LA-UR-12-25893
Approved for public release; distribution is unlimited.

Title:	Characterization of Delayed-Particle Emission Signatures for Pyroprocessing. Part 1: Fuel Assembly.
Author(s):	Durkee, Joe W. Jr. Fensin, Michael Lorne Zhang, Jinsuo
Intended for:	Report

Characterization of Delayed-Particle Emission Signatures for Pyroprocessing Part 1: Fuel Assembly

Joe W. Durkee, Jr., Michael L. Fensin, Jinsuo Zhang
Los Alamos National Laboratory
jdurkee@lanl.gov
505-665-0530
Fax: 505-665-2897
PO Box 1663, MS C921
Los Alamos, NM 87545

ABSTRACT

An initial study was conducted with nondestructive assay analysis using the MCNP6 Monte Carlo radiation-transport code to calculate delayed-neutron and delayed- gamma emission signature monitors to characterize burnup and isotopic composition for pyroprocessing. The study consists of five parts. In Part 1, a generic Westinghouse fuel assembly model was modified to create models with 3% and 5% ^{235}U enrichments, 20, 30, 40, and 50 GWd/MTU burnups, and 3-, 5-, 10-, 20-, and 30-year cooling times. MCNP6 was used to create detail-rich delayed-particle source terms for fuel assembly. Delayed-gamma activity ratios were then developed for conventional ^{134}Cs/^{137}Cs, ^{134}Cs/^{154}Eu, and ^{154}Eu/^{137}Cs markers as a function of burnup and of actinide mass for elemental uranium, neptunium, plutonium, americium, and curium. In addition, data mining using photon tally data was employed to discover potential new delayed-gamma activity ratios. The data mining effort was streamlined by the creation and use of several utility codes to extract and process data. The study confirms behavior for burnup dependence of ^{134}Cs/^{137}Cs, ^{134}Cs/^{154}Eu, and ^{154}Eu/^{137}Cs markers. A process for the discovery of potential new delayed-gamma markers has been developed, and results are presented. The actinide and nonactinide inventories for the fuel assembly models are used as source materials for the electrorefining models. Parts 2–5 contain analysis of a pyrochemical separations model that includes an MCNP6 mockup of the INL Mark IV electrorefiner (see companion documents). Part 2 focuses on delayed-particle emissions from the electrorefiner with loaded fuel dissolution baskets before electrorefining. Part 3 investigates delayed-particle emissions from the electrorefiner following electrorefining. Part 4 presents delayed-particle emissions from other pyroprocessing units that contain material developed by the electrorefining process in Part 3. Part 5 parallels Part 4, except for a 10 wt% plutonium reduction.

KEYWORDS: MCNP6; pyroprocessing; electrorefiner; delayed neutrons; delayed gammas, activity ratio.

CONTENTS

FIGURES

TABLES

ACRONYMS

3D	Three-Dimensional
AR	Activity Ratio
BAMF-DRT	Burnup Automation MCNPX File-Data Retrieval Tool
DA	Destructive Assay
DG	Delayed Gamma
DN	Delayed Neutron
ENSDF	Evaluated Nuclear Structure Data File
HEU	Highly Enriched Uranium
HPGe	High-Purity Germanium
LANL	Los Alamos National Laboratory
MPI	Message Passing Interface
NaI	Sodium Iodide
NDA	Nondestructive Assay
PC	Personal Computer
QA	Quality Assurance
SMR	Small Modular Reactor
VBA	Visual Basic

1. INTRODUCTION

The quantification of burnup and fissile content for irradiated nuclear fuels is of interest for fuel reprocessing and safeguards applications. Destructive assay (DA) and nondestructive assay (NDA) techniques have been developed and are used for such purposes (Hsue et al., 1978). DA methods, including mass spectroscopy and radiochemical assay, provide accurate characterizations, but involve chemical dissolution of spent fuel in a laboratory setting.

NDA entails delayed-gamma (DG) and/or delayed-neutron (DN) assay. The merit of NDA techniques is founded on the relationship between fission-product yield and number of fissions, or fuel burnup. NDA techniques are useful for laboratory and field assessment. The goal of NDA analysis is to provide a means of determining burnup and isotopic composition (fissile content) from measured DG or DN signals.

The gamma activity distribution can be assessed using both absolute and gamma ratio techniques. The absolute assay technique is used to correlate measured DG data with burnup for individual isotopes. The DG activity ratio (AR) technique uses pairs of isotopes to construct ARs that are proportional to fluence.

Accurate absolute DG activity measurement (Hsue et al., 1978) requires (1) knowledge of absolute detector efficiency and (2) measurement under strictly controlled geometry. These constraints cause absolute activity assay to be challenging for field inspection.

The DG AR technique, which has been investigated experimentally since 1971 (Hsue et al., 1978), (1) requires knowledge of relative detector efficiency and (2) is less sensitive to geometrical arrangement. This method is valid only if the measured nuclides have the same spatial distribution within the fuel pin or assembly. ARs are sensitive to migration effects (Hsue et al., 1978).

The activity distribution within a fuel assembly depends on two major factors (Hsue et al., 1978): (1) the burnup distribution as a function of irradiation and (2) fission-product migration relative to heavy metals. Migration exhibits dependence on fuel characteristics and the diffusing species (Hsue et al., 1978; Lee and Durkee, 1984). It has been reported that ^{134}Cs and ^{137}Cs migrate in a similar manner, whereas ^{95}Zr, ^{144}Ce, and ^{154}Eu do not migrate significantly in either the radial or axial directions relative to the heavy metal (Hsue et al., 1978; Pan, 1989; Tsao and Pan, 1993; Dennis and Usman, 2008).

In instances when DG emission data can be correlated with the burnup, plots of DG ARs exhibit linear or weakly nonlinear dependence on burnup. In this case, the DG activity isotopes are useful markers.

Suitable fission-product and actinide burnup monitors should have the following characteristics (Hsue et al., 1978) so that a DG AR is proportional to the fluence:

- approximately equal fission yields for the major fissioning nuclides;
- low neutron-capture cross sections (including capture by precursors);
- long half-life relative to irradiation duration;
- low migration (including precursors) in the fuel; and
- readily resolvable gamma-ray spectra with high-energy gamma rays to minimize attenuation.

Several suitable burnup monitors have been reported (Hsue et al., 1978) and are listed in Table 1. The data in Table 1 are updated to ENDF/B-VI using data from MCNP6 delayed-particle data contained in file cindergl.dat (Pelowitz, 2011).

Table 1. Burnup Monitor Nuclides (Hsue et al., 1978; cindergl.dat)

Isotope	Half-Life	Thermal Fission Yield		Principal Gamma	
		^{235}U	^{239}Pu	Energy (eV)	γ /100 decay
^{95}Zr	64.0 d	6.48	4.85	7.2420e5	81.0
				7.5673e5	100.0
^{106}Ru-^{106}Rh	371.6 d	0.53	4.10	5.1184e5	1000.0
				6.1617e5	37.0
				6.2194e5	487.0
				8.7348e5	21.5
				1.0504e6	76.4
				1.1280e6	19.8
^{134}Cs	2.06 y	7.62	7.66	5.6325e5	8.4
				5.6931e5	15.4
				6.0470e5	97.6
				7.9595e5	85.4
				8.0193e5	8.7
				1.3652e6	3.0
^{137}Cs-^{137m}Ba	30.0 y	6.32	6.71	6.6166e5	100.0
^{144}Ce-^{144}Pr	284.9 d	5.24	3.62	6.9649e5	1000.0
				1.4891e6	203.0
				2.1857e6	522.0
^{154}Eu	8.6 y	0.07	0.26	5.9181e5	13.6
				7.2330e5	55.5
				8.7319e5	32.4
				9.9632e5	29.0
				1.0048e6	50.4

Hsue et al. (1978) provide simple algebraic expressions that are based on the aforementioned characteristics which underpin the DG AR technique (Equations 12 and 13 of their report). To better understand why these characteristics are needed and how those expressions and DG AR expressions are developed and related to burnup and fissile content, consider the production chains for ^{134}Cs and ^{137}Cs (Hsue et al., 1978):

$$fission: {}^{133}I \xrightarrow[21h]{} {}^{133}Xe \xrightarrow[5.27d]{} {}^{133}Cs \xrightarrow[(n,\gamma)]{} {}^{134}Cs \xrightarrow[2.1y]{} {}^{134}Ba \tag{1}$$

and

$$fission: {}^{137}I \xrightarrow[24s]{} {}^{137}Xe \xrightarrow[4.2m]{} {}^{137}Cs \xrightarrow[30.0y]{} {}^{137m}Ba \xrightarrow[2.6m]{} {}^{137}Ba \tag{2}$$

The isotopic diffusion-reaction-decay equations for ^{133}Cs, ^{134}Cs and ^{137}Cs can be written as

$$\begin{aligned}
\frac{\partial N^{Cs3}}{\partial t} &= \vec{\nabla}\cdot D^{Cs3}\vec{\nabla}N^{Cs3} + \gamma^{Cs3}\varphi\Sigma_f - \varphi\sigma_{n,\gamma}^{Cs3}N^{Cs3} \\
\frac{\partial N^{Cs4}}{\partial t} &= \vec{\nabla}\cdot D^{Cs4}\vec{\nabla}N^{Cs4} + \varphi\sigma_{n,\gamma}^{Cs3}N^{Cs3} - \varphi\sigma_c^{Cs4}N^{Cs4} - \lambda^{Cs4}N^{Cs4} \\
\frac{\partial N^{Cs7}}{\partial t} &= \vec{\nabla}\cdot D^{Cs7}\vec{\nabla}N^{Cs7} + \gamma^{Cs7}\varphi\Sigma_f - \varphi\sigma_c^{Cs7}N^{Cs7} - \lambda^{Cs7}N^{Cs7}.
\end{aligned} \tag{3}$$

where φ is the spectrum-averaged flux and N^{Cs3}, N^{Cs4}, and N^{Cs7} are the concentrations (a/b-cm) of ^{133}Cs, ^{134}Cs, and ^{137}Cs, respectively. Characteristic 1 presumes that the fission yields γ^{Cs3} and γ^{Cs7} (implicit via the ^{133}I and ^{137}I fission production and rapid decay to ^{133}Cs and ^{137}Cs) are approximately equivalent; we call this yield γ. Characteristic 2 presumes that the terms containing these capture cross sections σ_c^{Cs4} and σ_c^{Cs7} are small. Characteristic 3 presumes that terms with the decay constants λ^{Cs4} and λ^{Cs7} are small. Characteristic 4 presumes that the diffusion (migration) terms with the diffusion coefficients D^{Cs3}, D^{Cs4}, and D^{Cs7} are negligible. Provided these characteristics are satisfied, then the expressions in Eq.(3) simplify to

$$\begin{aligned}
\frac{dN^{Cs3}}{dt} &= \gamma\varphi\Sigma_f - \varphi\sigma_{n,\gamma}^{Cs3}N^{Cs3} \\
\frac{dN^{Cs4}}{dt} &= \varphi\sigma_{n,\gamma}^{Cs3}N^{Cs3} \\
\frac{dN^{Cs7}}{dt} &= \gamma\varphi\Sigma_f.
\end{aligned} \tag{4}$$

Solving the first and third expressions in Eq.(4) gives

$$N^{Cs3}(t) = \frac{\gamma\Sigma_f}{\sigma_{n,\gamma}^{Cs3}}\left[1-\exp\left(-\varphi\sigma_{n,\gamma}^{Cs3}t\right)\right]$$
$$N^{Cs7}(t) = \gamma\varphi\Sigma_f t. \tag{5}$$

Substituting the expression for $N^{Cs3}(t)$ in Eq.(5) into the expression for $N^{Cs4}(t)$ in Eq.(4) and solving gives

$$N^{Cs4}(t) = \gamma\varphi\Sigma_f t + \frac{\gamma\Sigma_f}{\sigma_{n,\gamma}^{Cs3}}\left[\exp\left(-\varphi\sigma_{n,\gamma}^{Cs3}t\right)-1\right] . \tag{6}$$

The DG AR formed using Equations (5) and (6) is

$$\frac{N^{Cs4}(t)}{N^{Cs7}(t)} = \frac{\gamma\varphi\Sigma_f t + \frac{\gamma\Sigma_f}{\sigma_{n,\gamma}^{Cs3}}\left[\exp\left(-\varphi\sigma_{n,\gamma}^{Cs3}t\right)-1\right]}{\gamma\varphi\Sigma_f t} , \tag{7}$$

which does not appear to be proportional to the fluence, $\varphi t,$ as has been asserted by others (Hsue et al., 1978). Note however that a first-order Taylor series approximation for $N^{Cs3}(t)$ in Eq.(5) is

$$N^{Cs3}(t) = \gamma\varphi\Sigma_f t , \tag{8}$$

which becomes increasingly valid at later times. Using Eq.(8) in the expression for $N^{Cs4}(t)$ in Eq.(4) and solving gives

$$N^{Cs4}(t) = \gamma\varphi^2\sigma_{n,\gamma}^{Cs3}\Sigma_f\frac{t^2}{2} . \tag{9}$$

Using the expressions for $N^{Cs4}(t)$ in Eq.(9) and $N^{Cs7}(t)$ in Eq.(5) yields the quotient

$$\frac{N^{Cs4}(t)}{N^{Cs7}(t)} \sim \varphi t , \tag{10}$$

which suggests that, subject to the stipulated characteristics, the concentration ratio is proportional to the product of the flux and time (fluence).[†] The reasoning for the stipulated characteristics is now clear. If one or more of the characteristics is violated, then the simple expression in Eq.(10) is invalid. Equation (10) includes only a crude treatment of radiation transport.

[†] Also, if a second-order Taylor series approximation of the exponential term in Eq.(7) is used, then Equations (9) and (10) are obtained. A first-order expansion gives $N^{Cs4}(t)=0$. A second-order expansion is necessary because ^{134}Cs is the second isotope in the transmutation chain.

To see how, in principle, the ratio in Eq.(10) can be used as a burnup monitor, consider the following simplified fuel depletion formulation (Lamarsh, 1972). For a reactor that is fueled with a single isotope, the depletion of this isotope is given by

$$\frac{dN^F(\vec{r},t)}{dt} = -N^F(\vec{r},t)\bar{\sigma}_a^F\varphi(\vec{r},t) \ , \tag{11}$$

where $N^F(\vec{r},t)$ is the atom density of the isotope at point $\vec{r}$ and time *t*, $\bar{\sigma}_a^F$ is the absorption cross section, and $\varphi(\vec{r},t)$ is the spectrum-averaged flux. In general, the flux and the fuel concentrations are inter-related so that numerical evaluation of Eq.(11) is required. However, approximate solutions can be obtained. For example, if the flux is assumed to be constant over a time interval of interest, the constant-flux approximation (Duderstadt and Hamilton, 1976)

$$\varphi(\vec{r},t) = \varphi(\vec{r}) \ , \tag{12}$$

facilitates the analytic result

$$N^F(\vec{r},t) = N^F(\vec{r},0)\exp[-\bar{\sigma}_a^F\varphi(\vec{r})t] \ , \tag{13}$$

which is the isotopic depletion (burnup) for a fissile isotope. Equation (13) can be solved for the fluence in terms of the fissile content so that

$$\varphi(\vec{r})t = -\frac{1}{\bar{\sigma}_a^F}\ln\left[\frac{N^F(\vec{r},t)}{N^F(\vec{r},0)}\right] \sim \frac{N^{Cs4}(\vec{r},t)}{N^{Cs7}(\vec{r},t)} \tag{14}$$

where Eq.(10) has been included with positional dependence. Equation (14) shows the relationships between the fluence, fissile content, and the $^{134}Cs/^{137}Cs$ DG AR burnup monitor. Spatial dependence of the flux can be inferred using measured position-dependent $^{134}Cs/^{137}Cs$ DG AR (Ansari et al., 2007).

In effect, NDA analysis is an inverse problem. That is, given the DG and/or DN measured signal, perhaps with the irradiation history, the burnup and isotopic composition are determined. This formulation contrasts with the forward problem: determine the signal given reactor composition and irradiation history. Care must be exercised to formulate a well-posed inverse problem so that a unique solution can be obtained. In this report we have proceeded along an investigatory path that has been used by earlier investigators to examine this signature identification problem.

In the current study, burnup is defined as the integrated energy released from the fission of heavy nuclides initially present in fuel in GWd/MTU (gigawatt days per metric ton uranium initial). This definition facilitates the correlation of the number of fissions, or burnup, as desired for the reliance of NDA techniques for measured DG and DN data.

In this effort, NDA analysis has been used to characterize burnup and isotopic composition for pyroprocessing. The effort has consisted of two primary tasks: (1) assembly analysis and (2) pyroprocessing analysis.

The assembly analysis was designed to establish a baseline reference with which the pyroprocessing results could be compared. The assembly analysis uses a fuel assembly model to (1) generate DG and DN sources; (2) calculate DG emission ratios for $^{134}Cs/^{137}Cs$, $^{134}Cs/^{154}Eu$, and $^{154}Eu/^{137}Cs$ as a function of burnup and actinide mass; (3) evaluate DN current as a function of burnup and actinide mass; and (4) discover potential new DG emission ratio markers.

This radiation signature study has been executed using the MCNP6 Monte Carlo radiation-transport code. Los Alamos National Laboratory (LANL) develops and maintains the MCNP (Brown, 2003a; Brown, 2003b) and, before the code merger occurred (Goorley et al., 2012), the MCNPX™(Pelowitz, 2011) Monte Carlo N-Particle eXtended general-purpose radiation-transport codes. A merged version of MCNP and MCNPX, MCNP6, was released in 2012.

MCNP6 (Goorley et al., 2012), as with its recent predecessors, accommodates intricate three-dimensional (3D) geometrical models, continuous-energy transport of 36 different particle types plus heavy-ion transport, fuel burnup, and high-fidelity delayed-gamma emission. MCNP6 is written in Fortran 90, has been parallelized, has been threaded for kcode/burnup calculations, and works on platforms including single-processor personal computers (PCs), Sun workstations, Linux clusters, and supercomputers. MCNP6 has approximately 3000 users throughout the world working on endeavors that include radiation therapy, reactor design, and homeland security.

MCNP6 has a kcode/burnup feature that links Monte Carlo particle-transport and depletion capabilities. This feature enables isotopic transmutation studies of complex 3D geometries with exotic material combinations and highly anisotropic flux behavior, conditions that are expected to be exhibited by test reactors and new advanced reactor systems, such as small modular reactors (SMRs) and Generation 3+ and 4 systems (Cousin and Haeck, 2008; Ghrayeb et al., 2008; Sterbentz et al., 2011; Kim and Hartanto, 2011; Fensin et al., 2010). The Monte Carlo method is well suited for considering "details" because the simulation process has fewer approximations during the particle transport than deterministic methods. Such a lack of approximation is important for systems that have high anisotropy, large streaming effects, low capture-cross-section/high decay-yield isotopes (such as material characterization for nonproliferation), material combinations that result in appreciable spectra over varying significant resonances (such as high burnup or advanced clad systems), or a fuel/reflector interface for highly leaky systems (such as SMRs).

MCNP6 contains a delayed-particle feature to treat DN, DG, or DN and DG emission by radioactive decay of unstable fission or activation products.[†] The MCNP6 capability pertains to reactions where unstable residuals decay with half-lives ranging from microseconds to thousands of years. The DG feature can provide photon emission for scoping studies using 25-bin data or for detailed analyses using discrete (line) data. This delayed radiation can be exploited for a variety of purposes, including homeland security, health physics, instrumentation and equipment

[†] Less complete work for burnup monitoring using ORIGEN and MCNP techniques has been reported (e.g., Hawari et al., 2005). That treatment evidently considers only fission; activation is neglected.

design, and nuclear safeguards. The theoretical, computational, and data development effort supporting the MCNP6 DG feature is detailed in the literature (Durkee et al., 2009a, 2009b, 2009c, 2010, 2012; McKinney, 2012).

The kcode/burnup and delayed-particle features use CINDER'90 (Wilson et al., 1995) to provide time-dependent nuclide densities. CINDER'90 is an isotopic transmutation code that calculates nuclide inventories in spatially homogeneous regions created by neutron transmutation and radioactive decay. CINDER'90 accommodates 3400 nuclides with atomic numbers (Z) ranging from 1 to 103. Originally written as a standalone code, CINDER'90 was integrated into MCNPX to provide seamless simulation capability (Trellue et al., 2005).

The MCNP6 kcode/burnup and delayed-particle features function independently. Currently, MCNP6 contains no linkage to permit delayed-particle simulations using inventories produced by kcode/burnup calculations. Our analysis thus required the use of an auxiliary processing routine to create DG and DN sources using irradiated fuel inventories. This component of our study is discussed in Section 3.

In this study, MCNP6 has been used to execute kcode/burnup simulations to create irradiated material inventories for a fuel assembly. Those inventories are then used to produce delayed-particle source terms for DG AR and DN emission analyses. The analyses consider behavior as a function of fuel enrichment, burnup, and post-irradiation cooling time to develop a general characterization of behavior. The work considers the traditional DG AR markers $^{134}Cs/^{137}Cs$, $^{134}Cs/^{154}Eu$, and $^{154}Eu/^{137}Cs$ and begins an exploration for new markers.

The analysis considered here includes burnup treatment as a function of irradiation. Migration effects are not examined—all fuel, fission products, and actinides are treated as being *in situ*.

The computational procedure is discussed in the following sections. We also discuss limitations of the procedure and identify important upgrades that are required to achieve fuel reprocessing and safeguards endpoints.

2. FUEL ASSEMBLY BURNUP MODELS

The fuel assembly studies used a generic 17 x 17 Westinghouse infinitely reflected assembly (Fensin et al., 2009; OECD-NEA, 2012). Although core operating strategies, such as bundle placement affecting bundle-to-bundle leakage, do affect the ultimate buildup and depletion of nuclides, this study chose to examine only a generic average bundle; therefore, infinite reflection was deemed to be an acceptable boundary condition. The general assembly parameters are listed in Table 2. The UO_2 fuel pellets were encased in Zircaloy-4 cladding. The coolant was chosen to be a 660-ppm average boron concentration at a density of 0.7245 g/cm^3 and temperature of 575 K. To maximize the spatial resolution per fuel pin, the fuel assembly was modeled using the MCNP6 repeated structures capability with one-eighth-assembly symmetry. Using one-eighth-assembly symmetry results in 39 repeated fuel pin regions (diagonal rows of pins are shared amongst the one-eighth-assembly divisions). Figures 1a and 1b contain plots of the assembly made with the MCNP6 geometry plotter.

Table 2. Generic Westinghouse 17 x 17 Assembly Parameters

Parameter	Data
Assembly general data	
Lattice	17×17
Number of fuel rods	264
Number of guide tubes	24
Number of instrument tubes	1
Fuel rod data	
Type of fuel pellet	UO_2 (10.4538 g/cm^3)
Rod pitch	1.26 cm
Clad thickness	0.065 cm (no gap between fuel and clad)
Pellet diameter	0.410 cm
Active fuel length	365.76 cm
Fuel temperature	900 K
Clad temperature	620 K
Clad material	Zircaloy-4 (5.8736 g/cm^3)
Guide and Instrument tube data	
Inner radius	0.571 cm
Outer radius	0.613 cm
Material	Zircaloy-4 (5.8736 g/cm^3)

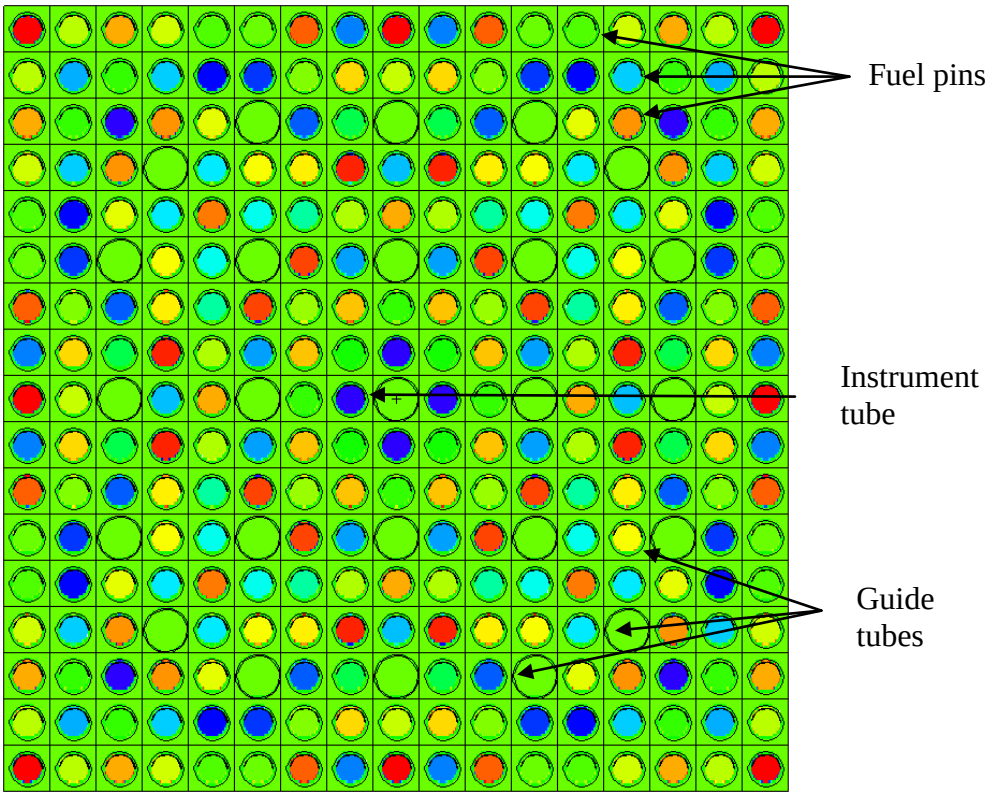

Figure 1a. MCNP6 mid-plane fuel assembly geometry plot.

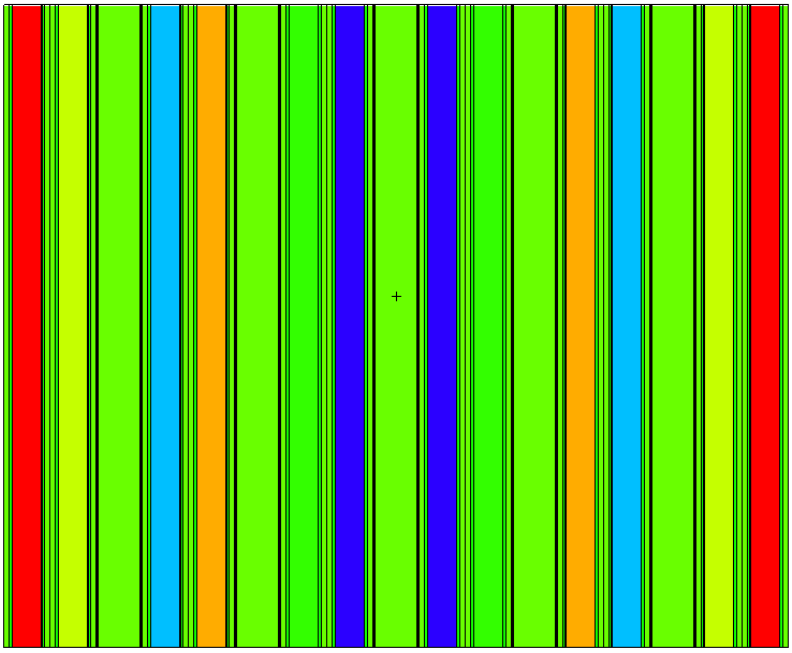

Figure 1b. MCNP6 axial fuel assembly geometry plot.

MCNP6 input files were prepared for 3% and 5% ^{235}U enrichment.[†] Each of these files was used to prepare models with burnups of 20, 30, 40, and 50 GWd/MTU. Each of the eight input files was prepared with post-irradiation cooling times of 3, 5, 10, 20, and 30 years.

The kcode/burnup models included materials and cross sections at realistic reactor temperatures. Fuel, clad, and water were treated at 900 K, 620 K, and 575 K, respectively.

These models were executed using the MCNP6 Tier 3 burnup inventory option. The Tier 3 option provides inventories for all ENDF/B-VII.0 fission products that have yield information in the CINDER'90 transmutation code (Pelowitz, 2011). The Tier 3 option provides the most comprehensive fission-product and actinide inventory available in MCNP6. Simulations with Tier 3 provided DG and DN sources to the fullest possible extent. The analysis presented here constitutes the first reported use of the Tier 3 option for signature analysis of spent fuel.

To enhance nuclide prediction, short time steps are taken at the beginning of each cycle to account for the equilibrium buildup of Xe and Sm fission-product poisons. After equilibrium Xe and Sm concentrations were achieved, longer time steps, ~ 2 GWD/MTU, were used. Each kcode time step used 10,000 particles per cycle, skipping the first 25 cycles for 155 cycles.

The complexity of the kcode/burnup models, inclusive of the comprehensive assortment of fission products and actinides, necessitated the use of the new MCNP6 threading capability (Fensin et al. 2012) to execute the data-intensive kcode/burnup calculations in a timely manner.

[†] Throughout the remainder of this series of reports, the enrichment terminology without specific reference to ^{235}U will be used for brevity.

Threading facilitates parallel execution using shared memory with reduced memory requirements. Message passing interface (MPI) execution alone enables parallel execution but requires copies of arrays—one per processor. Threading allows parallel execution with array sharing, thus reducing memory requirements.

A threaded Intel MPI MCNP6 executable was created on the LANL Pete Linux cluster (or Pete). Each of the eight kcode/burnup jobs required 4 to 7 days of execution time using 45 dedicated processors. Batch execution was done using a qsub[†] execution file (bumf4.qsub).

3. FUEL ASSEMBLY DELAYED-PARTICLE SOURCE MODELS

The output (outp) files for the source calculations were ported from Pete to the PC for processing to create models with DG and DN sources corresponding to the irradiated fuel inventories. Processing was done using the Burnup Automation MCNPX File-Data Retrieval Tool (BAMF-DRT) Visual Basic (VBA) code (Sandoval and Fensin, 2008; Fensin et al., 2011). BAMF-DRT was modified to generate fixed-source emission decks of the passive neutron and gamma signals at each cooling time.

BAMF-DRT uses modified Evaluated Nuclear Structure Data File (ENSDF) data (National Nuclear Data Center, 2012) to generate the passive gamma emission signature within each fuel region of the assembly, based on the activity of each individual gamma within each individual region. Because this analysis uses Tier 3 fission products, the BAMF-DRT gamma library file was modified to include all fission-product and actinide lines from the maximum amount of nuclides followed in MCNP burnup (390 isotopes with ENDF/B VII.0 transport data).

The BAMF-DRT framework was also modified to automatically generate SOURCES3A (Wilson et al., 1997) decks for each individual fuel region. SOURCES3A is a computer code that determines neutron production rates and spectra from (α, n) reactions, spontaneous fission, and DN emission from the decay of radionuclides in homogeneous media. BAMF-DRT ran SOURCES3A and then used the results to generate a neutron fixed-source emission deck. The sampling of each fuel region was based on the neutron activity in each region, and the energy spectra were based on the isotopics present in each region.

This processing procedure was used to prepare 40 input files with DG sources. Each deck contained 1-keV photon tally bins. Additionally, 40 input files were prepared with DN sources. Decks were prepared for each state point: 3% and 5% enrichment; 20, 30, 40, and 50 GWd/MTU burnup; and 3, 5, 10, 20, and 30 year post-irradiation cooling times.

For the DG models, the outgoing energy-dependent photon current was calculated using 1-keV bin resolution. For the DN models, the energy-integrated escaping neutron current surface was calculated. These currents were calculated using the MCNP6 “F1” tally, which counts the number of particles crossing a surface. This tally differs from the MCNP6 “F8” pulse-height tally, which mimics detectors by calculating the energy distribution of pulses created in a detector. The F8 tally mimics typical measurement strategies, such as high-purity germanium

[†] qsub is the command used for job submission to the cluster. The qsub file contains commands for job execution.

(HPGe) or sodium iodide (NaI) for photons (energy-dependent) and a helium tube or Bonner sphere for neutrons (energy integrated). The F1 tally was used throughout this study to simplify the analysis as basic capability—which focuses on distilling electrorefining concepts and data for use in radiation-transport models—is developed. The F1 tally surfaces throughout this study are large planes. The use of F8 detector tallies requires the creation and placement of detector models. F1 planar tallies with reliable quality require less model development, including execution using analog Monte Carlo and less computer time than F8 detector tallies, which can require implementation of clever variance-reduction techniques to obtain desired results. Such implementation is an art and can be time consuming to develop successfully. Consequently, we chose not to use F8 tallies with variance reduction in addition to the electrorefining/radiation-transport problem. The use of F8 tallies is left to a future study.

These models were ported to Pete for execution using a regular (non-threaded) Intel MPI build and 48 processors. Automated execution of these calculations and handling of the output files on Pete was done using new Perl scripts. Script **rundps.pl** guided the qsub file (dps.qsub) submission for each model, whereas **runopm.pl** handled file renaming. These scripts dive down from a higher-level directory to the various subdirectories to control function. The use of these scripts streamlined performance, eliminated tedium, and enabled tracking and reproducibility.

The DG fixed-source ("sdef") calculations were executed using 2×10^9 source photon histories, resulting in relative (fractional) errors[†] of 0.02 or less for the outgoing current F1 tallies in almost all tally bins <1 MeV. The 10 statistical checks[*] used by MCNP6 (Brown, 2003a, pp. 123–127) to help confirm the acceptability of the result were passed for the aggregate surface-integrated-current ("F1") tallies. Each model required 3 to 6 hours of execution time using 48 processors.

The DN sdef calculations were executed using 10^8 source neutron histories, resulting in relative errors of ~0.0001 for the F1 tallies. The 10 statistical checks were passed. Execution of each of the 40 models (2 enrichments, 4 burnups, and 5 cooling times) required ~1 hour of wall clock time.

Processing details for the DG and DN emission signals are presented in the following sections.

4. FUEL ASSEMBLY DG ARs VS BURNUP FOR ^{134}Cs/^{137}Cs, ^{134}Cs/^{154}Eu, AND ^{154}Eu/^{137}Cs

Once the delayed-particle source calculations were completed on Pete, the MCNP6 outp and mctal files were moved to the PC for postprocessing to produce plots of DG emission ratios as a function of burnup. The postprocessing procedure and calculated results are discussed next.

[†]The relative error is defined in MCNP6 as one estimated standard deviation of the mean divided by the estimated mean. Tally quality is interpreted as follows. Values < 0.10 are generally reliable, 0.1–0.2 are questionable, 0.2–0.5 are within a factor of a few, and 0.5–1 are not meaningful.
[*]MCNP6 uses 10 statistical checks to form statistically valid confidence intervals for each tally bin.

4.1. Tally Processing for Fuel Assembly DG AR Analysis

The data for DG AR analysis were obtained by first retrieving outgoing surface-integrated current (F1) tally data from the outp files for emissions for the key signaling radioisotopes ^{134}Cs, ^{137}Cs, and ^{154}Eu (Hsue et al., 1978; Tsao and Pan, 1993; Willman et al., 2006). Then quotients of the tally data were calculated to form the DG ARs for ^{134}Cs/^{137}Cs, ^{134}Cs/^{154}Eu, and ^{154}Eu/^{137}Cs.

The MCNP6 F1 photon-current tallies were calculated using 1-keV energy bins. Contributions to the F1 tally in each bin can originate from multiple nuclides. Correct analysis requires identification of the nuclides contributing to the signal in each tally bin. However, MCNP6 currently does not have the diagnostic capability required to identify the individual nuclides producing DGs that contribute to the F1 tally in each energy bin. For the moment, the approximate treatment conducted here using the aggregate tally bin values is the best that can be provided. The approximate treatment used the bin-wise tally data based on the premise that the prominent DGs for the energy bins of interest are emitted by ^{134}Cs, ^{137}Cs, and ^{154}Eu. Consequently, conclusions drawn from this analysis must be viewed with caution because other radionuclides can emit photons that contribute to the tally in an energy bin.

The DG emission energies for these isotopes were obtained from the cindergl.dat data file.[†] Tables 2a and 2b list DG emission data for ^{134}Cs and ^{154}Eu. The prominent lines selected for ratio analysis are highlighted in blue fonts. A single emission energy of 0.662 MeV was used for ^{137}Cs.

Table 2a. ^{134}Cs Gamma Emission Energies

```
Radiation type: gamma
Average decay energy: 1.5550E+06 (4.0000E+03) eV
Discrete spectrum normalization: 1.0000E-02 (0.0000E+00)
  12 discrete lines given     Gammas per
     E(eV)   Uncertainty   100 decay Uncertainty
    2.4269E+05 (4.0000E+01)    0.0210 (  0.0008)
    3.2651E+05 (1.0000E+02)    0.0144 (  0.0006)
    4.7535E+05 (5.0000E+01)    1.4600 (  0.0400)
    5.6323E+05 (1.5000E+01)    8.3800 (  0.0500)
    5.6931E+05 (1.5000E+01)   15.4300 (  0.1100)
    6.0470E+05 (1.5000E+01)   97.6000 (  0.3000)
    7.9585E+05 (2.2000E+01)   85.4000 (  0.4000)
    8.0193E+05 (2.2000E+01)    8.7300 (  0.0400)
    8.4702E+05 (2.5000E+01)    0.0003 (  0.0001)
    1.0386E+06 (2.6000E+01)    1.0000 (  0.0100)
    1.1679E+06 (2.6000E+01)    1.8050 (  0.0260)
    1.3652E+06 (3.2000E+01)    3.0400 (  0.0400)
```

[†] The cindergl.dat file contains ENDF/B-VI photon-emission data for 979 nuclides (Durkee et al., 2009a).

Table 2b. ^{154}Eu Gamma Emission Energies

Radiation type: gamma
Average decay energy: 1.2420E+06 (7.1000E+04) eV
Discrete spectrum normalization: 3.5500E-03 (2.0000E-04)
174 discrete lines given

5.8400E+04	(0.0000E+00)	0.0110	(0.0010)
8.0400E+04	(0.0000E+00)	0.0080	(0.0040)
8.1990E+04	(2.0000E+01)	0.0095	(0.0050)
1.2307E+05	(4.0000E+00)	114.0000	(2.0000)
1.2539E+05	(0.0000E+00)	0.0200	(0.0060)
1.2840E+05	(0.0000E+00)	0.0280	(0.0000)
1.2950E+05	(0.0000E+00)	0.0390	(0.0060)
1.3157E+05	(3.5000E+01)	0.0580	(0.0060)
1.3484E+05	(0.0000E+00)	0.0280	(0.0030)
1.3580E+05	(0.0000E+00)	0.0310	(0.0000)
1.3839E+05	(0.0000E+00)	0.0028	(0.0000)
1.4300E+05	(0.0000E+00)	0.0020	(0.0000)
1.4603E+05	(2.5000E+01)	0.0730	(0.0000)
1.5494E+05	(0.0000E+00)	0.0014	(0.0000)
1.5631E+05	(1.0000E+02)	0.0280	(0.0000)
1.5990E+05	(0.0000E+00)	0.0028	(0.0000)
1.6209E+05	(0.0000E+00)	0.0028	(0.0014)
1.6591E+05	(0.0000E+00)	0.0065	(0.0014)
1.8073E+05	(0.0000E+00)	0.0130	(0.0030)
1.8468E+05	(8.0000E+01)	0.0115	(0.0031)
1.8825E+05	(1.3000E+01)	0.6400	(0.0200)
1.9550E+05	(5.0000E+02)	0.0056	(0.0028)
2.0940E+05	(4.0000E+02)	0.0068	(0.0023)
2.1940E+05	(0.0000E+00)	0.0065	(0.0025)
2.2900E+05	(5.0000E+02)	0.0056	(0.0023)
2.3201E+05	(5.0000E+01)	0.0630	(0.0100)
2.3700E+05	(0.0000E+00)	0.0170	(0.0110)
2.4794E+05	(8.0000E+00)	18.6000	(0.4000)
2.6090E+05	(0.0000E+00)	0.0056	(0.0023)
2.6540E+05	(0.0000E+00)	0.0045	(0.0000)
2.6744E+05	(0.0000E+00)	0.0390	(0.0000)
2.6744E+05	(0.0000E+00)	0.0390	(0.0000)
2.6980E+05	(0.0000E+00)	0.0200	(0.0030)
2.7400E+05	(0.0000E+00)	0.0110	(0.0000)
2.7540E+05	(0.0000E+00)	0.0001	(0.0000)
2.7990E+05	(0.0000E+00)	0.0085	(0.0000)
2.9000E+05	(0.0000E+00)	0.0096	(0.0000)
2.9570E+05	(0.0000E+00)	0.0068	(0.0000)
2.9600E+05	(1.0000E+03)	0.0039	(0.0025)
3.0125E+05	(0.0000E+00)	0.0280	(0.0000)
3.0512E+05	(0.0000E+00)	0.0500	(0.0000)
3.0820E+05	(0.0000E+00)	0.0045	(0.0000)
3.1228E+05	(0.0000E+00)	0.0410	(0.0000)
3.1542E+05	(0.0000E+00)	0.0130	(0.0000)
3.2000E+05	(1.0000E+03)	0.0030	(0.0020)
3.2201E+05	(5.0000E+01)	0.1900	(0.0000)
3.2948E+05	(0.0000E+00)	0.0340	(0.0060)
3.4672E+05	(5.0000E+01)	0.0850	(0.0000)
3.5200E+05	(0.0000E+00)	0.0025	(0.0000)

```
3.6821E+05 (0.0000E+00)    0.0085 (  0.0000)
3.7071E+05 (0.0000E+00)    0.0150 (  0.0040)
3.7520E+05 (5.0000E+02)    0.0050 (  0.0030)
3.8200E+05 (5.0000E+01)    0.0280 (  0.0000)
3.9714E+05 (0.0000E+00)    0.0850 (  0.0000)
4.0130E+05 (5.0000E+01)    0.5900 (  0.0200)
4.0355E+05 (5.0000E+01)    0.0760 (  0.0000)
4.1430E+05 (0.0000E+00)    0.0140 (  0.0000)
4.1940E+05 (0.0000E+00)    0.0110 (  0.0060)
4.2208E+05 (0.0000E+00)    0.0034 (  0.0000)
4.3178E+05 (0.0000E+00)    0.0079 (  0.0000)
4.3590E+05 (0.0000E+00)    0.0073 (  0.0000)
4.4444E+05 (7.0000E+01)    1.4200 (  0.0400)
4.6020E+05 (0.0000E+00)    0.0079 (  0.0000)
4.6390E+05 (0.0000E+00)    0.0120 (  0.0000)
4.6792E+05 (5.0000E+01)    0.1600 (  0.0000)
4.7826E+05 (5.0000E+01)    0.6100 (  0.0200)
4.8061E+05 (0.0000E+00)    0.0140 (  0.0000)
4.8374E+05 (0.0000E+00)    0.0140 (  0.0000)
4.8464E+05 (0.0000E+00)    0.0110 (  0.0000)
4.8636E+05 (0.0000E+00)    0.0062 (  0.0000)
4.8826E+05 (0.0000E+00)    0.0200 (  0.0090)
5.0640E+05 (0.0000E+00)    0.0170 (  0.0060)
5.0988E+05 (0.0000E+00)    0.1030 (  0.0000)
5.1203E+05 (0.0000E+00)    0.0920 (  0.0200)
5.1800E+05 (5.0000E+01)    0.1300 (  0.0000)
5.3284E+05 (0.0000E+00)    0.0310 (  0.0060)
5.3305E+05 (1.4000E+02)    0.0650 (  0.0000)
5.3506E+05 (1.4000E+02)    0.0650 (  0.0000)
5.4560E+05 (0.0000E+00)    0.0300 (  0.0030)
5.5756E+05 (5.0000E+01)    0.7200 (  0.0200)
5.6923E+05 (0.0000E+00)    0.0280 (  0.0000)
5.8200E+05 (5.0000E+01)    2.3700 (  0.0700)
5.9181E+05 (4.0000E+01)   13.6000 (  0.3000)
5.9750E+05 (0.0000E+00)    0.0160 (  0.0000)
5.9831E+05 (0.0000E+00)    0.0170 (  0.0000)
6.0000E+05 (0.0000E+00)    0.0170 (  0.0110)
6.0281E+05 (5.0000E+01)    0.0960 (  0.0000)
6.1200E+05 (0.0000E+00)    0.0170 (  0.0000)
6.1326E+05 (5.0000E+01)    0.2600 (  0.0000)
6.2052E+05 (0.0000E+00)    0.0260 (  0.0000)
6.2522E+05 (5.0000E+01)    0.8700 (  0.0300)
6.4240E+05 (0.0000E+00)    0.0110 (  0.0060)
6.4944E+05 (5.0000E+01)    0.2100 (  0.0000)
6.5060E+05 (0.0000E+00)    0.0280 (  0.0000)
6.6070E+05 (0.0000E+00)    0.0082 (  0.0000)
6.6468E+05 (5.0000E+01)    0.0820 (  0.0000)
6.6890E+05 (0.0000E+00)    0.0340 (  0.0080)
6.7659E+05 (5.0000E+01)    0.3940 (  0.0120)
6.9241E+05 (5.0000E+01)    4.7700 (  0.1000)
7.0170E+05 (0.0000E+00)    0.0130 (  0.0000)
7.1576E+05 (5.0000E+01)    0.4900 (  0.0200)
7.2330E+05 (4.0000E+01)   55.5000 (  1.1000)
7.2730E+05 (0.0000E+00)    0.2100 (  0.0000)
7.3765E+05 (0.0000E+00)    0.0210 (  0.0030)
7.5687E+05 (5.0000E+01)   12.2000 (  0.3000)
7.7440E+05 (0.0000E+00)    0.0280 (  0.0140)
```

```
7.9012E+05 (0.0000E+00)    0.0310 (  0.0080)
8.0020E+05 (0.0000E+00)    0.0920 (  0.0140)
8.1555E+05 (5.0000E+01)    1.3100 (  0.0400)
8.3038E+05 (0.0000E+00)    0.0140 (  0.0000)
8.4539E+05 (5.0000E+01)    1.5500 (  0.0500)
8.5064E+05 (5.0000E+01)    0.6500 (  0.0200)
8.7319E+05 (5.0000E+01)   32.4000 (  0.6000)
8.8061E+05 (5.0000E+01)    0.2300 (  0.0000)
8.9273E+05 (5.0000E+01)    1.3000 (  0.0400)
8.9837E+05 (0.0000E+00)    0.0056 (  0.0014)
9.0405E+05 (5.0000E+01)    2.3200 (  0.0700)
9.0610E+05 (0.0000E+00)    0.0340 (  0.0000)
9.1924E+05 (0.0000E+00)    0.0350 (  0.0000)
9.2449E+05 (5.0000E+01)    0.1700 (  0.0000)
9.2840E+05 (0.0000E+00)    0.0140 (  0.0000)
9.8130E+05 (0.0000E+00)    0.0230 (  0.0060)
9.8450E+05 (0.0000E+00)    0.0180 (  0.0110)
9.9632E+05 (4.0000E+01)   29.0000 (  0.6000)
1.0048E+06 (4.0000E+01)   50.4000 (  0.9000)
1.0128E+06 (2.0000E+02)    0.0082 (  0.0034)
1.0230E+06 (1.0000E+03)    0.0200 (  0.0080)
1.0334E+06 (0.0000E+00)    0.0340 (  0.0000)
1.0474E+06 (1.0000E+02)    0.4000 (  0.0000)
1.0494E+06 (1.0000E+02)    0.0490 (  0.0000)
1.0722E+06 (0.0000E+00)    0.0110 (  0.0000)
1.1100E+06 (0.0000E+00)    0.0085 (  0.0056)
1.1185E+06 (1.0000E+02)    0.2900 (  0.0100)
1.1242E+06 (0.0000E+00)    0.0200 (  0.0030)
1.1284E+06 (1.0000E+02)    0.7500 (  0.0200)
1.1361E+06 (0.0000E+00)    0.0210 (  0.0030)
1.1409E+06 (1.0000E+02)    0.6100 (  0.0200)
1.1531E+06 (5.0000E+02)    0.0390 (  0.0110)
1.1606E+06 (0.0000E+00)    0.1240 (  0.0000)
1.1700E+06 (5.0000E+02)    0.0120 (  0.0060)
1.1886E+06 (0.0000E+00)    0.2300 (  0.0000)
1.2168E+06 (0.0000E+00)    0.0100 (  0.0000)
1.2321E+06 (5.0000E+02)    0.0260 (  0.0170)
1.2416E+06 (2.0000E+02)    0.3700 (  0.0100)
1.2462E+06 (2.0000E+02)    2.5300 (  0.0600)
1.2744E+06 (9.0000E+01)  100.0000 (  2.0000)
1.2900E+06 (2.0000E+02)    0.0320 (  0.0000)
1.2920E+06 (2.0000E+02)    0.0370 (  0.0000)
1.2955E+06 (2.0000E+02)    0.0110 (  0.0000)
1.3270E+06 (0.0000E+00)    0.0056 (  0.0000)
1.3870E+06 (5.0000E+02)    0.0560 (  0.0060)
1.4000E+06 (0.0000E+00)    0.0085 (  0.0028)
1.4085E+06 (2.0000E+02)    0.0590 (  0.0080)
1.4150E+06 (5.0000E+02)    0.0110 (  0.0000)
1.4185E+06 (2.0000E+02)    0.0060 (  0.0000)
1.4192E+06 (2.0000E+02)    0.0190 (  0.0050)
1.4259E+06 (5.0000E+02)    0.0037 (  0.0023)
1.4680E+06 (1.0000E+03)    0.0070 (  0.0000)
1.4896E+06 (2.0000E+02)    0.0085 (  0.0014)
1.4944E+06 (3.0000E+02)    1.8300 (  0.0600)
1.5100E+06 (5.0000E+02)    0.0140 (  0.0030)
1.5220E+06 (1.0000E+03)    0.0017 (  0.0000)
1.5220E+06 (1.0000E+03)    0.0017 (  0.0000)
```

```
1.5314E+06 (0.0000E+00)    0.0170 (  0.0010)
1.5378E+06 (0.0000E+00)    0.1400 (  0.0100)
1.5540E+06 (0.0000E+00)    0.0040 (  0.0000)
1.5930E+06 (2.0000E+02)    2.9000 (  0.3000)
1.5965E+06 (1.5000E+02)    5.1500 (  0.2600)
1.6673E+06 (0.0000E+00)    0.0056 (  0.0008)
1.6736E+06 (0.0000E+00)    0.0039 (  0.0011)
1.7169E+06 (0.0000E+00)    0.0017 (  0.0011)
1.7730E+06 (1.0000E+03)    0.0008 (  0.0006)
1.8380E+06 (5.0000E+02)    0.0023 (  0.0006)
1.8950E+06 (1.0000E+03)    0.0017 (  0.0006)
```

The F1 tally data from the outp files for ^{134}Cs, ^{137}Cs, and ^{154}Eu were obtained and summed for selected prominent emission energies. The summed tally data were then used to form DG emission ratios as a function of burnup (GWd/MTU) for ^{134}Cs/^{137}Cs, ^{134}Cs/^{154}Eu, and ^{154}Eu/^{137}Cs.

This data postprocessing process required handling 40 files and extensive amounts of data. To manage this effort, a Fortran utility code and a Perl script were written. In addition, graphics plots were created using gnuplot (Williams and Kelley, 2007). Automation of the postprocessing process streamlined the operations, eliminated errors, and facilitated reproducibility. The use of Fortran, Perl, and gnuplot ensures portability.

The Fortran code **extractt.f** was written to (1) parse the outp files;(2) locate the bins and tally data corresponding to the ^{134}Cs, ^{137}Cs, and ^{154}Eu DG lines; (3) sum the lines for these respective isotopes; (4) calculate the ratios ^{134}Cs/^{137}Cs, ^{134}Cs/^{154}Eu, and ^{154}Eu/^{137}Cs; and (5) write these three ratios to output file rtalo.
The Perl script **runrtal.pl** was created to 1) guide the execution of extractt.exe for each of the outp files; 2) input the values in the rtalo files (each contains the three ratio values); and 3) create GNUFILE files containing the ratio values for each highly enriched uranium (HEU) enrichment and for each ratio value (named crtaloe3r1, crtaloe3r2, crtaloe3r3, crtaloe5r1, crtaloe5r2, crtaleoe5r3). Execution of **runrtal.pl** for the 40 DG models requires approximately two minutes.

Plotting was done using the gnuplot utility. The gnuplot file **gnupdgbf.plt** was created and used to plot each of the crtaleo files. Results are presented next.

4.2. Fuel Assembly DG AR Analysis as a Function of Burnup

Figures 2–7 contain plots of the ^{134}Cs/^{137}Cs, ^{134}Cs/^{154}Eu, and ^{154}Eu/^{137}Cs DG ARs as a function of burnup for 3% and 5% enrichment at 3, 5, 10, 20, and 30 years following irradiation. From Table 1, the half-life of ^{134}Cs is 2.06 y; thus, the merit of the ^{134}Cs/^{137}Cs and ^{134}Cs/^{154}Eu ARs diminish after 10 years. The ^{154}Eu/^{137}Cs ratio is useful for at least 30 years post-irradiation because the ^{154}Eu half-life is 8.6 y.

Figures 8 and 9 show the DG spectra (F1 tallies) for the fuel assembly at 3- and 30-year cooling times for 3% enrichment and 20 GWd/MTU burnup. The tally data for 3-year cooling in Fig. 8 show that the photon tallies in the energy bins corresponding to the primary emission lines for ^{134}Cs and ^{154}Eu are prominent. Tallies for energy bins in the proximity of the ^{134}Cs and ^{154}Eu emission energies are nonzero. At 30-year cooling, as seen in Fig. 9, the tallies containing the

prominent ^{134}Cs and ^{154}Eu emission lines have approximately the same values as the adjacent energy bins. The adjacent energy bins likely contain contributions from nuclides emitting at these energies, as well as scattered photons. Despite this, the AR signals are well classified at late cooling times, as evidenced by the separation in AR profiles in Figs. 3 and 6.

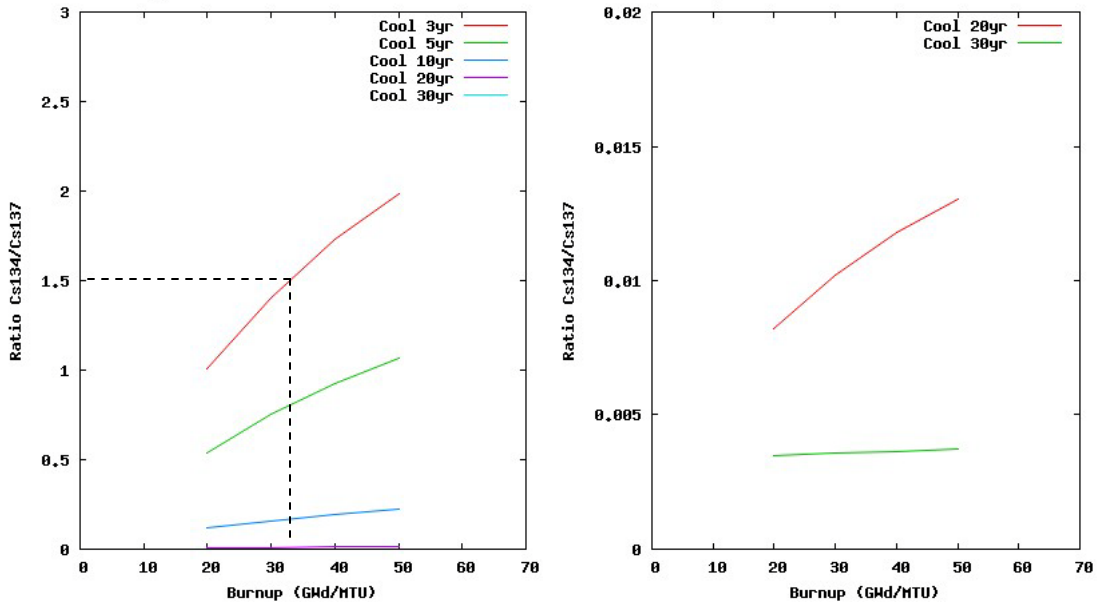

Figure 2. ^{134}Cs/^{137}Cs DG ARs as a function of burnup for 3% enrichment at 3, 5, 10, 20, and 30 years following irradiation.

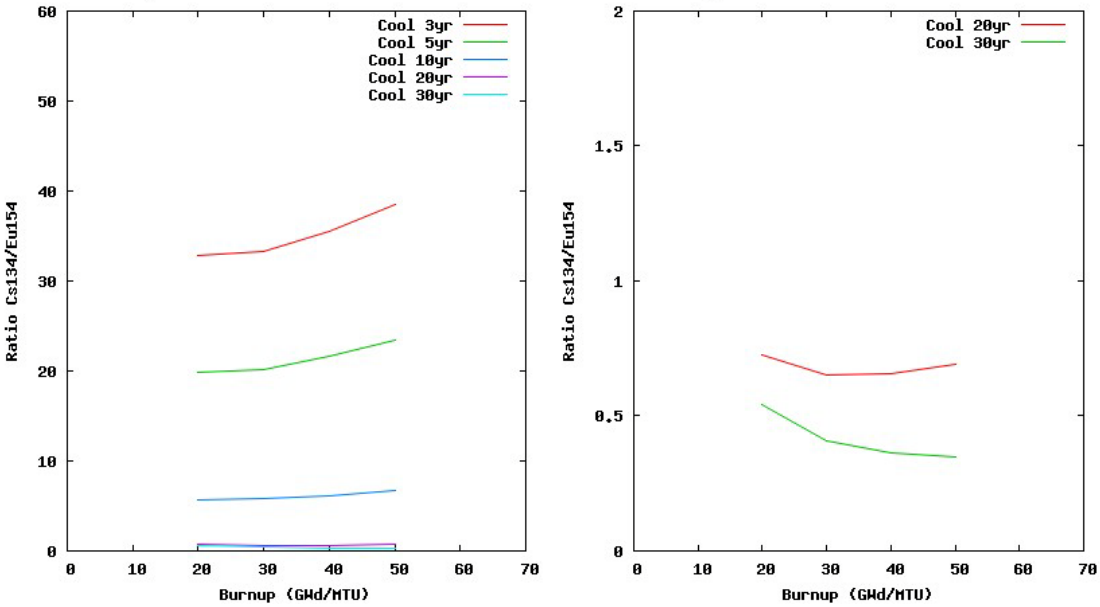

Figure 3. ^{134}Cs/^{154}Eu DG ARs as a function of burnup for 3% enrichment at 3, 5, 10, 20, and 30 years following irradiation.

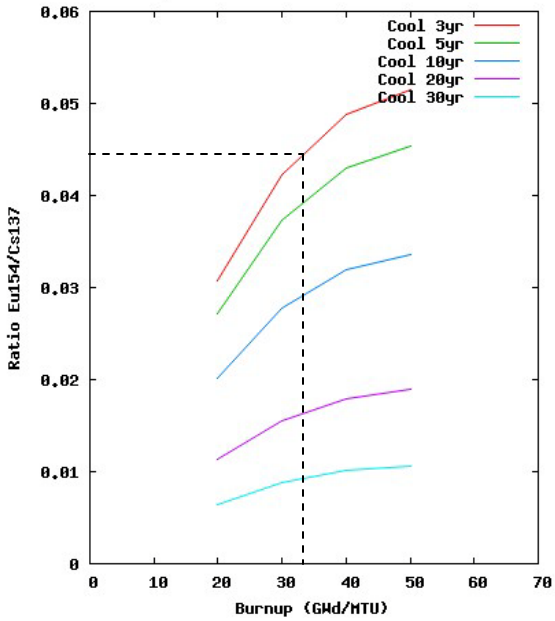

Figure 4. $^{154}Eu/^{137}Cs$ DG ARs as a function of burnup for 3% enrichment at 3, 5, 10, 20, and 30 years following irradiation.

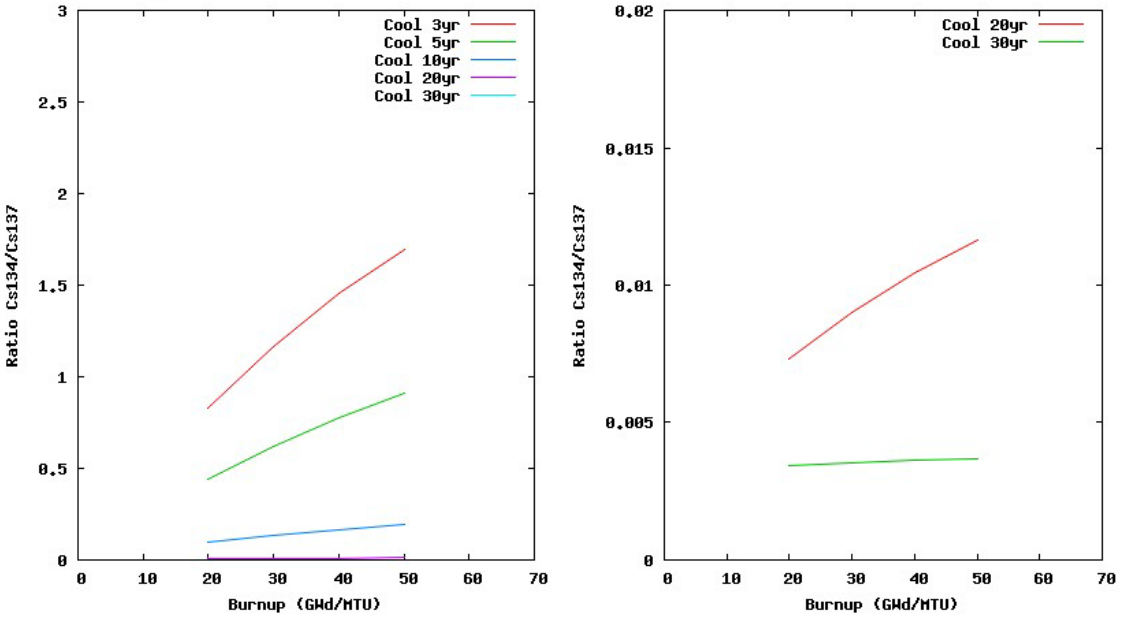

Figure 5. $^{134}Cs/^{137}Cs$ DG ARs as a function of burnup for 5% enrichment at 3, 5, 10, 20, and 30 years following irradiation.

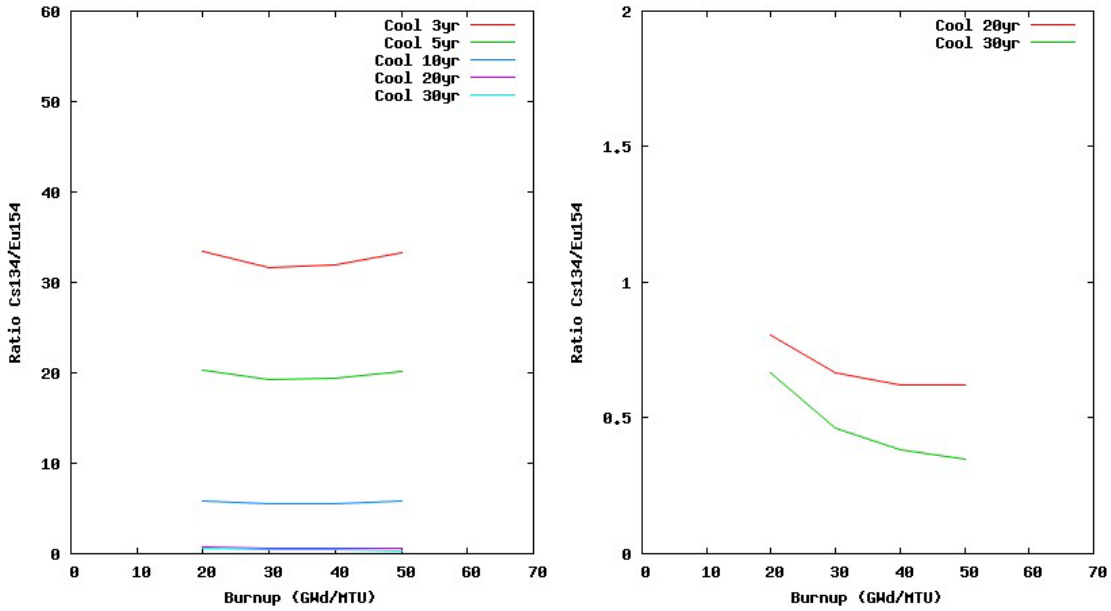

Figure 6. $^{134}Cs/^{154}Eu$ DG ARs as a function of burnup for 5% enrichment at 3, 5, 10, 20, and 30 years following irradiation.

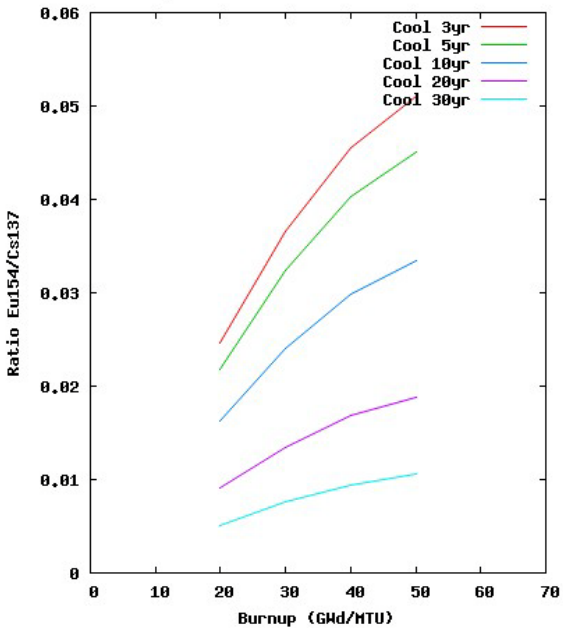

Figure 7. $^{154}Eu/^{137}Cs$ DG ARs as a function of burnup for 5% enrichment at 3, 5, 10, 20, and 30 years following irradiation.

Unambiguous determination of burnup and enrichment is done by using information from two DG ARs (Hawari and Chen, 2005). For example, if the cooling time is 3 years and the (measured) $^{134}Cs/^{137}Cs$ and $^{154}Eu/^{137}Cs$ DG ARs are 1.5 and 0.044, respectively, then Figures 2 and 4 show (dashed lines) that the initial ^{235}U enrichment is 3% and the burnup must be ~32 GWd/MTU.

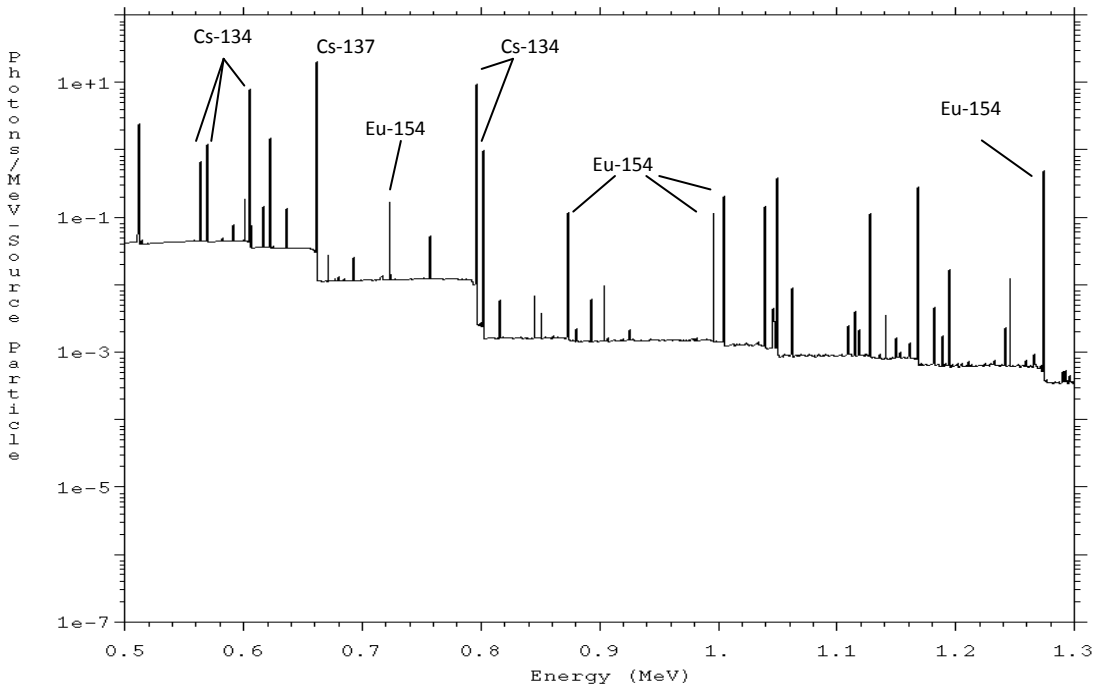

Figure 8. Delayed-gamma current for the spent fuel assembly for 3% enrichment and 20 GWd/MTU burnup at 3 years following irradiation. Prominent ^{134}Cs lines are at 0.56323, 0.56931, 0.60470, 0.79585, 0.80193 MeV. Prominent ^{154}Eu lines are at 0.72330, 0.87319, 0.99632, 1.0048, and 1.2744 MeV.

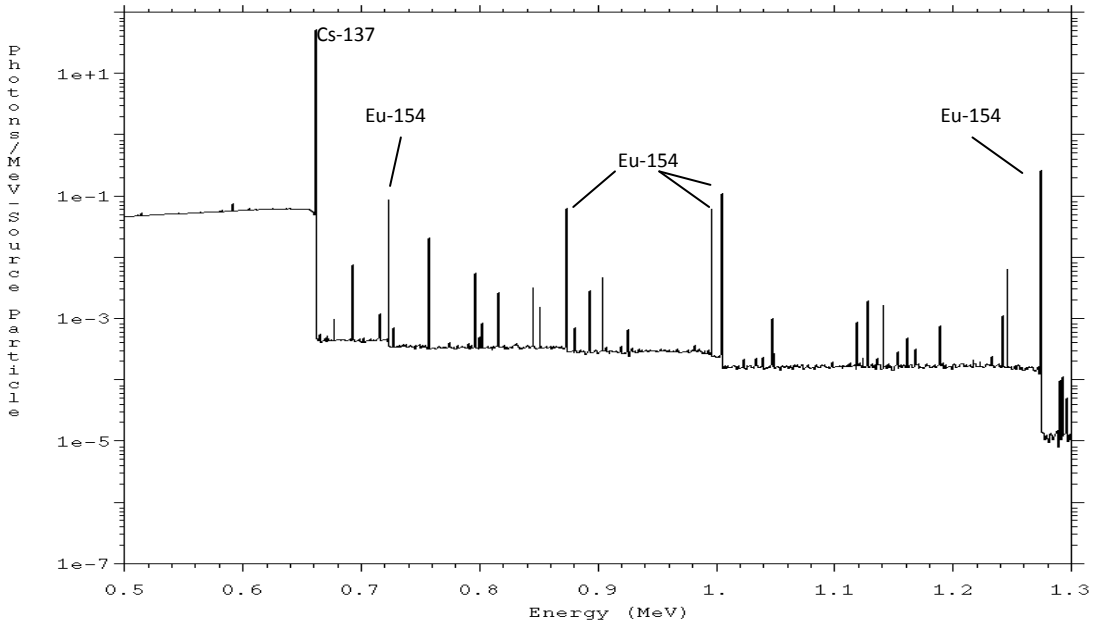

Figure 9. Delayed-gamma current for the spent fuel assembly for 3% enrichment and 20 GWd/MTU burnup at 30 years following irradiation. Because of radioactive decay, prominent ^{134}Cs lines are virtually absent, whereas the prominent ^{154}Eu lines are still apparent.

A least-squares fit of each of the profiles in Figs. 2–7 was made with a straight line using the gnuplot "fit" function. Table 3 contains the calculated slopes and their associated errors. Fits with small slopes and large errors—such as the 5% enrichment DG ARs for $^{134}Cs/^{154}Eu$ at 3-, 5-, and 10-year cooling times—are virtually horizontal profiles (see Fig. 6 left).

Table 3. Slopes of the $^{134}Cs/^{137}Cs$, $^{134}Cs/^{154}Eu$, and $^{154}Eu/^{137}Cs$ DG ARs as a Function of Burnup for 3% and 5% Enrichment at 3, 5, 10, 20, and 30 Years Following Irradiation Obtained Using gnuplot Fit Function with Line f(x)=mx+b (Data from fit.log)

Enrichment	Cooling Time (yr)	Slope and Error of Fit ("m")		
		$^{134}Cs/^{137}Cs$	$^{134}Cs/^{154}Eu$	$^{154}Eu/^{137}Cs$
3%	3	3.261e-2 +/-2.250e-3(6.9%)	1.962e-1 +/- 4.161e-2(21.2%)	6.874e-4 +/- 1.390e-3 (20.2%)
	5	1.744e-2 +/-1.203e-3(6.9%)	0.1203 +/- 2.635e-2(21.9%)	6.0304e-4 +/-1.243e-4 (20.6%)
	10	3.652e-3 +/-2.516e-4(6.9%)	3.282e-2 +/- 7.826e-3(23.8%)	4.455e-4 +/- 9.194e-5 (20.6%)
	20	1.612e-4 +/- 1.108e-5(6.9%)	-9.761e-4 +/- 1.688e-3(172.9%)	2.501e-4 +/- 5.197e-5 (20.7%)
	30	8.123e-6 +/- 5.684e-7(7.0%)	-6.2648e-3 +/- 2.021e-3(32.2%)	1.400e-4 +/- 2.975e-5 (21.2%)
5%	3	2.902e-2 +/- 1.438e-3(5.0%)	-5.52e-3 +/- 5.025e-2(910.3%)	8.800e-4 +/- 1.028e-4 (11.6%)
	5	1.553e-2 +/- 7.667e-4(4.9%)	-3.790e-3 +/- 3.023e-2(797.6%)	7.771e-4 +/- 9.018e-5 (11.6%)
	10	3.252e-3 +/- 1.600e-4(4.9%)	-3.691e-3 +/- 9.375e-3(254%)	5.773e-4 +/- 6.779e-5 (11.7%)
	20	1.450e-4 +/- 7.664e-6(5.3%)	-9.761e-4 +/- 2.180e-3(36.4%)	3.243e-4 +/- 3.834e-5 (11.8%)
	30	8.252e-6 +/- 6.072e-7(7.4%)	-6.2648e-3 +/- 2.731e-3(26.1%)	1.815e-4 +/- 2.124e-5 (11.7%)

5. 5. FUEL ASSEMBLY DG ARs VS ACTINIDE MASS FOR $^{134}Cs/^{137}Cs$, $^{134}Cs/^{154}Eu$, AND $^{154}Eu/^{137}Cs$

The preceding section presents results for DG emission ratios as a function of burnup expressed as energy obtained from fuel irradiation (GWd/MTU). A similar process was performed to provide plots of DG emission ratios as a function of burnup characterized in terms of actinide mass.

The MCNP6 isotopic actinide mass data are contained in the outp files created for the fuel-assembly kcode/burnup calculations (see Section 1). Thus, eight files were treated for the two enrichments and four burnup times.

The pertinent data were identified using a two-step process. First, print table 210, which lists neutronics and burnup data as a function of burn step, was located. The summary data are listed for (1) burn steps inclusive of the relevant flux and (2) zero-flux cooldown. For safeguards monitoring proposes, the data for spent fuel corresponding to post-irradiation zero-flux conditions is of interest. Table 4 contains the print table 210 for the 3% enrichment/20 GWd/MTU kcode/burnup model. Data for irradiation and cooldown conditions are highlighted in red and blue fonts, respectively.

Table 4. MCNP6 outp File Print Table 210 for the 3%-Enrichment/20-GWd/MTU kcode/Burnup Model

1burnup summary table by material print table 210

nuclides with atom fractions below 1.000E-10 for a material are zeroed and deleted from print tables after t=0

neutronics and burnup data

step	duration (days)	time (days)	power (MW)	keff	flux	ave. nu	ave. q (GWd/MTU)	burnup	source (nts/sec)
0	0.000E+00	0.000E+00	1.790E+01	1.25072	2.934E+14	2.459	200.985	0.000E+00	1.367E+18
1	1.300E+00	1.300E+00	1.790E+01	1.21100	3.015E+14	2.460	200.990	4.952E-02	1.367E+18
2	2.000E+01	2.130E+01	1.790E+01	1.19468	3.057E+14	2.474	201.293	8.114E-01	1.373E+18
3	3.000E+01	5.130E+01	1.790E+01	1.18313	3.092E+14	2.495	201.740	1.954E+00	1.381E+18
4	5.251E+01	1.038E+02	1.790E+01	1.16047	3.160E+14	2.525	202.383	3.954E+00	1.394E+18
5	5.251E+01	1.563E+02	1.790E+01	1.13729	3.229E+14	2.550	202.914	5.955E+00	1.404E+18
6	5.251E+01	2.088E+02	1.790E+01	1.11454	3.306E+14	2.572	203.374	7.955E+00	1.413E+18
7	5.251E+01	2.613E+02	1.790E+01	1.09398	3.376E+14	2.592	203.778	9.955E+00	1.421E+18
8	5.251E+01	3.138E+02	1.790E+01	1.07407	3.452E+14	2.611	204.145	1.196E+01	1.428E+18
9	5.251E+01	3.664E+02	1.790E+01	1.05573	3.522E+14	2.628	204.485	1.396E+01	1.435E+18
10	5.251E+01	4.189E+02	1.790E+01	1.03752	3.594E+14	2.643	204.798	1.596E+01	1.442E+18
11	5.251E+01	4.714E+02	1.790E+01	1.02123	3.664E+14	2.659	205.096	1.796E+01	1.448E+18
12	5.251E+01	5.239E+02	1.790E+01	1.00454	3.734E+14	2.673	205.372	1.996E+01	1.454E+18
13	1.170E+00	5.251E+02	1.790E+01	1.00230	3.745E+14	2.673	205.380	2.000E+01	1.454E+18
14	1.096E+03	1.621E+03	0.000E+00	1.02143	0.000E+00	0.000	0.000	2.000E+01	undefined
15	7.305E+02	2.351E+03	0.000E+00	1.01737	0.000E+00	0.000	0.000	2.000E+01	undefined
16	1.826E+03	4.178E+03	0.000E+00	1.00461	0.000E+00	0.000	0.000	2.000E+01	undefined
17	3.652E+03	7.830E+03	0.000E+00	0.99056	0.000E+00	2.500	200.000	2.000E+01	0.000E+00
18	3.652E+03	1.148E+04	0.000E+00	0.98092	0.000E+00	2.500	200.000	2.000E+01	0.000E+00

Second, print table 220, which lists isotopic actinide inventories at the end of each irradiation or cooling step, was located. The data for each cooling step are of interest. Table 5 contains the print table 220 data at the end of step 14 (the first cooling step, 3 years post-irradiation) for the 3%-enrichment/20-GWd/MTU kcode/burnup model. The isotopes and isotopic masses are listed in columns 2 and 3, respectively (highlighted in blue). For this study, uranium, neptunium, plutonium, americium, and curium data are considered.

Table 5. MCNP6 outp File Print Table 220 Actinide Inventory at the End of Step 14 for the 3%-Enrichment/20-GWd/MTU kcode/Burnup Model

actinide inventory for sum of materials at end of step 14, time 1.621E+03 (days), power 0.000E+00 (MW)

no.	zaid	mass (gm)	activity (Ci)	sp. act. (Ci/gm)	atom den. (a/b-cm)	atom fr.	mass fr.
1	90232	1.790E-04	1.963E-11	1.097E-07	9.110E-12	1.294E-10	3.359E-10
2	92233	4.125E-04	3.975E-06	9.636E-03	2.090E-11	2.968E-10	7.742E-10
3	92234	9.989E-01	6.211E-03	6.218E-03	5.041E-08	7.158E-07	1.875E-06
4	92235	6.305E+03	1.363E-02	2.161E-06	3.168E-04	4.498E-03	1.184E-02
5	92236	1.354E+03	8.757E-02	6.467E-05	6.775E-05	9.620E-04	2.542E-03
6	92238	4.489E+05	1.509E-01	3.361E-07	2.227E-02	3.162E-01	8.427E-01
7	93236	3.023E-04	3.982E-06	1.317E-02	1.512E-11	2.148E-10	5.674E-10
8	93237	1.015E+02	7.153E-02	7.047E-04	5.056E-06	7.180E-05	1.905E-04
9	94238	2.012E+01	3.445E+02	1.712E+01	9.979E-07	1.417E-05	3.776E-05
10	94239	2.289E+03	1.420E+02	6.205E-02	1.131E-04	1.606E-03	4.296E-03
11	94240	6.735E+02	1.528E+02	2.269E-01	3.313E-05	4.705E-04	1.264E-03
12	94241	3.281E+02	3.391E+04	1.033E+02	1.607E-05	2.283E-04	6.159E-04
13	94242	7.980E+01	3.157E-01	3.956E-03	3.894E-06	5.530E-05	1.498E-04
14	94244	1.554E-03	2.845E-08	1.831E-05	7.517E-11	1.067E-09	2.916E-09
15	95241	5.741E+01	1.968E+02	3.427E+00	2.812E-06	3.993E-05	1.078E-04
16	95242	3.844E-02	4.028E-01	1.048E+01	1.876E-09	2.664E-08	7.216E-08
17	95243	9.709E+00	1.938E+00	1.996E-01	4.717E-07	6.698E-06	1.822E-05
18	96242	1.545E-02	5.116E+01	3.311E+03	7.539E-10	1.070E-08	2.901E-08
19	96243	1.805E-02	9.315E-01	5.161E+01	8.770E-10	1.245E-08	3.388E-08
20	96244	1.437E+00	1.163E+02	8.095E+01	6.956E-08	9.877E-07	2.698E-06
21	96245	6.013E-02	1.032E-02	1.716E-01	2.898E-09	4.114E-08	1.129E-07
22	96246	2.636E-03	8.098E-04	3.072E-01	1.265E-10	1.797E-09	4.949E-09
	totals	4.602E+05	3.492E+04	7.589E-02	2.283E-02	3.242E-01	8.637E-01

The desired aggregate, or elemental, actinide mass was obtained by summing the isotopic masses. The elemental actinide mass was obtained for each cooling time for each of the eight models.

This data extraction and processing procedure was automated as follows. First, the Fortran code **extractm.f** was written to (1) parse the outp files to identify the cooldown steps in print table 210; (2) find the masses in print table 220 at the 3-, 5-, 10-, 20-, and 30-year post-irradiation cooling times; (3) sum the masses of the actinide isotopes to provide total (elemental) mass at each cooling time; and (4) write the elemental mass data to file totmo.[†] This utility code

[†] File totmo contains the integer cooldown data (years) and elemental actinide mass data (g). This content is suitable for easy processing using the **runmass.pl** Perl script. For easier quality assurance (QA), identical data are also written to file totmasso with ascii labeling of the quantities.

dynamically determines which actinides are present and have data in the outp file at each cooldown step.

These outp files are approximately 4 million lines long, so these files were first zipped on Pete ("gzip") to reduce storage needs. These files were then ported to the PC. Each file was unzipped ("gunzip") for data extraction. Because of the file size, several seconds were required to unzip, parse, and extract data.

Second, the Perl script **runmassp.pl** was created to streamline the execution process for **extractm.f** for DG signal ratios as a function of elemental mass. This Perl script serves to (1) unzip/zip the outp files;(2) guide the execution of extractm.exe (Fortran executable) for each of the kcode/burnup outp files; (3) input the values in the totmo files (each contains the three ratio values); and (4) create GNUFILE plot input files containing the ratio values as a function of actinide mass for each ^{235}U enrichment and for each ratio value (for plutonium, the files dgvsmPue3r1, dgvsmPue3r2, dgvsmPue3r3, dgvsmPue5r1, dgvsmPue5r2, dgvsmPue5r3, and similar names are used for the other actinides).

Because tally data from the DG sources are needed, **runmassp.pl** also contains the coding contained in **runrtal.pl**. The outp files for the assembly kcode/burnup models (see Section 1) and the DG sources (see Section 2) are stored on separate directories (for QA). Consequently, **runmassp.pl** executes **extractt.f** by changing to the directory where the DG outp files are located. The necessary tally data and ratios are obtained so that the GNUFILE files contain the DG emission ratios for ^{134}Cs/^{137}Cs, ^{134}Cs/^{154}Eu, and ^{154}Eu/^{137}Cs as a function of actinide mass.

Execution of **runmassp.pl** for the 8 kcode/burnup models and the 40 DG models requires ~20 minutes on the PC.

The following subsections contain calculated results for the ^{134}Cs/^{137}Cs, ^{134}Cs/^{154}Eu, and ^{154}Eu/^{137}Cs DG ARs as a function of elemental mass for 3% and 5% enrichment at 3, 5, 10, 20, and 30 years following irradiation. Data are reported here for uranium, neptunium, plutonium, americium, and curium. The abscissa values—i.e., the actinide masses—vary as a function of cooling time. These plots were created using **gnudgmU.plt**, **gnudgmNp.plt**, **gnudgmPu.plt**, **gnudgmAm.plt**, and **gnudgmCm.plt** for uranium, neptunium, plutonium, americium, and curium, respectively.

5.1. DG ARs as a Function of Uranium Mass

Figures 10–15 contain plots of the $^{134}Cs/^{137}Cs$, $^{134}Cs/^{154}Eu$, and $^{154}Eu/^{137}Cs$ DG ARs as a function of elemental uranium mass for 3% and 5% enrichment at 3, 5, 10, 20, and 30 years following irradiation. General features observed for ARs as a function of burnup in terms of energy obtained by fuel irradiation in the Section 4 are again observed, albeit with different profile slopes. The ^{134}Cs 2.06-year half-life limits the merit of the $^{134}Cs/^{137}Cs$ and $^{134}Cs/^{154}Eu$ ARs to approximately 10 years. The $^{154}Eu/^{137}Cs$ ratio is useful for at least 30 years post-irradiation because the ^{154}Eu half-life is 8.6 y.

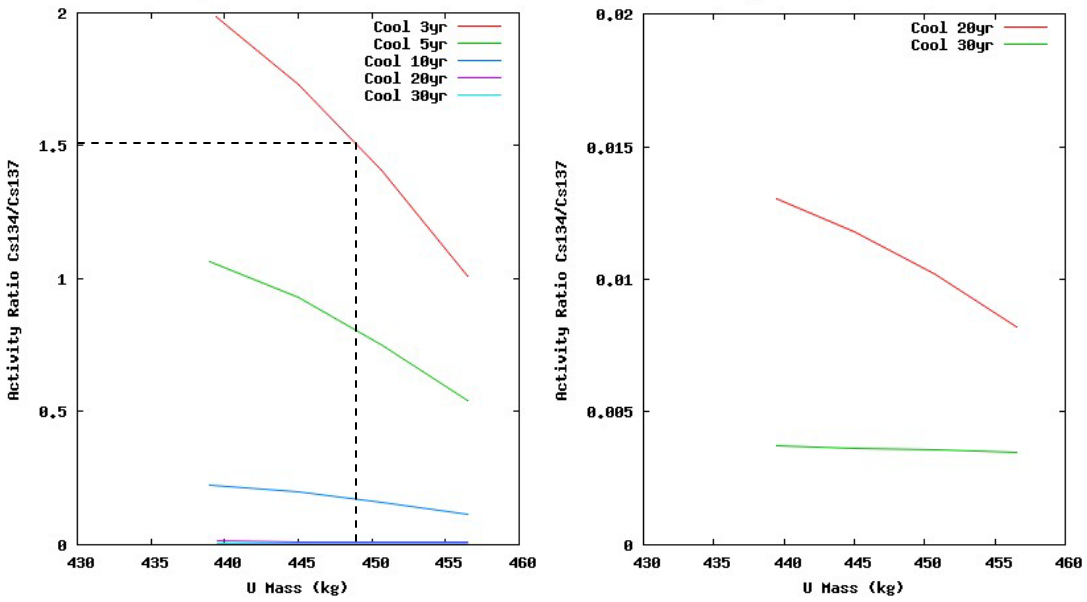

Figure 10. $^{134}Cs/^{137}Cs$ DG ARs as a function of elemental uranium mass for 3% enrichment at 3, 5, 10, 20, and 30 years following irradiation.

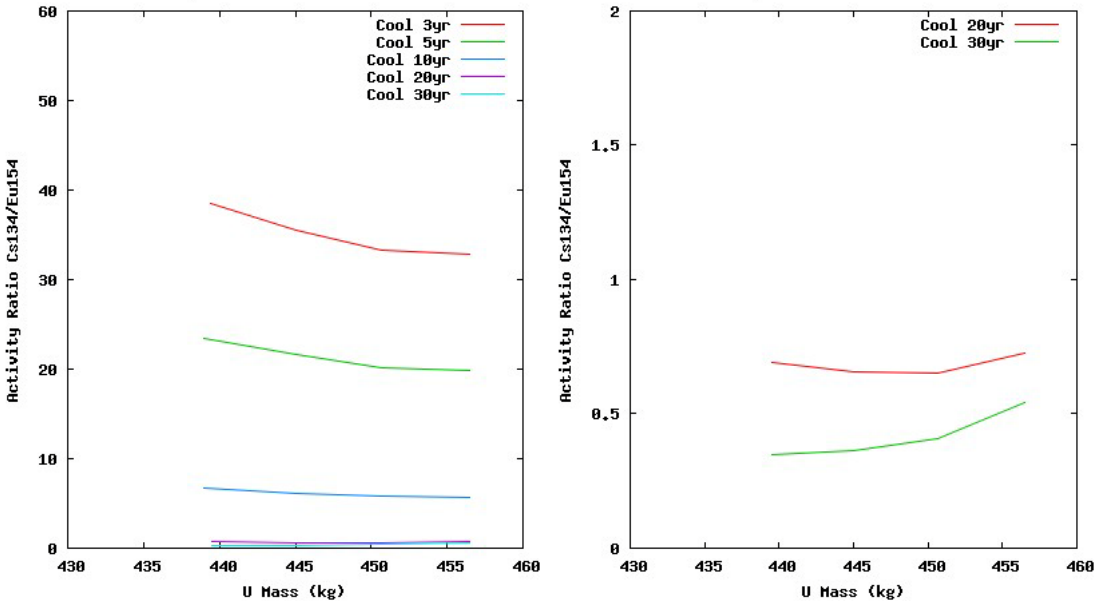

Figure 11. $^{134}Cs/^{154}Eu$ DG ARs as a function of elemental uranium mass for 3% enrichment at 3, 5, 10, 20, and 30 years following irradiation.

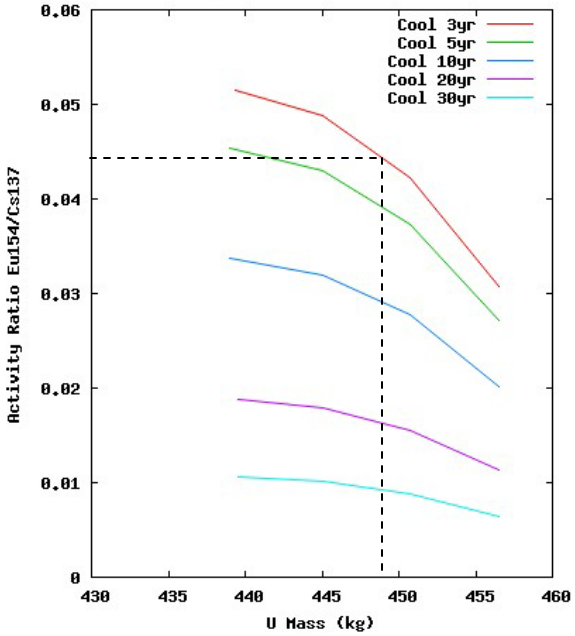

Figure 12. $^{154}Eu/^{137}Cs$ DG ARs as a function of elemental uranium mass for 3% enrichment at 3, 5, 10, 20, and 30 years following irradiation.

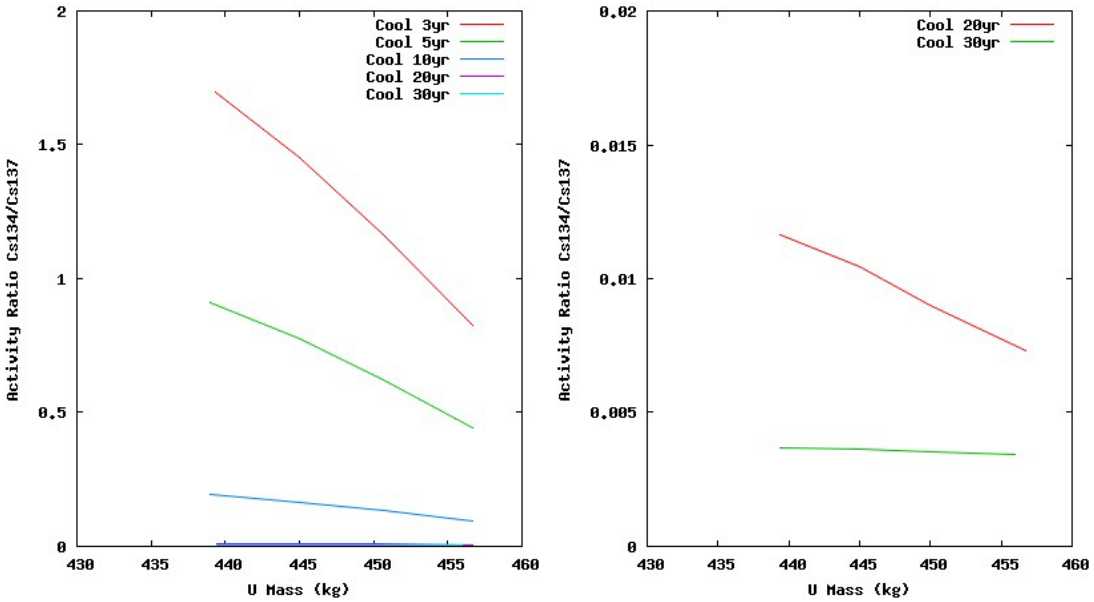

Figure 13. $^{134}Cs/^{137}Cs$ DG ARs as a function of elemental uranium mass for 5% enrichment at 3, 5, 10, 20, and 30 years following irradiation.

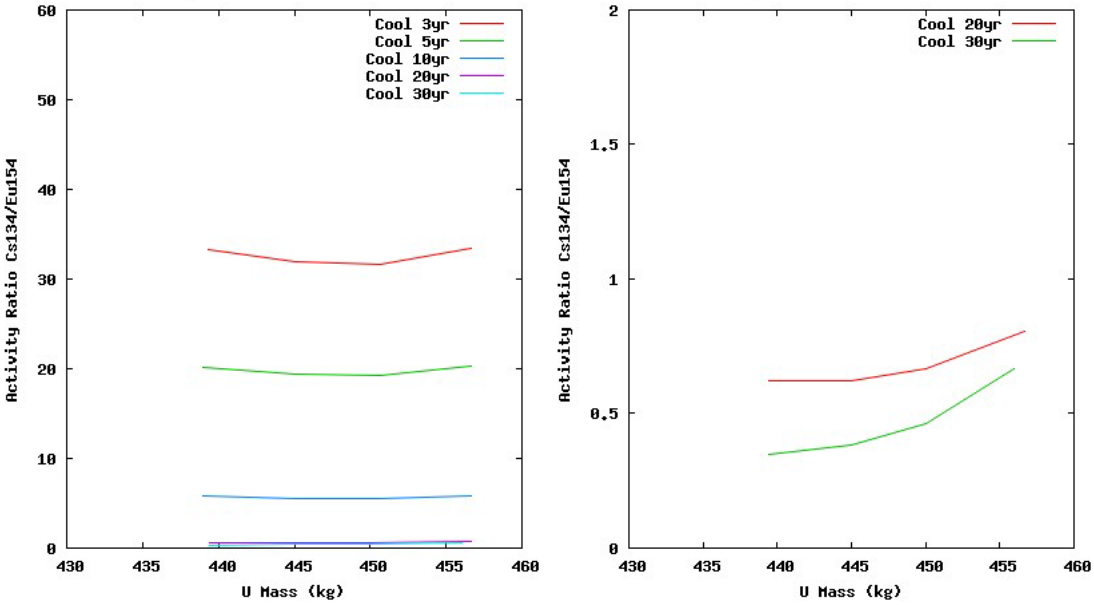

Figure 14. $^{134}Cs/^{154}Eu$ DG ARs as a function of elemental uranium mass for 5% enrichment at 3, 5, 10, 20, and 30 years following irradiation.

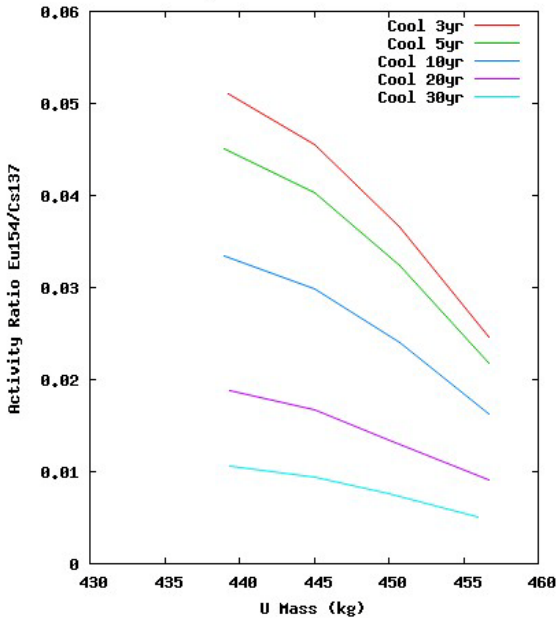

Figure 15. $^{154}Eu/^{137}Cs$ DG ARs as a function of elemental uranium mass for 5% enrichment at 3, 5, 10, 20, and 30 years following irradiation.

The elemental uranium mass can be determined once the cooling time and initial ^{235}U enrichment are determined (see previous section). For example, if the cooling time is 3 years, the initial enrichment is 3%, and the (measured) $^{134}Cs/^{137}Cs$ and $^{154}Eu/^{137}Cs$ DG ARs are 1.5 and 0.044, respectively, then Figures 10 and 12 show (dashed lines) that the elemental uranium mass is ~448 kg. This mass compares to 450.7 kg for the 30 GWd/MTU and 3 year cooling in print table 220 of the MCNP6 output file, which should be slightly more for 30 GWd/MTU than 448 kg at ~ 32 GWd/MTU.

A least-squares fit of each of the profiles in Figs.10–15 was made with a straight line using the gnuplot "fit" function with **gnudgmU.plt**. Table 6 contains the calculated slope and its associated error for the $^{134}Cs/^{137}Cs$, $^{134}Cs/^{154}Eu$, and $^{154}Eu/^{137}Cs$ DG ARs as a function of total uranium mass.

Table 6. Slopes of the $^{134}Cs/^{137}Cs$, $^{134}Cs/^{154}Eu$, and $^{154}Eu/^{137}Cs$ DG ARs as a Function of Total Uranium Mass for 3% and 5% Enrichment at 3, 5, 10, 20, and 30 Years Following Irradiation Obtained Using gnuplot Fit Function with line f(x)=mx+b (Data from fit.log)

Enrichment	Cooling Time (yr)	Slope and Error of Fit ("m")		
		$^{134}Cs/^{137}Cs$	$^{134}Cs/^{154}Eu$	$^{154}Eu/^{137}Cs$
3%	3	4.693e-4 +/- 1.018e-5(2.1%)	2.683e-3 +/- 8.406e-4(31.3%)	-6.345e-3 +/- 1.246e-3 (19.6%)
	5	2.510e-4 +/- 5.446e-6(2.1%)	1.643e-3 +/- 5.272e-4(32.0%)	-7.168e-3 +/- 1.431e-3 (19.9%)
	10	5.256e-5 +/- 1.146e-6(2.1%)	4.467e-4 +/- 1.528e-4(34.2%)	-9.602e-3 +/- 1.918e-3 (19.9%)
	20	2.320e-6 +/- 5.026e-8(2.1%)	-1.814e-5 +/- 2.276e-5(125.4%)	-1.71314e-2 +/- 3.432e-3 (20.0%)
	30	1.169e-7 +/- 2.286e-9(1.9%)	-9.416e-5 +/- 2.083e-5(22.1%)	-3.029e-2 +/- 6.146e-3 (20.2%)
5%	3	3.679e-4 +/- 1.179e-5(3.2%)	-1.723e-4 +/- 6.261e-4(363.4%)	-8.924e-3 +/- 1.518e-3 (17.0%)
	5	1.969e-4 +/- 6.343e-6(3.2%)	-1.095e-4 +/- 3.762e-4(343.3%)	-1.009e-2 +/- 1.707e-3 (16.9%)
	10	4.122e-5 +/- 1.334e-6(3.2%)	-6.560e-5 +/- 1.141e-4(173.9%)	-1.3585e-2 +/- 2.315e-3 (17.0%)
	20	1.839e-6 +/- 5.244e-8(2.8%)	-7.954e-5 +/- 2.133e-5(26.8%)	-2.428e-2 +/- 4.159e-3 (17.1%)
	30	1.049e-7 +/- 9.418e-10(0.9%)	-1.36678e-4 +/- 2.381e-5(17.4%)	-4.277e-2 +/- 7.29e-3 (17.0%)

5.2. DG ARs as a Function of Neptunium Mass

Figures 16–21 contain plots of the $^{134}Cs/^{137}Cs$, $^{134}Cs/^{154}Eu$, and $^{154}Eu/^{137}Cs$ DG ARs as a function of elemental neptunium mass for 3% and 5% enrichment at 3, 5, 10, 20, and 30 years following irradiation.

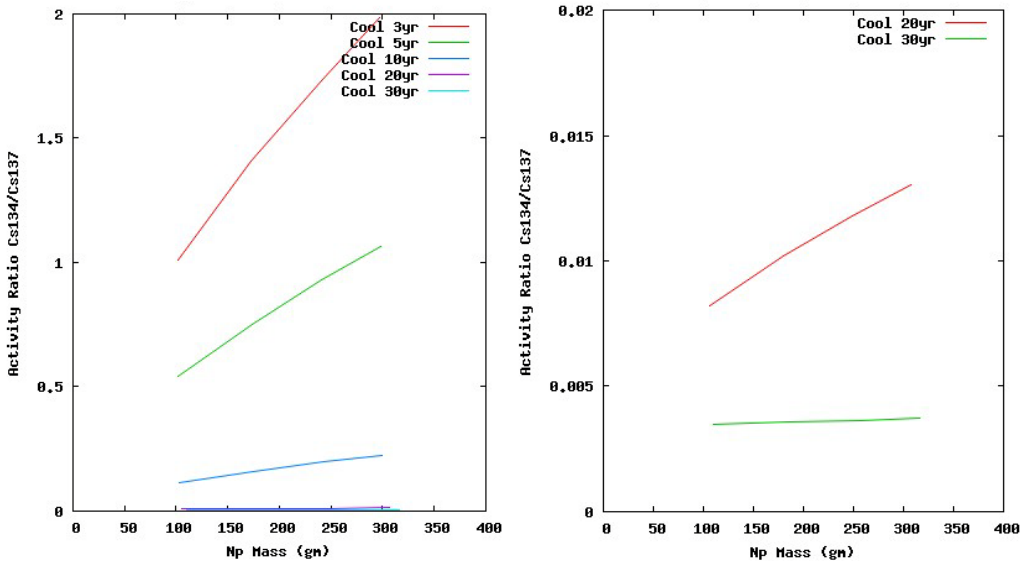

Figure 16. $^{134}Cs/^{137}Cs$ DG ARs as a function of elemental neptunium mass for 3% enrichment at 3, 5, 10, 20, and 30 years following irradiation.

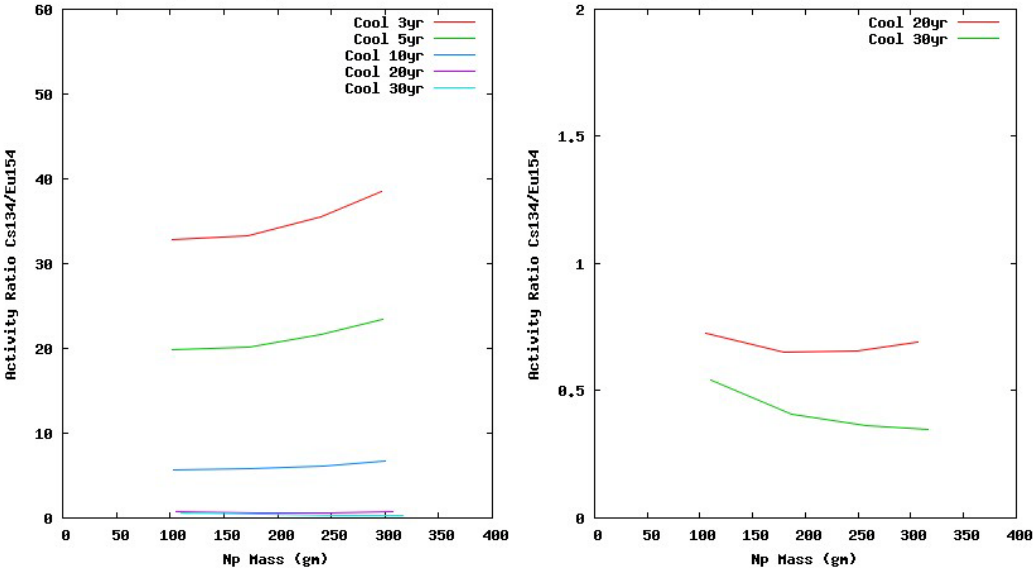

Figure 17. $^{134}Cs/^{154}Eu$ DG ARs as a function of elemental neptunium mass for 3% enrichment at 3, 5, 10, 20, and 30 years following irradiation.

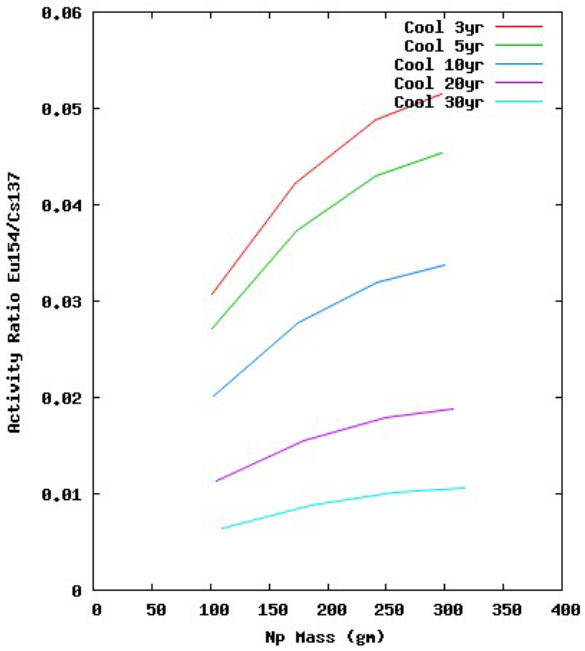

Figure 18. $^{154}Eu/^{137}Cs$ DG ARs as a function of elemental neptunium mass for 3% enrichment at 3, 5, 10, 20, and 30 years following irradiation.

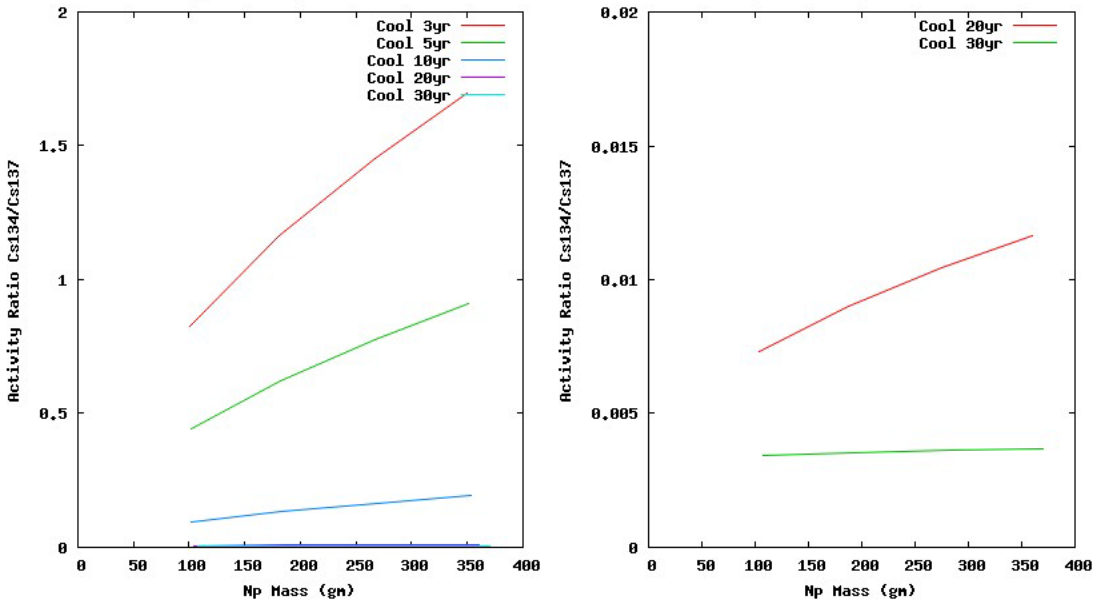

Figure 19. $^{134}Cs/^{137}Cs$ DG ARs as a function of elemental neptunium mass for 5% enrichment at 3, 5, 10, 20, and 30 years following irradiation.

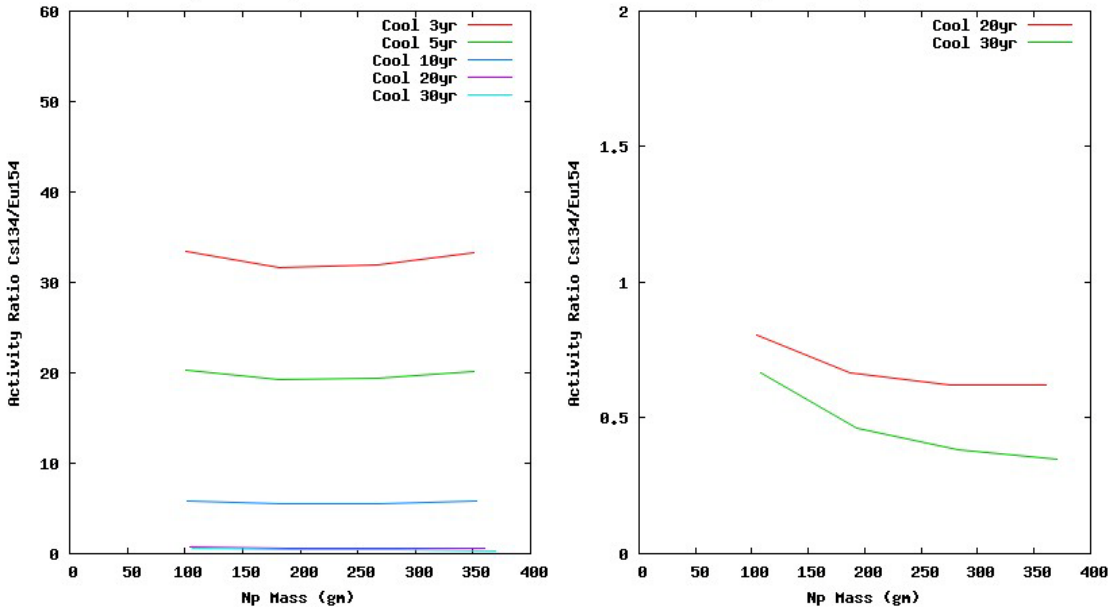

Figure 20. $^{134}Cs/^{154}Eu$ DG ARs as a function of elemental neptunium mass for 5% enrichment at 3, 5, 10, 20, and 30 years following irradiation.

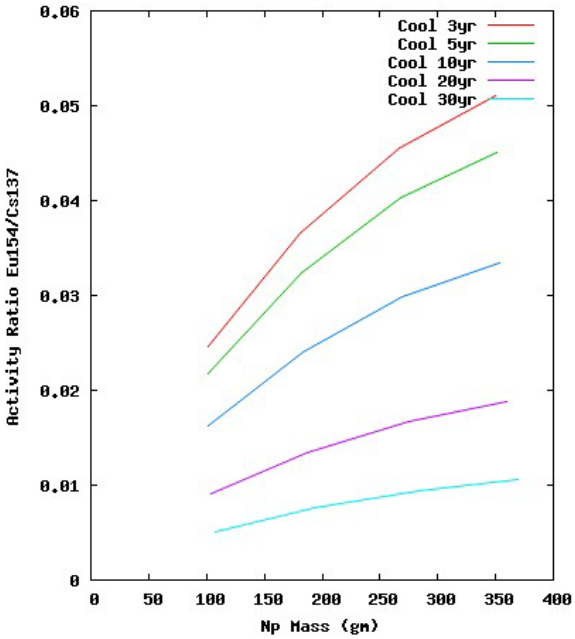

Figure 21. $^{154}Eu/^{137}Cs$ DG ARs as a function of elemental neptunium mass for 5% enrichment at 3, 5, 10, 20, and 30 years following irradiation.

A least-squares fit of each of the profiles in Figs. 16–21 was made with a straight line using the gnuplot "fit" function using gnupdgNp.plt. Table 7 contains the calculated slope and its associated error for the $^{134}Cs/^{137}Cs$, $^{134}Cs/^{154}Eu$, and $^{154}Eu/^{137}Cs$ DG ARs as a function of total neptunium mass.

Table 7. Slopes of the $^{134}Cs/^{137}Cs$, $^{134}Cs/^{154}Eu$, and $^{154}Eu/^{137}Cs$ DG ARs as a Function of Total Neptunium Mass for 3% and 5% Enrichment at 3, 5, 10, 20, and 30 Years Following Irradiation Obtained Using gnuplot Fit Function with line f(x)=mx+b (data from fit.log)

Enrichment	Cooling Time (yr)	Slope and Error of Fit ("m")		
		$^{134}Cs/^{137}Cs$	$^{134}Cs/^{154}Eu$	$^{154}Eu/^{137}Cs$
3%	3	4.991e-3 +/- 1.722e-4(3.4%)	2.947e-2 +/- 0.007343(24.9%)	1.062e-4 +/- 1.757e-5 (16.5%)
	5	2.666e-3 +/- 9.068e-5(3.4%)	1.802e-2 +/- 4.659e-3(25.8%)	9.307e-5 +/- 1.573e-5 (16.9%)
	10	5.554e-4 +/- 1.871e-5(3.3%)	4.882e-3 +/- 1.354e-3(27.7%)	6.839e-5 +/- 1.152e-5 (16.8%)
	20	2.402e-5 +/- 7.745e-7(3.2%)	-1.626e-4 +/- 2.452e-4(150.8%)	3.762e-5 +/- 6.331e-6 (16.8%)
	30	1.180e-6 +/- 3.700e-8 (3.1%)	-9.274e-4 +/- 2.578e-4(27.8%)	2.058e-5 +/- 3.499e-6 (17%)
5%	3	3.481e-3 +/- 1.926e-4(5.5%)	-5.894e-4 +/- 6.053e-3(1027%)	1.054e-4 +/- 1.288e-5 (12.2%)
	5	1.860e-3 +/- 1.021e-4(5.4%)	-4.376e-4 +/- 3.617e-3(826.5%)	9.298e-5 +/- 1.129e-5 (12.1%)
	10	3.870e-4 +/- 2.101e-5(5.4%)	-4.276e-4 +/- 1.118e-3(261.4%)	6.866e-5 +/- 8.39e-6 (12.2%)
	20	1.695e-5 +/- 9.50e-7(5.6%)	-6.956e-4 +/- 2.577e-4(37.0%)	3.785e-5 +/- 4.597e-6 (12.1%)
	30	9.408e-7 +/- 7.03e-8(7.4%)	-1.186e-3 +/- 3.146e-4(26.5%)	2.067e-5 +/- 2.454e-6 (11.8%)

5.3. DG ARs as a Function of Plutonium Mass

Figures 22–27 contain plots of the $^{134}Cs/^{137}Cs$, $^{134}Cs/^{154}Eu$, and $^{154}Eu/^{137}Cs$ DG ARs as a function of elemental plutonium mass for 3% and 5% enrichment at 3, 5, 10, 20, and 30 years following irradiation.

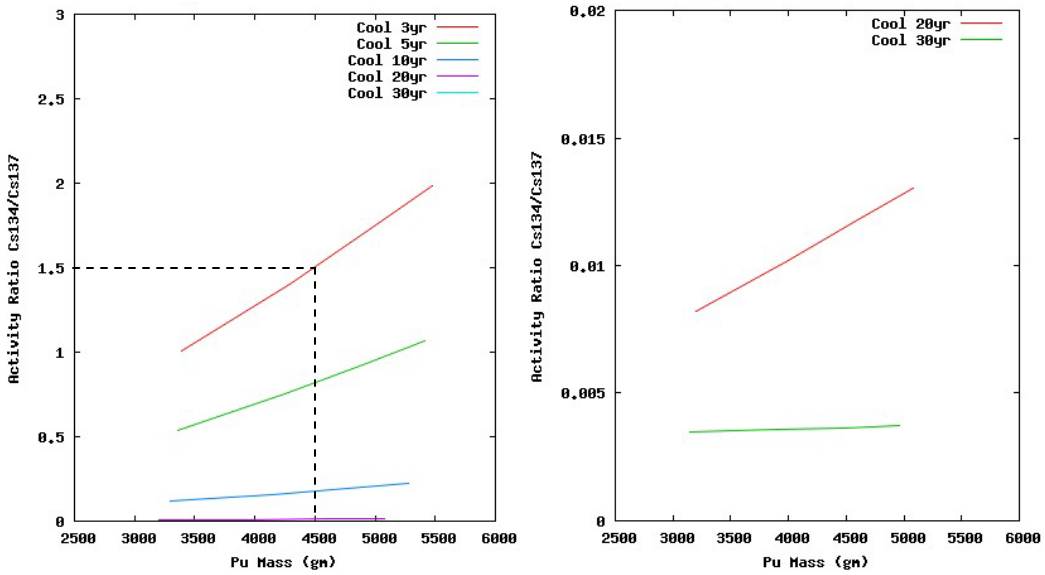

Figure 22. $^{134}Cs/^{137}Cs$ DG ARs as a function of elemental plutonium mass for 3% enrichment at 3, 5, 10, 20, and 30 years following irradiation.

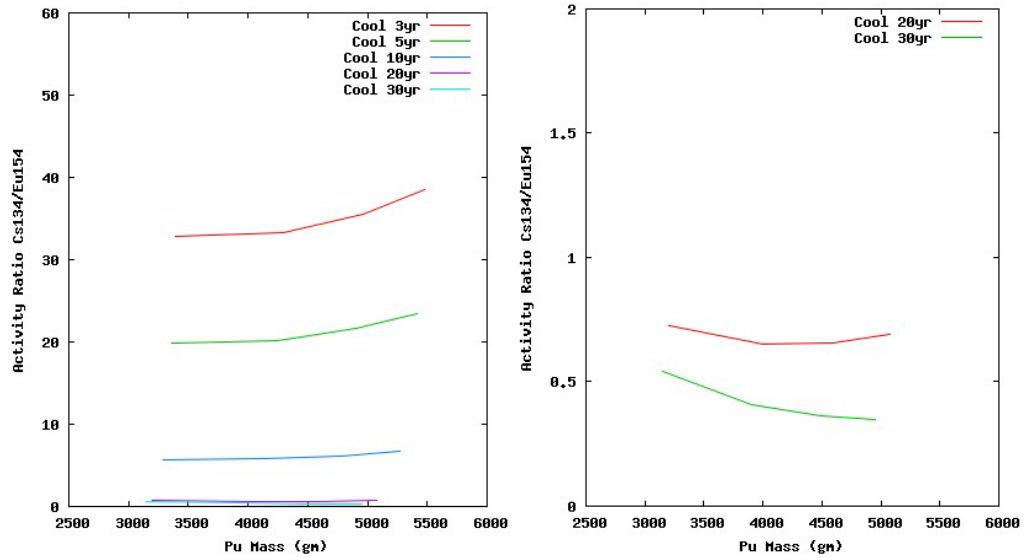

Figure 23. $^{134}Cs/^{154}Eu$ DG ARs as a function of elemental plutonium mass for 3% enrichment at 3, 5, 10, 20, and 30 years following irradiation.

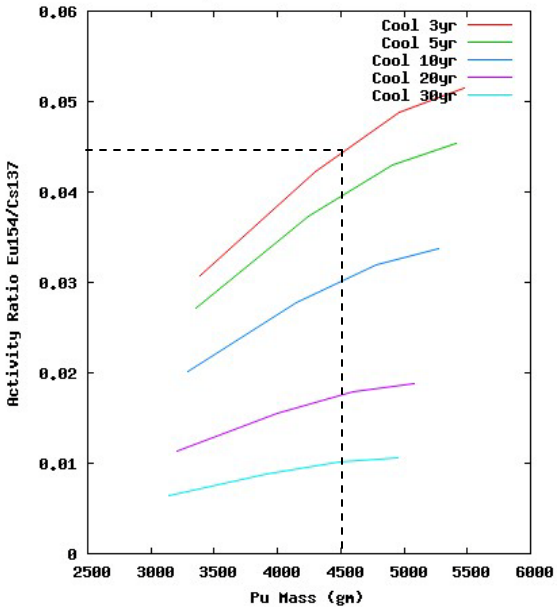

Figure 24. $^{154}Eu/^{137}Cs$ DG ARs as a function of elemental plutonium mass for 3% enrichment at 3, 5, 10, 20, and 30 years following irradiation.

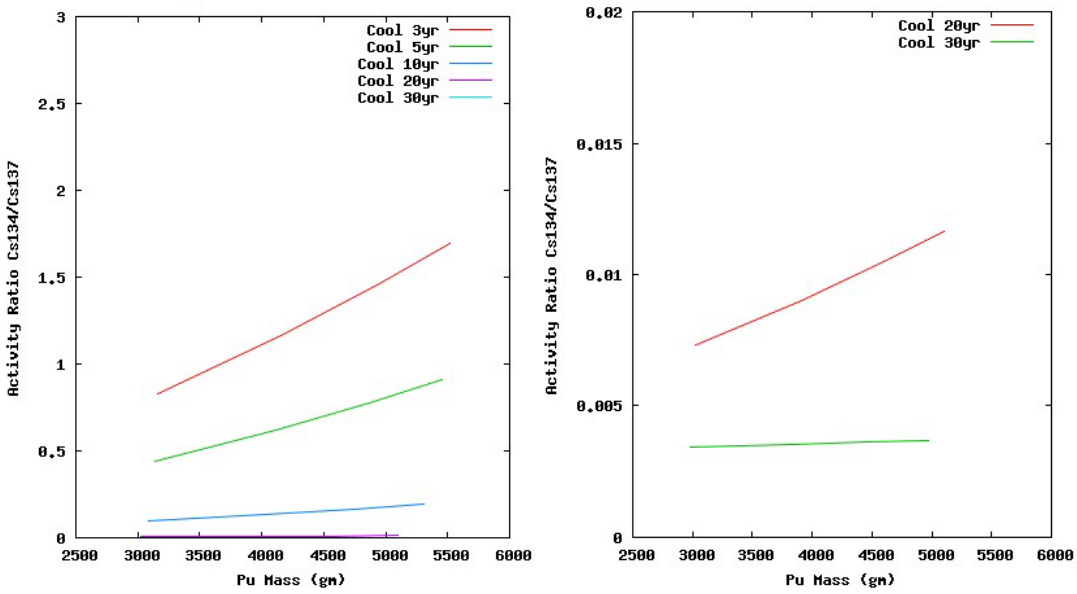

Figure 25. $^{134}Cs/^{137}Cs$ DG ARs as a function of elemental plutonium mass for 5% enrichment at 3, 5, 10, 20, and 30 years following irradiation.

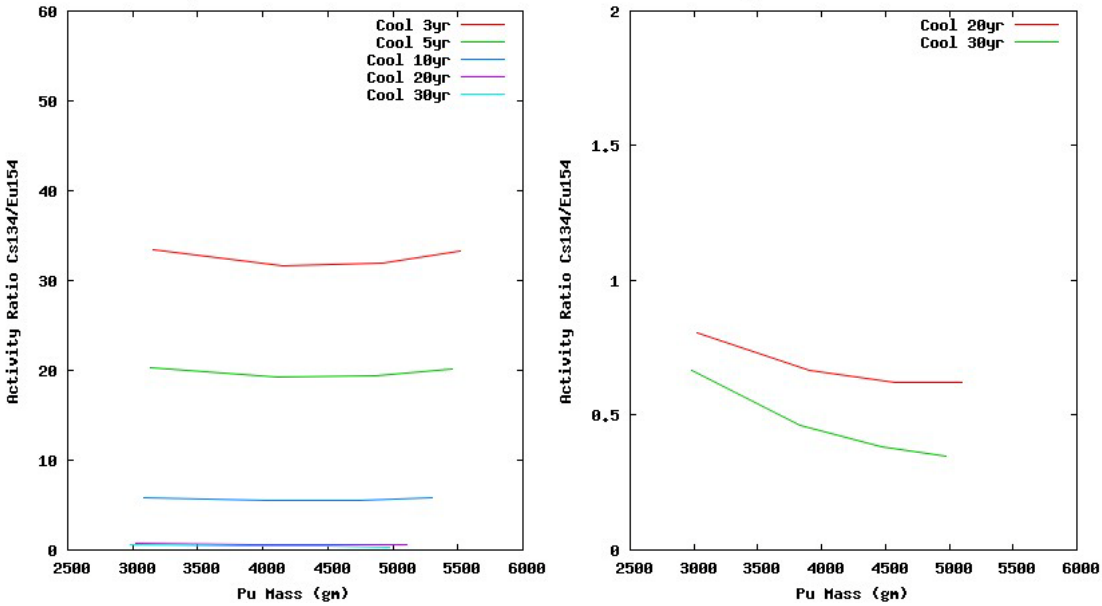

Figure 26. $^{134}Cs/^{154}Eu$ DG ARs as a function of elemental plutonium mass for 5% enrichment at 3, 5, 10, 20, and 30 years following irradiation.

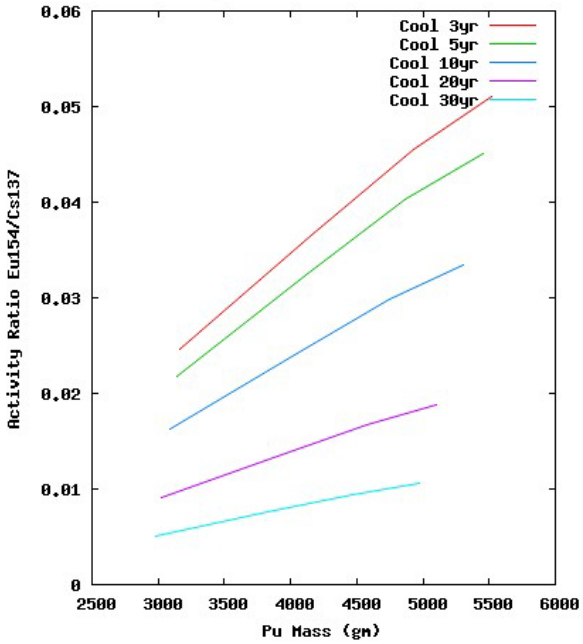

Figure 27. $^{154}Eu/^{137}Cs$ DG ARs as a function of elemental plutonium mass for 5% enrichment at 3, 5, 10, 20, and 30 years following irradiation.

The elemental plutonium mass can be determined once the cooling time and initial ^{235}U enrichment are determined (see Section 4.2). For example, if the cooling time is 3 years, the initial enrichment is 3%, and the (measured) $^{134}Cs/^{137}Cs$ and $^{154}Eu/^{137}Cs$ DG ARs are 1.5 and 0.044, respectively, then Figures 22 and 24 show (dashed lines) that the elemental plutonium mass is ~4500 g. This mass compares to 4295 g for the 30 GWd/MTU and 3 year cooling in print

table 220 of the MCNP6 output file, which should be slightly less for 30 GWd/MTU than 4500 g at ~ 32 GWd/MTU.

A least-squares fit of each of the profiles in Figs. 20–25 was made with a straight line using the gnuplot "fit" function using **gnudgmPu.plt**. Table 8 contains the calculated slope and its associated error for the $^{134}Cs/^{137}Cs$, $^{134}Cs/^{154}Eu$, and $^{154}Eu/^{137}Cs$ DG ARs as a function of total plutonium mass.

Table 8. Slopes of the $^{134}Cs/^{137}Cs$, $^{134}Cs/^{154}Eu$, and $^{154}Eu/^{137}Cs$ DG ARs as a Function of Total Plutonium Mass for 3% and 5% Enrichment at 3, 5, 10, 20, and 30 Years Following Irradiation Obtained Using gnuplot Fit Function with line f(x)=mx+b (data from fit.log)

Enrichment	Cooling Time (yr)	Slope and Error of Fit ("m")		
		$^{134}Cs/^{137}Cs$	$^{134}Cs/^{154}Eu$	$^{154}Eu/^{137}Cs$
3%	3	4.691e-4 +/- 1.005e-5 (2.1%)	2.684e-3 +/- 8.394e-4 (31.2%)	4.691e-4 +/- 1.005e-5 (2.1%)
	5	2.552e-4 +/- 5.216e-6 (2.0%)	1.672e-3 +/- 5.367e-4(32.1%)	2.552e-4 +/- 5.216e-6 (2.0%)
	10	5.540e-5 +/- 1.006e-6 (1.8%)	4.717e-4 +/- 1.593e-4(33.7%)	5.540e-5 +/- 1.006e-6 (1.8%)
	20	2.584e-6 +/- 3.460e-8 (1.3%)	-1.977e-5 +/- 2.553e-5(129.1%)	2.584e-6 +/- 3.46e-8 (1.3%)
	30	1.349e-7 +/- 1.193e-9 (0.8%)	-1.08104e-4 +/- 2.525e-5 (23.3%)	1.349e-7 +/- 1.193e-9 (0.8%)
5%	3	3.677e-4 +/- 1.169e-5 (3.1%)	-1.722e-4 +/- 6.279e-4(364.5%)	1.012e-5 +/- 1.104e-6 (10.9%)
	5	2.007e-4 +/- 6.469e-6 (3.2%)	-1.143e-4 +/- 3.827e-4(334.8%)	9.038e-6 +/- 1.028e-6 (11.3%)
	10	4.389e-5 +/- 1.446e-6 (3.2%)	-6.999e-5 +/- 1.214e-4(173.4%)	6.915e-6 +/- 8.048e-7 (11.6%)
	20	2.089e-6 +/- 6.327e-8 (3.0%)	-9.037e-5 +/- 2.41e-5 (26.6%)	4.095e-6 +/- 5.046e-7 (12.3%)
	30	1.247e-7 +/- 1.475e-9 (1.1%)	-1.623e-4 +/- 2.79e-5 (17.1%)	2.378e-6 +/- 3.107e-7 (13.0%)

5.4. DG ARs as a Function of Americium Mass

Figures 28–33 contain plots of the $^{134}Cs/^{137}Cs$, $^{134}Cs/^{154}Eu$, and $^{154}Eu/^{137}Cs$ DG ARs as a function of elemental americium mass for 3% and 5% enrichment at 3, 5, 10, 20, and 30 years following irradiation.

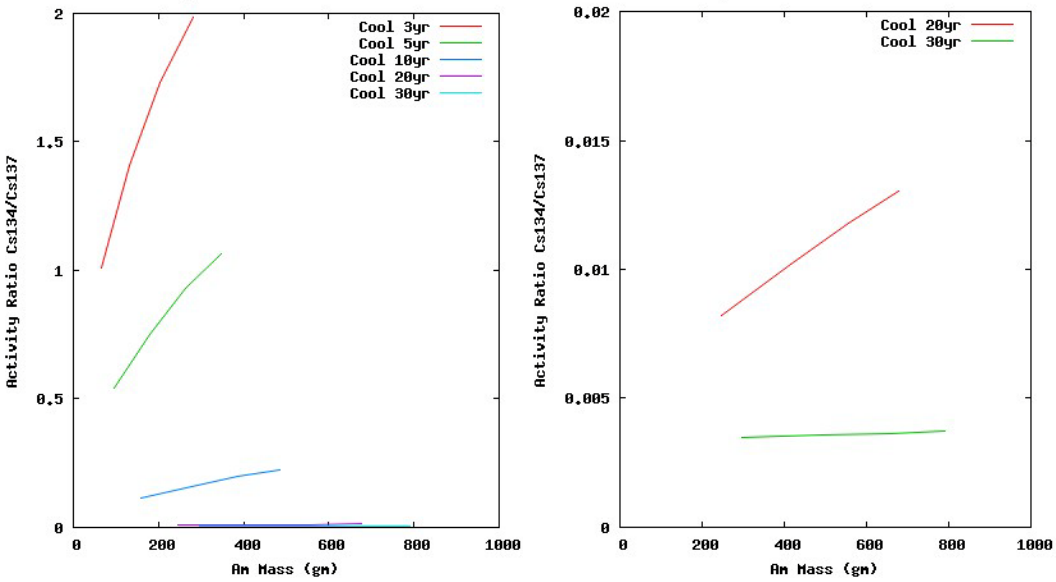

Figure 28. $^{134}Cs/^{137}Cs$ DG ARs as a function of elemental americium mass for 3% enrichment at 3, 5, 10, 20, and 30 years following irradiation.

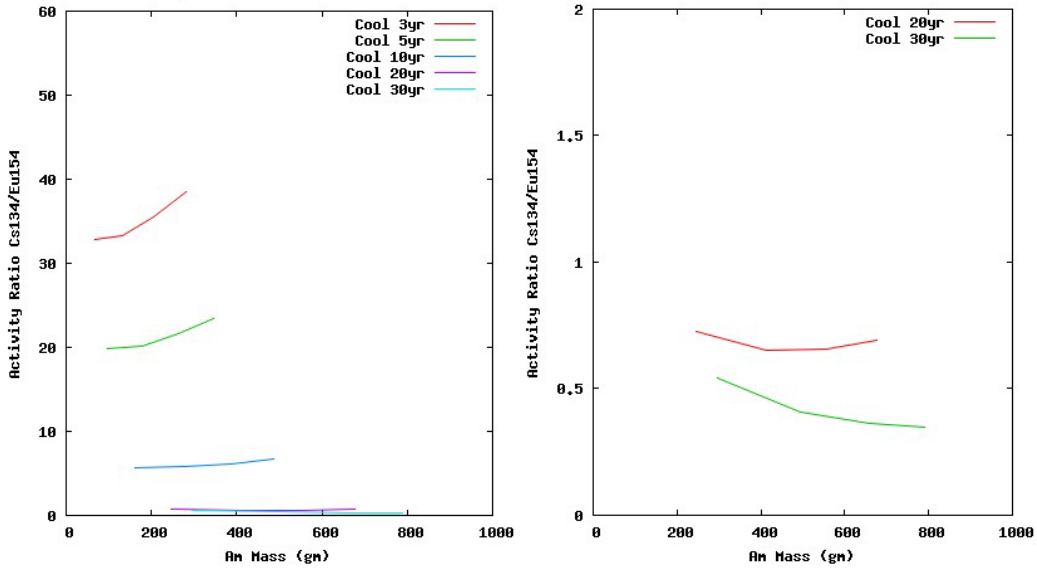

Figure 29. $^{134}Cs/^{154}Eu$ DG ARs as a function of elemental americium mass for 3% enrichment at 3, 5, 10, 20, and 30 years following irradiation.

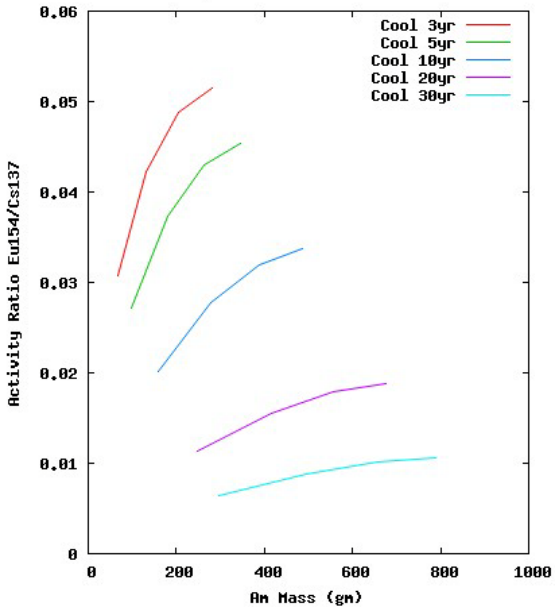

Figure 30. $^{154}Eu/^{137}Cs$ DG ARs as a function of elemental americium mass for 3% enrichment at 3, 5, 10, 20, and 30 years following irradiation.

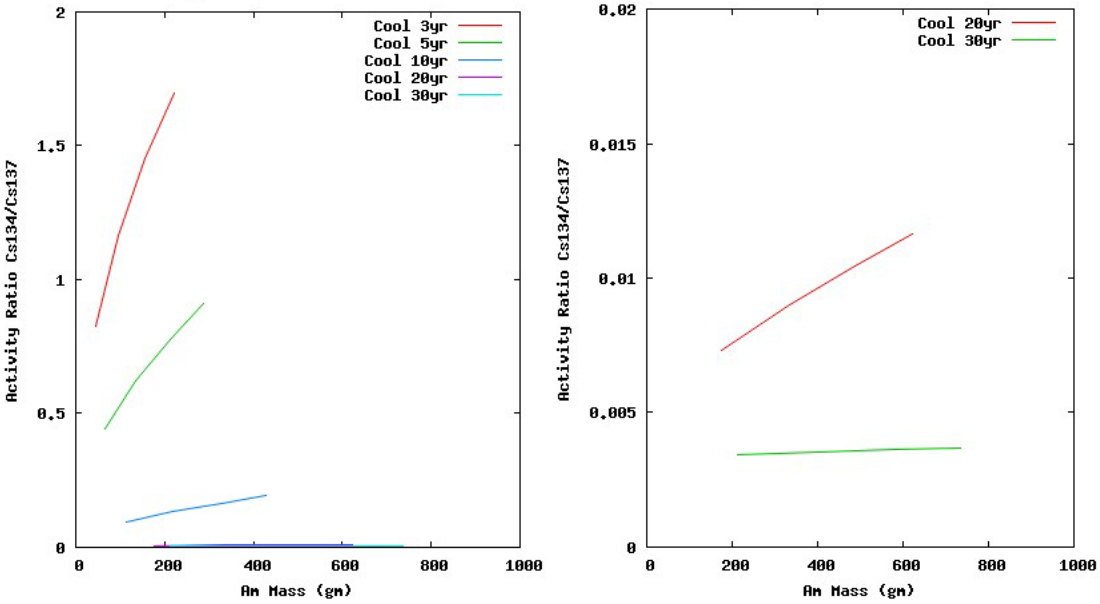

Figure 31. $^{134}Cs/^{137}Cs$ DG ARs as a function of elemental americium mass for 5% enrichment at 3, 5, 10, 20, and 30 years following irradiation.

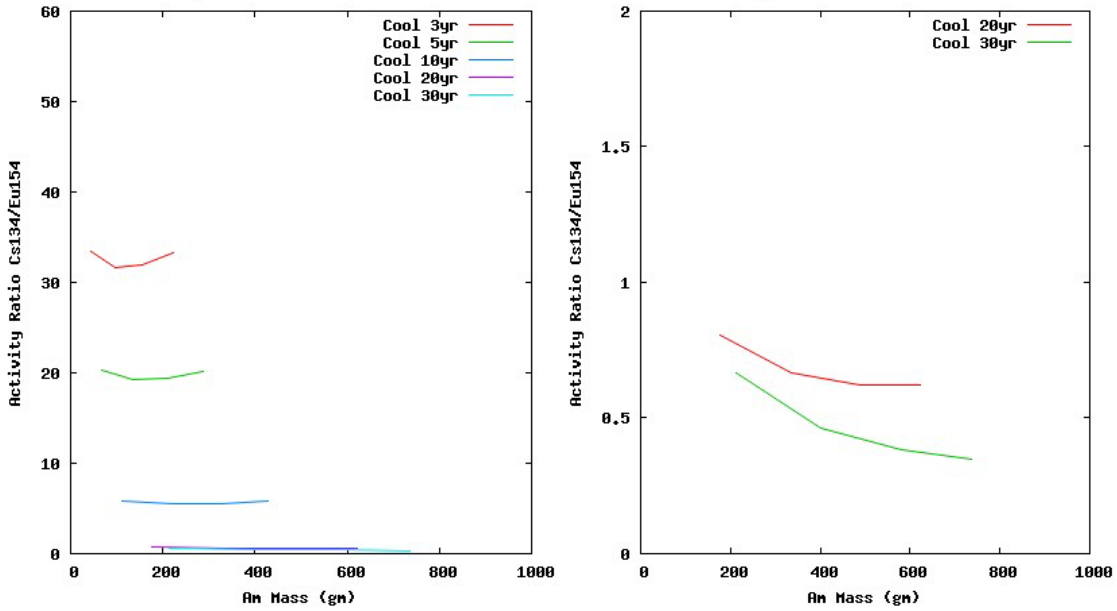

Figure 32. $^{134}Cs/^{154}Eu$ DG ARs as a function of elemental americium mass for 5% enrichment at 3, 5, 10, 20, and 30 years following irradiation.

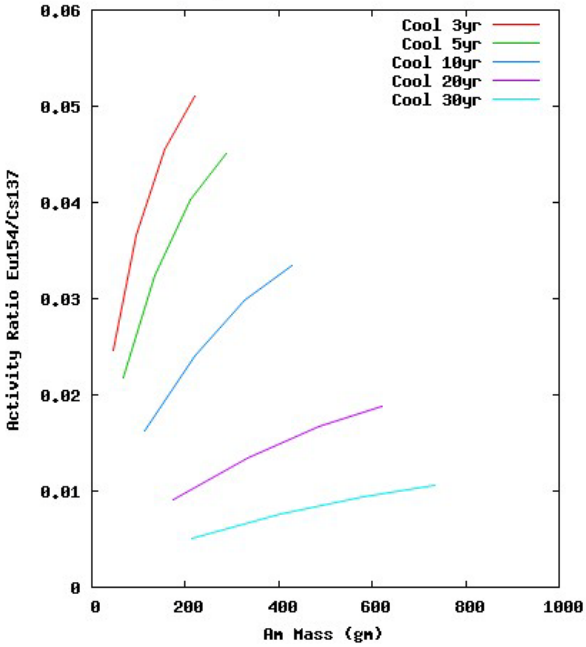

Figure 33. $^{154}Eu/^{137}Cs$ DG ARs as a function of elemental americium mass for 5% enrichment at 3, 5, 10, 20, and 30 years following irradiation.

A least-squares fit of each of the profiles in Figs. 28–33 was made with a straight line using the gnuplot "fit" function with gnudgmAm.plt. Table 9 contains the calculated slope and its associated error for the $^{134}Cs/^{137}Cs$, $^{134}Cs/^{154}Eu$, and $^{154}Eu/^{137}Cs$ DG ARs as a function of total americium mass.

Table 9. Slopes of the $^{134}Cs/^{137}Cs$, $^{134}Cs/^{154}Eu$, and $^{154}Eu/^{137}Cs$ DG ARs as a Function of Total Americium Mass for 3% and 5% Enrichment at 3, 5, 10, 20, and 30 Years Following Irradiation Obtained Using gnuplot Fit Function with line f(x)=mx+b (data from fit.log)

Enrichment	Cooling Time (yr)	Slope and Error of Fit ("m")		
		$^{134}Cs/^{137}Cs$	$^{134}Cs/^{154}Eu$	$^{154}Eu/^{137}Cs$
3%	3	4.555e-3 +/-4.318e-4(9.4%)	2.781e-2 +/- 5.119e-3(18.4%)	9.540e-5 +/- 2.194e-5 (23%)
	5	2.092e-3 +/- 1.493e-4(7.1%)	1.445e-2 +/- 3.144e-3(21.7%)	7.232e-5 +/- 1.51e-5 (20.8%)
	10	3.370e-4 +/- 1.343e-5(3.9%)	2.973e-3 +/- 8.051e-4(27.0%)	4.144e-5 +/- 7.249e-6 (17.4%)
	20	1.126e-5 +/- 1.732e-7(1.5%)	-8.007e-5 +/- 1.135e-4(141.7%)	1.771e-5 +/- 2.67e-6 (15.0%)
	30	4.959e-7 +/- 3.323e-9(0.6%)	-3.945e-4 +/- 9.862e-5(24.9%)	8.711e-6 +/- 1.26e-6 (14.4%)
5%	3	4.893e-3 +/- 4.404e-4(9.0%)	-2.471e-4 +/- 8.569e-3(3467%)	1.475e-4 +/- 2.332e-5 (15.8%)
	5	02.096e-3 +/- 1.404e-4(6.6%)	-3.958e-4 +/- 4.088e-3(1033%)	1.046e-4 +/- 1.402e-5 (13.4%)
	10	3.081e-4 +/- 1.260e-5(4.0%)	-3.637e-4 +/- 8.840e-4(243.1%)	5.476e-5 +/- 5.941e-6 (10.8%)
	20	9.752e-6 +/- 2.638e-7(2.7%)	-4.074e-4 +/- 1.361e-4(33.4%)	2.186e-5 +/- 1.996e-6 (9.1%)
	30	4.742e-7 +/- 1.926e-8(4.0%)	-6.055e-4 +/- 1.379e-4(22.7%)	1.045e-5 +/- 8.759e-7 (8.3%)

5.5. DG ARs as a Function of Curium Mass

Figures 34–39 contain plots of the $^{134}Cs/^{137}Cs$, $^{134}Cs/^{154}Eu$, and $^{154}Eu/^{137}Cs$ DG ARs as a function of elemental curium mass for 3% and 5% enrichment at 3, 5, 10, 20, and 30 years following irradiation.

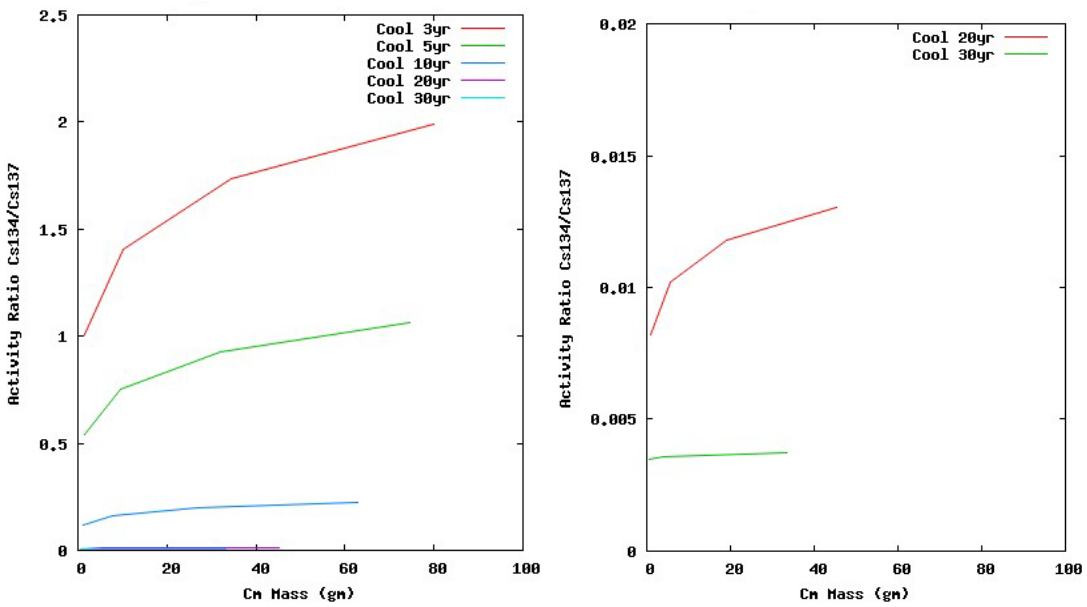

Figure 34. $^{134}Cs/^{137}Cs$ DG ARs as a function of elemental curium mass for 3% enrichment at 3, 5, 10, 20, and 30 years following irradiation.

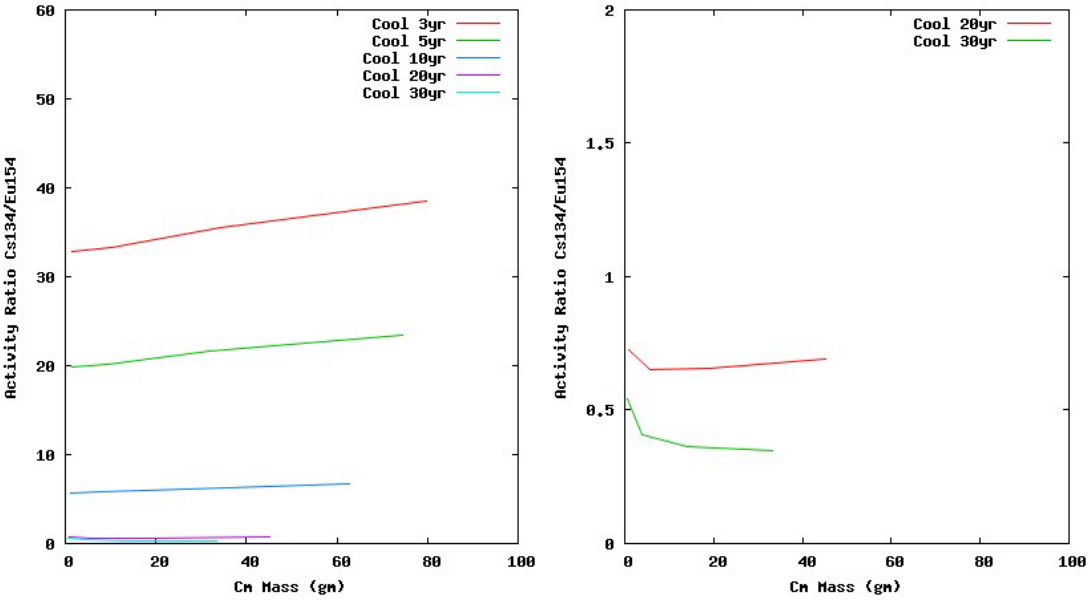

Figure 35. $^{134}Cs/^{154}Eu$ DG ARs as a function of elemental curium mass for 3% enrichment at 3, 5, 10, 20, and 30 years following irradiation.

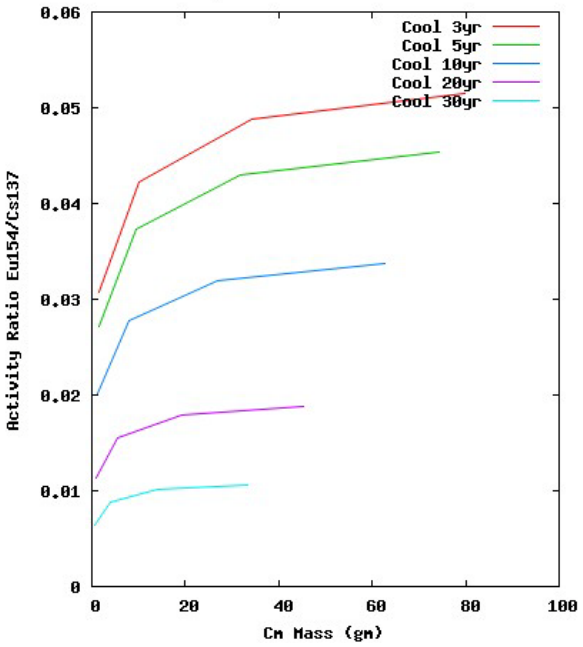

Figure 36. $^{154}Eu/^{137}Cs$ DG ARs as a function of elemental curium mass for 3% enrichment at 3, 5, 10, 20, and 30 years following irradiation.

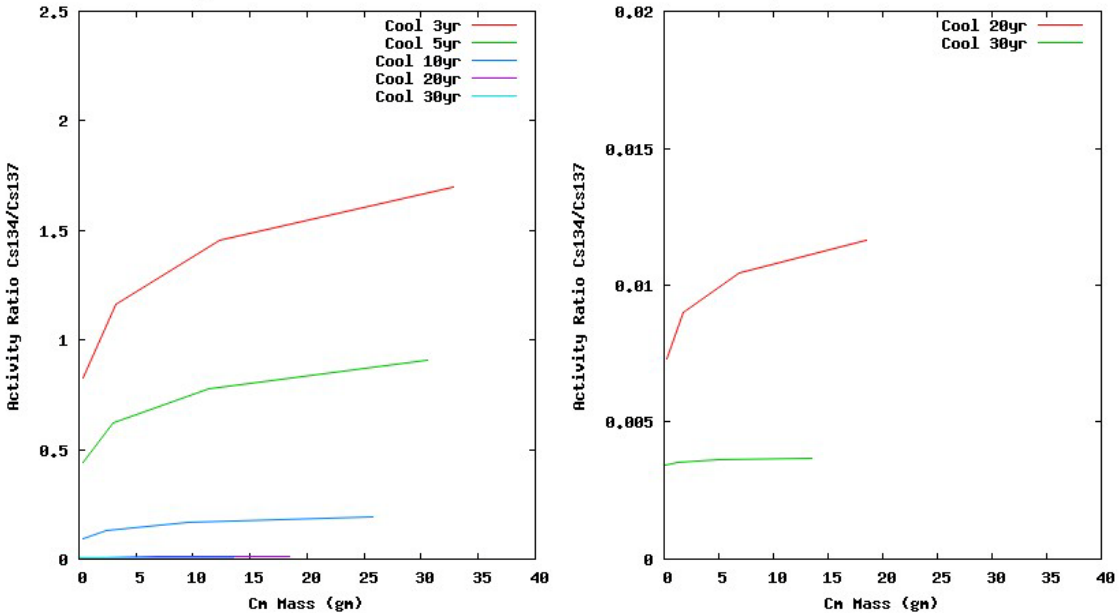

Figure 37. $^{134}Cs/^{137}Cs$ DG ARs as a function of elemental curium mass for 5% enrichment at 3, 5, 10, 20, and 30 years following irradiation.

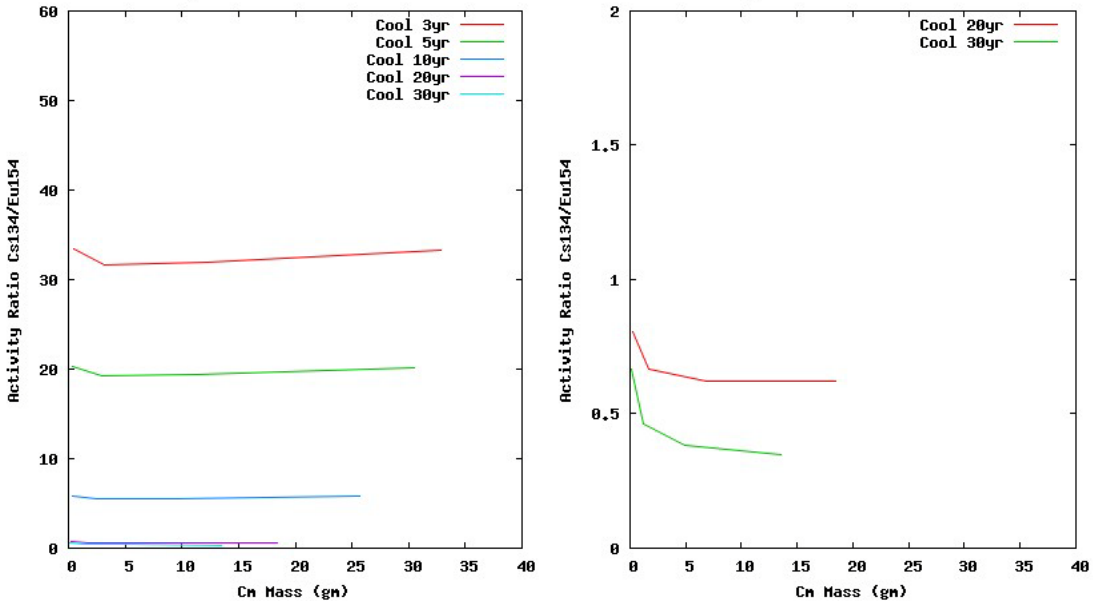

Figure 38. $^{134}Cs/^{154}Eu$ DG ARs as a function of elemental curium mass for 5% enrichment at 3, 5, 10, 20, and 30 years following irradiation.

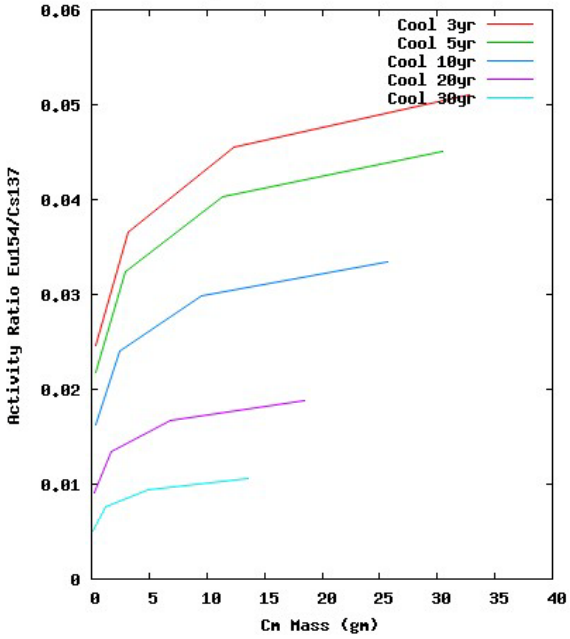

Figure 39. $^{154}Eu/^{137}Cs$ DG ARs as a function of elemental curium mass for 5% enrichment at 3, 5, 10, 20, and 30 years following irradiation.

A least-squares fit of each of the profiles in Figs. 34–39 was made with a straight line using the gnuplot "fit" function using **gnudgmCm.plt**. Table 10 contains the calculated slope and its associated error for the $^{134}Cs/^{137}Cs$, $^{134}Cs/^{154}Eu$, and $^{154}Eu/^{137}Cs$ DG ARs as a function of total curium mass.

Table 10. Slopes of the $^{134}Cs/^{137}Cs$, $^{134}Cs/^{154}Eu$, and $^{154}Eu/^{137}Cs$ DG ARs as a Function of Total Curium Mass for 3% and 5% Enrichment at 3, 5, 10, 20, and 30 Years Following Irradiation Obtained Using gnuplot Fit Function with line f(x)=mx+b (data from fit.log)

Enrichment	Cooling Time (yr)	Slope and Error of Fit ("m")		
		$^{134}Cs/^{137}Cs$	$^{134}Cs/^{154}Eu$	$^{154}Eu/^{137}Cs$
3%	3	1.106e-2 +/-3.369e-3(30.4%)	7.514e-2 +/- 3.902e-3(5.1%)	2.190e-4 +/- 1.029e-4 (46.9%)
	5	6.346e-3 +/- .935e-3(30.4%)	4.954e-2 +/- 2.729e-3(5.5%)	2.05608e-4 +/- 9.773e-5 (47.5%)
	10	1.573e-3 +/-4.818e-4(30.6%)	1.611e-2 +/- 9.986e-4(6.1%)	1.798e-4 +/- 8.568e-5 (47.6%)
	20	9.607e-5 +/-2.971e-5(30.9%)	-1.399e-4 +/- 1.176e-3(840.6%)	1.392e-4 +/- 6.721e-5 (48.2%)
	30	6.549e-6 +/-2.052e-6(31.3%)	-4.467e-3 +/- 2.879e-3(64.4%)	1.053e-4 +/- 5.195e-5 (49.3%)
5%	3	2.329e-2 +/-7.544e-3(32.3%)	1.696e-2 +/- 4.288e-2(252.7%)	6.804e-4 +/- 2.773e-4 (40.7%)
	5	1.339e-2 +/-4.342e-3(32.4%)	1.035e-2 +/- 2.773e-2(267.8%)	6.457e-4 +/- 2.632e-4 (40.7%)
	10	3.325e-3 +/-1.081e-3(32.5%)	1.242e-3 +/- 1.088e-2(875.5%)	5.682e-4 +/- 2.332e-4 (41.0%)
	20	2.058e-4 +/-6.807e-5(33.0%)	-7.067e-3 +/- 5.485e-3(77.6%)	4.4295e-4 +/- 1.834e-4 (41.4%)
	30	1.577e-5 +/-5.661e-6(35.9%)	-1.792e-2 +/- 1.095e-2(61.0%)	3.377e-4 +/- 1.404e-4 (41.5%)

6. FUEL ASSEMBLY DELAYED-NEUTRON EMISSION RATIOS VS BURNUP

Attention is now turned from DG emission to DN emission. Calculations were performed to evaluate DN emission signals as a function of burnup. The neutron emission rate depends primarily on the quantity of curium isotopes (Hsue et al., 1978). Curium is not initially present in the fuel but is produced as a result of isotopic transmutation during irradiation. At the conclusion of irradiation, most of the DNs are produced by ^{242}Cm ($t_{1/2}$ = 162.8d). After about 2 years of cooling, DN production is dominated by ^{244}Cm ($t_{1/2}$ = 18.11yr). Discussions of processing and results follow.

6.1. Tally Processing for DN Current Analysis

These fixed-source (SDEF) calculations were executed using the irradiated fuel assembly DN emission as the radiation-transport sources. A description of the source-term generation processing is given in Section 3. The calculations were executed as a function of enrichment, burnup, and cooling time.

Once the calculations were completed on Pete, the MCNP6 outp and mctal files were moved to the PC for postprocessing to produce plots of DN emission ratios as a function of burnup. The necessary data were obtained by retrieving surface-integrated neutron current (F1) tally data from the outp files.

Data postprocessing for plot creation required the handling of 40 files and extensive amounts of data. The Fortran code **extrctnt.f** was written to (1) parse the outp files, (2) locate the bins and tally data, and (3) write the F1 tally data to output file talno.

The Perl script **runtaln.pl** was created to (1) guide the execution of extrctnt.exe for each of the outp files, (2) input the values in the talno files (each contains the surface- integrated current value), and (3) create GNUFILE files containing the ratio values for each HEU enrichment and for each ratio value (named dnvsbue3 and dnvsbue5). Execution of runrtal.pl for the 40 DN models requires approximately 10 seconds.

The gnuplot file **gnupdn.plt** was created and used to plot each of the dnvsbu files. Results are presented next.

6.2. Fuel Assembly DN Current Simulation Results

Figure 40 contains plots of the DN current as a function of burnup for 3% and 5% enrichment at 3, 5, 10, 20, and 30 years following irradiation. The general tendencies include (1) for a given enrichment and burnup, the DN signal decreases with cooling time; (2) for a given enrichment and cooling time, the DN signal increases with burnup; (3) for a given burnup and cooling time, the DN signal decreases with increasing enrichment (constant power operation results in fewer fissions with increasing enrichment); and (4) DN signals exhibit quasi-cubic dependence on burnup for all considered enrichment and cooling times (Reilly et al., 1991).

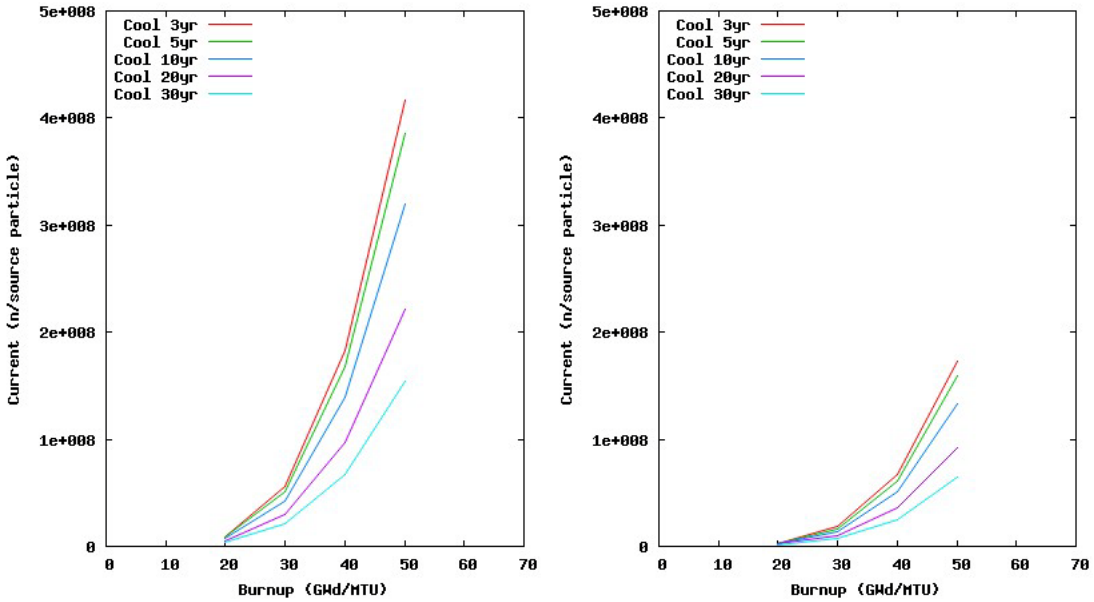

Figure 40. Delayed-neutron current as a function of burnup at 3, 5, 10, 20, and 30 years following irradiation for a) 3% enrichment and b) 5% enrichment.

A least-squares fit of each of the profiles in Fig. 40 was made with a straight line using the gnuplot "fit" function (executed using **gnupdnf.plt**). Table 11 contains the calculated slopes and their associated errors.

Table 11. Slopes of the DN Current as a Function of Burnup for 3% and 5% Enrichment at 3, 5, 10, 20, and 30 Years Following Irradiation Obtained Using gnuplot Fit Function with line f(x)=mx+b (data from fit.log)

Enrichment	Cooling Time (yr)	Slope and Error of Fit ("m")
3%	3	1.350e+7 +/- 2.98e+6(22.0%)
	5	1.248e+7 +/- 2.76e+6(22.1%)
	10	1.035e+7 +/- 2.29e+6(22.4%)
	20	7.141e+6 +/- 1.58e+6(22.1%)
	30	4.952e+6 +/- 1.09e+6(22.1%)
5%	3	5.595e+6 +/- 1.44e+6(25.8%)
	5	5.160e+6 +/- 1.34e+6(25.9%)
	10	4.281e+6 +/- 1.10e+6(25.9%)
	20	2.960e+6 +/- 7.62e+5(25.7%)
	30	2.057e+6 +/- 5.24e+5(25.5%)

7. FUEL ASSEMBLY DELAYED-NEUTRON EMISSION VS ACTINIDE MASS

Analysis of the DN emission current as a function of actinide mass was conducted. The procedure mirrors that used for the DG analysis (see Section 5). Isotopic actinide mass data are contained in the outp files created for the fuel-assembly kcode/burnup calculations (see Section 2). The Perl script **runmassn.pl** was created to guide the execution process for **extractm.f** for DN emission as a function of mass. This Perl script serves to (1) unzip/zip the outp files, (2) guide the execution of extractm.exe (Fortran executable) for each of the kcode/burnup outp files, (3) input the values in the totmo files (each contains a single neutron current value), and (4) create GNUFILE plot input files containing the neutron current data as a function of actinide mass for each HEU enrichment (files dnvsmAme3, dnvsmAme5, dnvsmPu3e, dnvsmPue5, etc.).

Because the tally data from the DN sources are needed, **runmassn.pl** also contains the coding contained in **runtaln.pl**. The outp files for the assembly kcode/burnup models (see Section 1) and the DN sources (see Section 5) are stored on separate directories (for QA). Consequently, runmassn.pl executes extrctnt.f by changing to the directory where the delayed-particle outp files are located. Processing creates GNUFILE files containing actinide mass and DN emission current tally data.

Execution of **runmassn.pl** for the eight kcode/burnup models and the 40 DN models requires ~20 minutes on the PC. Results for uranium, neptunium, plutonium, americium, and curium are presented next.

7.1. DN Current as a Function of Uranium Mass

Figure 41 contains plots of the DN currents as a function of uranium mass for 3% and 5% enrichment at 3, 5, 10, 20, and 30 years following irradiation. DN emission (1) decreases with increasing uranium mass for constant-power operation, (2) decreases with increasing cooling time, and (3) decreases with increasing enrichment for constant-power operation. These plots were created using **gnudnmU.plt**.

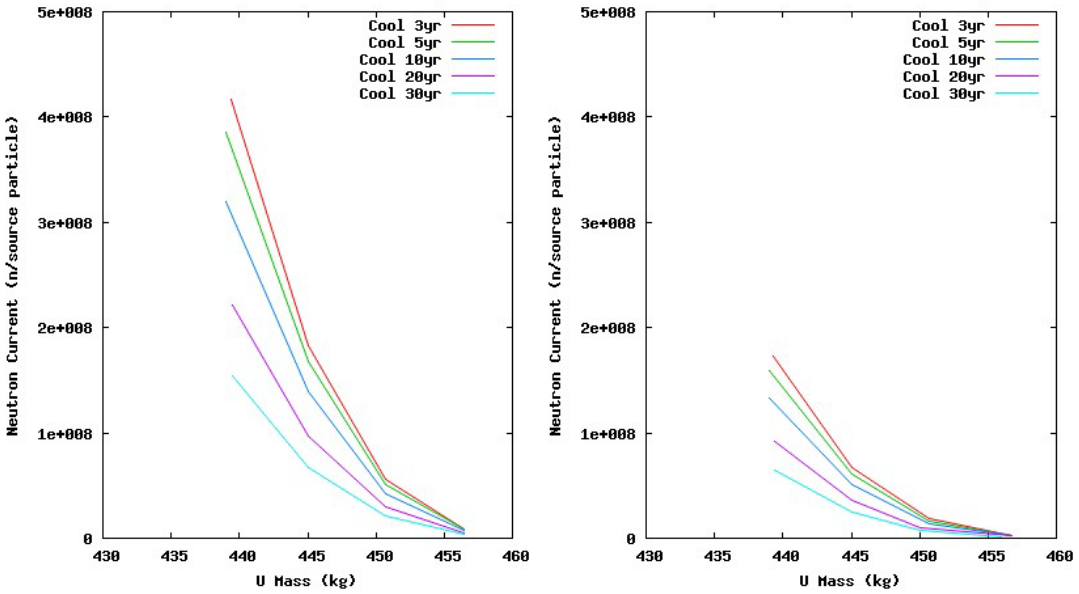

Figure 41. Delayed-neutron current as a function of uranium mass at 3, 5, 10, 20, and 30 years following irradiation for (a) 3% and (b) 5% enrichment.

A least-squares fit of each of the profiles in Fig. 41 was made with a straight line using the gnuplot "fit" function using **gnudnmU.plt**. Table 12 contains the calculated slope and its associated error for the DN current as a function of total uranium mass.

Table 12. Slopes of the DN Current as a Function of Uranium Mass for 3% and 5% Enrichment at 3, 5, 10, 20, and 30 Years Following Irradiation Obtained Using gnuplot Fit Function with line f(x)=mx+b (data from fit.log)

Enrichment	Cooling Time (yr)	Slope and Error of Fit ("m")
3%	3	-2.362e+7 +/- 5.359e+6 (22.6%)
	5	-2.150e+7 +/- 4.627e+6 (21.5%)
	10	-1.783e+7 +/- 3.837e+6 (21.5%)
	20	-1.254e+7 +/- 2.896e+6 (23.0%)
	30	-8.699e+6 +/- 2.010e+6 (23.1%)
5%	3	-9.624e+6 +/- 2.576e+6 (26.7%)
	5	-8.782e+6 +/- 2.273e+6 (25.8%)
	10	-7.284e+6 +/- 1.881e+6 (25.8%)
	20	-5.113e+6 +/- 1.484e+6 (29.0%)
	30	-3.733e+6 +/- 9.941e+5 (26.6%)

7.2. DN Current as a Function of Neptunium Mass

Figure 42 contains plots of the DN currents as a function of neptunium mass for 3% and 5% enrichment at 3, 5, 10, 20, and 30 years following irradiation. These plots were created using **gnudnmNp.plt**.

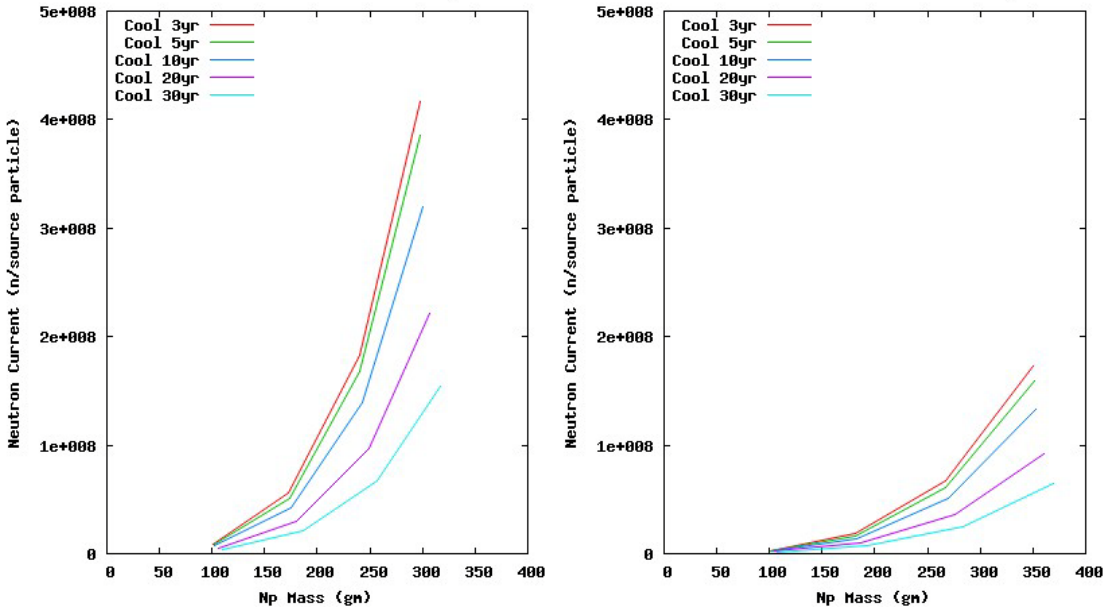

Figure 42. Delayed-neutron current as a function of neptunium mass at 3, 5, 10, 20, and 30 years following irradiation for a) 3% and b) 5% enrichment.

A least-squares fit of each of the profiles in Fig. 42 was made with a straight line using the gnuplot "fit" function using **gnudnmNp.plt**. Table 13 contains the calculated slope and its associated error for the DN current as a function of total neptunium mass.

Table 13. Slopes of the DN Current as a Function of Neptunium Mass for 3% and 5% Enrichment at 3, 5, 10, 20, and 30 Years Following Irradiation Obtained Using gnuplot Fit Function with line f(x)=mx+b (data from fit.log)

Enrichment	Cooling Time (yr)	Slope and Error of Fit ("m")
3%	3	2.024e+6 +/-5.273e+5(26.0%)
	5	1.869e+6 +/-4.886e+5(26.1%)
	10	1.540e+6 +/-4.037e+5(26.2%)
	20	1.040e+6 +/-2.749e+5(26.4%)
	30	7.027e+5 +/-1.877e+5(26.7%)
5%	3	6.730e+5 +/-1.711e+5(25.4%)
	5	6.197e+5 +/-1.580e+5(25.5%)
	10	5.107e+5 +/-1.303e+5(25.5%)
	20	3.462e+5 +/-8.827e+4(25.4%)
	30	2.345e+5 +/-5.970e+4 (25.4%)

7.3. DN Current as a Function of Plutonium Mass

Figure 43 contains plots of the DN currents as a function of plutonium mass for 3% and 5% enrichment at 3, 5, 10, 20, and 30 years following irradiation. For a given enrichment, the signals are not clearly identified because of their overlapping behavior as a function of mass for each cooling time. The signals do exhibit uniqueness as a function of enrichment. These plots were created using **gnudnmPu.plt**.

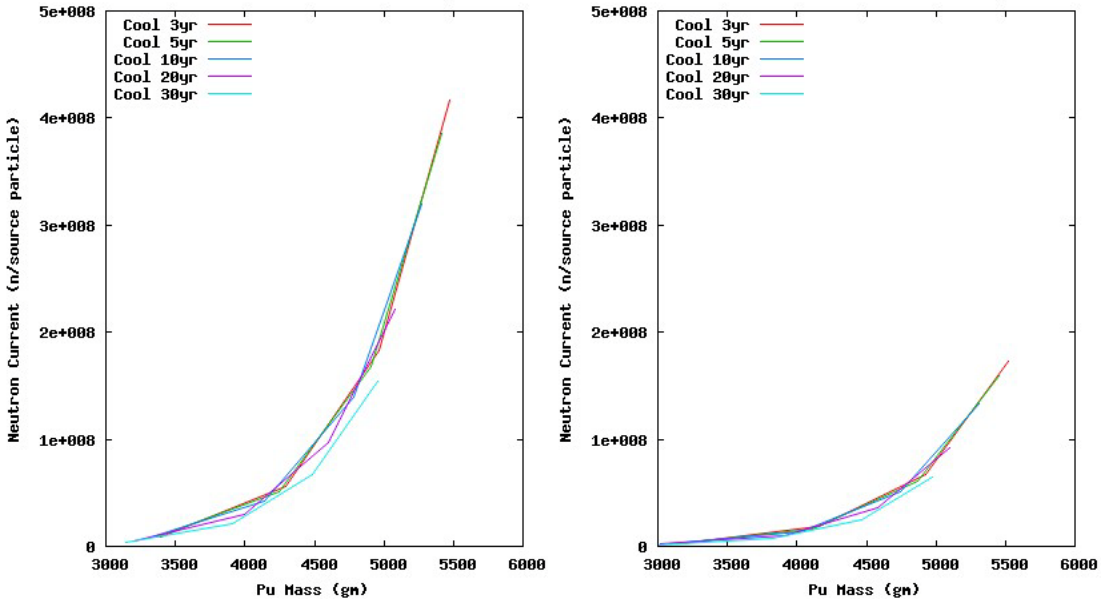

Figure 43. Delayed-neutron current as a function of plutonium mass at 3, 5, 10, 20, and 30 years following irradiation for a) 3% and b) 5% enrichment.

A least-squares fit of each of the profiles in Fig. 43 was made with a straight line using the gnuplot "fit" function using gnudnmNp.plt. Table 14 contains the calculated slope and its associated error for the DN current as a function of total plutonium mass.

Table 14. Slopes of the DN Current as a Function of Plutonium Mass for 3% and 5% Enrichment at 3, 5, 10, 20, and 30 Years Following Irradiation Obtained Using gnuplot Fit Function with line f(x)=mx+b (data from fit.log)

Enrichment	Cooling Time (yr)	Slope and Error of Fit ("m")
3%	3	1.843e+5 +/- 5.935e+4 (32.1%)
	5	1.736e+5 +/- 5.575e+4 (32.1%)
	10	1.493e+5 +/- 4.75e+4 (31.8%)
	20	1.091e+5 +/- 3.41e+4 (31.2%)
	30	7.864e+4 +/- 2.429e+4 (30.8%)
5%	3	6.741e+4 +/- 2.387e+4 (35.4%)
	5	6.342e+4 +/- 2.251e+4 (35.4%)
	10	5.493e+4 +/- 1.950e+4 (35.4%)
	20	4.049e+4 +/- 1.431e+4 (35.3%)
	30	4.873e+4 +/- 1.402e+4 (28.7%)

7.4. DN Current as a Function of Americium Mass

Figure 44 contains plots of the DN currents as a function of americium mass for 3% and 5% enrichment at 3, 5, 10, 20, and 30 years following irradiation. These plots were created using **gnudnmAm.plt**.

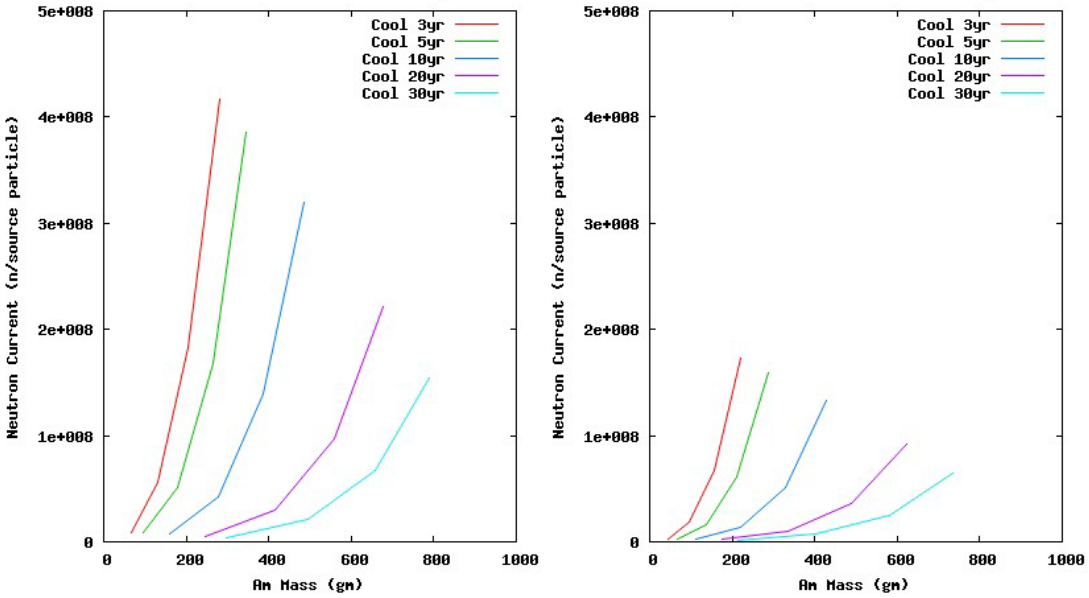

Figure 44. Delayed-neutron current as a function of americium mass at 3, 5, 10, 20, and 30 years following irradiation for a) 3% and b) 5% enrichment.

A least-squares fit of each of the profiles in Fig. 44 was made with a straight line using the gnuplot "fit" function using **gnudnmAm.plt**. Table 15 contains the calculated slope and its associated error for the DN current as a function of total americium mass.

Table 15. Slopes of the DN Current as a Function of Americium Mass for 3% and 5% Enrichment at 3, 5, 10, 20, and 30 Years Following Irradiation Obtained Using gnuplot Fit Function with line f(x)=mx+b (data from fit.log)

Enrichment	Cooling Time (yr)	Slope and Error of Fit ("m")
3%	3	1.912e+6 +/- 3.71e+5 (19.4%)
	5	1.499e+6 +/- 3.29e+5 (21.9%)
	10	9.389e+5 +/- 2.38e+5 (25.4%)
	20	4.831e+5 +/- 1.36e+5 (28.2%)
	30	2.913e+5 +/- 8.55e+4 (29.3%)
5%	3	9.662e+5 +/- 2.08e+5 (21.6%)
	5	7.037e+5 +/- 1.69e+5 (24.1%)
	10	4.033e+5 +/- 1.08e+5 (26.9%)
	20	1.956e+5 +/- 5.63e+4 (28.8%)
	30	1.155e+5 +/- 3.39e+4 (29.3%)

7.5. DN Current as a Function of Curium Mass

Figure 45 contains plots of the DN currents as a function of curium mass for 3% and 5% enrichment at 3, 5, 10, 20, and 30 years following irradiation. The half-lives of DN emitters ^{242}Cm and ^{244}Cm are 162.8 d and 18.11 y, respectively. All profiles are virtually linear as a function of curium mass. The profiles virtually overlap as a function of curium mass and cooling time. Consequently, the approximate curium content can be determined from the neutron current regardless of cooling time. These plots were created using **gnudnmCm.plt**.

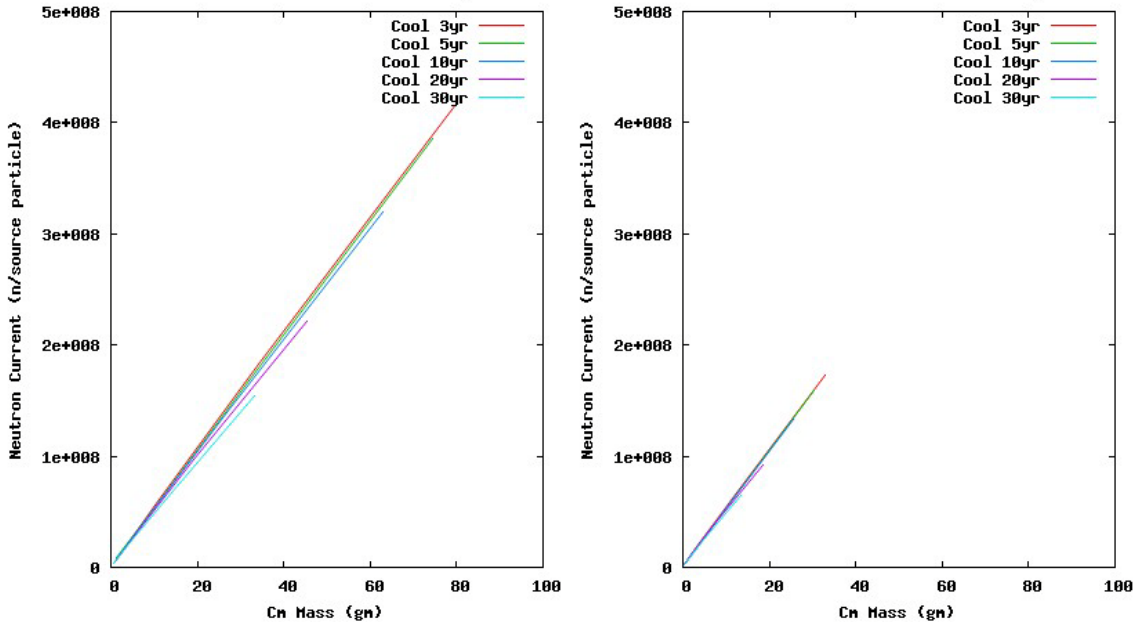

Figure 45. Delayed-neutron current as a function of curium mass at 3, 5, 10, 20, and 30 years following irradiation for (a) 3% and (b) 5% enrichment.

A least-squares fit of each of the profiles in Fig. 45 was made with a straight line using the gnuplot "fit" function using **gnudnmCm.plt**. Table 16 contains the calculated slope and its associated error for the DN current as a function of total curium mass.

Table 16. Slopes of the DN Current as a Function of Curium Mass for 3% and 5% Enrichment at 3, 5, 10, 20, and 30 Years Following Irradiation Obtained Using gnuplot Fit Function with line f(x)=mx+b (data from fit.log)

Enrichment	Cooling Time (yr)	Slope and Error of Fit ("m")
3%	3	5.2e+6 +/- 2.413e+4 (0.4%)
	5	5.159e+6 +/- 2.408e+4 (0.4%)
	10	5.067e+6 +/- 2.808e+4 (0.5%)
	20	4.841e+6 +/- 3.802e+4 (0.7%)
	30	4.555e+6 +/- 4.854e+4 (1.0%)
5%	3	5.248e+6 +/- 3.237e+4 (0.6%)
	5	5.204e+6 +/- 3.177e+4 (0.6%)
	10	5.119e+6 +/- 3.881e+4 (0.7%)
	20	4.917e+6 +/- 5.512e+4 (1.1%)
	30	4.658e+6 +/- 7.347e+4 (1.5%)

8. 8. FUEL ASSEMBLY DG ARs VS BURNUP FOR NEW DG RATIOS

Exploratory work was done to examine whether robust DG ARs other than $^{134}Cs/^{137}Cs$, $^{134}Cs/^{154}Eu$, and $^{154}Eu/^{137}Cs$ can be identified for the fuel assembly data. The postprocessing procedure and calculated results are discussed next.

8.1. Tally Processing for Fuel Assembly DG Ratio Analysis

This analysis was performed using the existing MCNP6 code capabilities. As already described (see Section 3.1), MCNP6 can only calculate aggregate contributions made by multiple nuclides to the F1 photon-current tally. That is, MCNP6 cannot discern the nuclide-specific contributions to each tally bin. Consequently, we explored DG ratios other than $^{134}Cs/^{137}Cs$, $^{134}Cs/^{154}Eu$, and $^{154}Eu/^{137}Cs$ using only the aggregate tally data for each bin.

To understand the processing technique, consider first the plots of the DG current at the surface of the assembly for the 3% enrichment and 20-GWd/MTU burnup at 3, 5, 10, 20, and 30 years post-irradiation, as shown in Fig. 46. The profiles show a baseline structure with as series of prominent discrete peaks. The emission profiles become less pronounced with time as the emitting radionuclides decay.

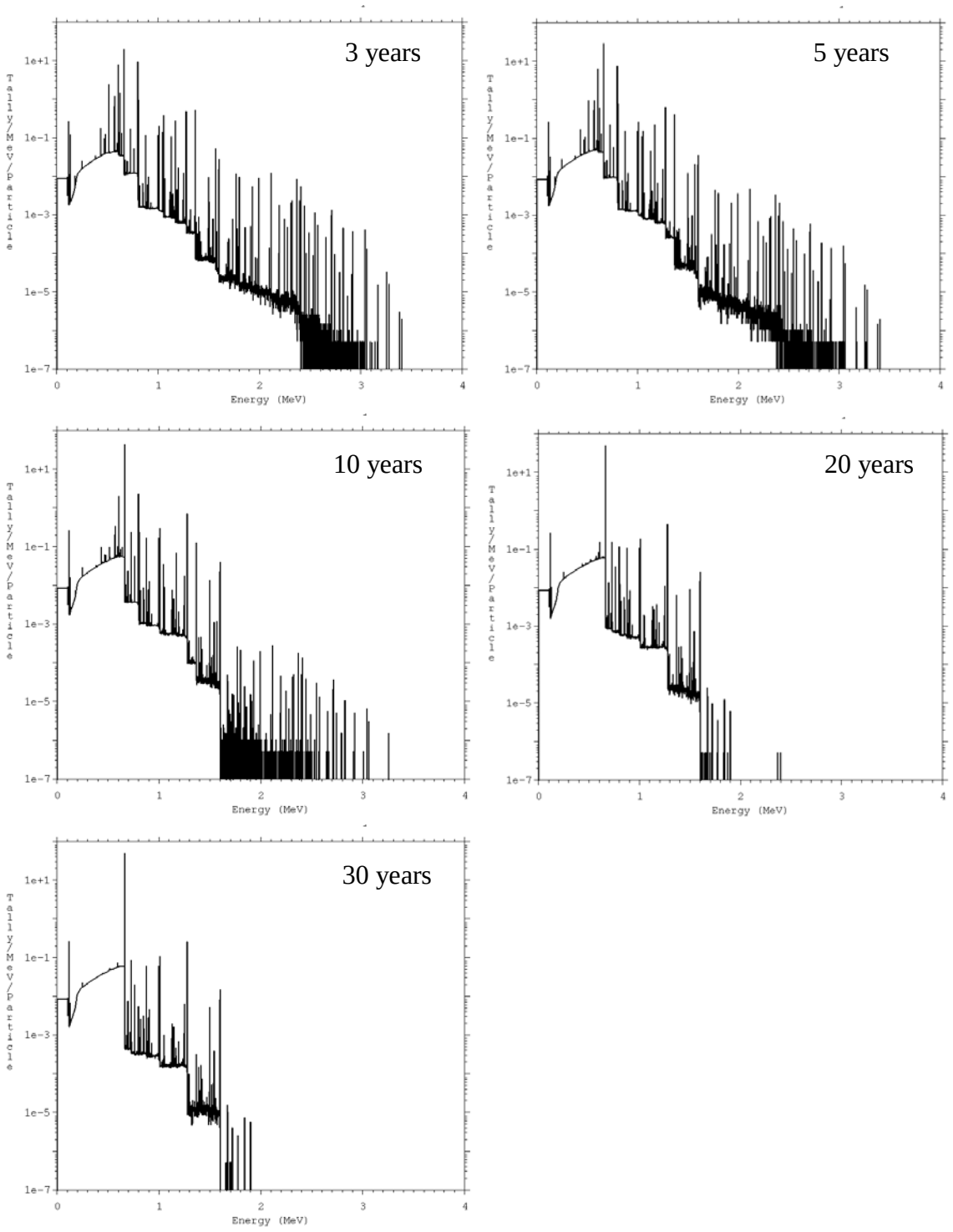

Figure 46. Assembly delayed-gamma current for 3% enrichment and 20 GWd/MTU burnup at 3, 5, 10, 20, and 30 years post irradiation.

The data for DG ratio analysis was executed following essentially the same underlying basic procedure used for the $^{134}Cs/^{137}Cs$, $^{134}Cs/^{154}Eu$, and $^{154}Eu/^{137}Cs$ ARs. However, instead of having a set of *a priori* emission energies and tally bins, all tally bins were considered. To do this, nested-loop combinations of all tally bins with nonzero values were used to calculate DG ratios. Thus, as illustrated in Table 17, DG ratios were calculated using the tally data in bins 1 and 2, 1 and 3, 1 and 4, etc. Next, DG ratios for bins 2 and 3, 2 and 4, etc., were calculated. The process was repeated until all combinations were calculated.

Table 17. A Portion of the Calculated (outp file) F1 Photon Current Tally for the 3% Enrichment and 20-GWd/MTU Burnup at 3 Years Post Irradiation

```
angle bin:  0.90000E+02 to 0.00000E+00 degrees
bin# surface:      a
   energy    tally   rel.uncert.
 1  1.0000E-01  8.84538E-04 0.0008
 2  1.0096E-01  3.16250E-06 0.0126
 3  1.0192E-01  3.44200E-06 0.0121
 4  1.0288E-01  3.50900E-06 0.0119
 5  1.0384E-01  3.50950E-06 0.0119
...
5000 4.9990E+00  0.00000E+00 0.0000
5001 5.0000E+00  0.00000E+00 0.0000
```

This set of calculations was done for the least and the most irradiated conditions, i.e., 20 and 50 GWd/MTU. For each pair of bins, a ratio of the DG emission was then calculated using the least and the most irradiated conditions. This procedure provided an assessment of the steepness of the profile for the DG ratio at the least and the most irradiated conditions for each pair of bins. The DG ratios with the largest quotients (nrmax) were saved and used for plotting diagnostics. This analysis was done without treating error propagation associated with the tallies.

Currently, no coding has been implemented to provide the identities of the nuclides producing the lines. In earlier work, pre-alpha-version coding was developed to give the nuclide identities for photon lines (Durkee et al., 2009a, b). That capability was developed for models executed with DG production ("dng_model"). The current effort uses a fixed (SDEF) source of delayed gammas rather than calculating DG emission during execution. Consequently, the earlier alpha coding cannot be directly used here: additional development is required. The results here are thus limited to DG ARs with unidentified nuclides.

This data postprocessing process required handling 40 files (2 enrichments, 4 burnups, and 5 cooling times). The Fortran utility code **extralle.f** was created to extract the tally bin energies. The Fortran utility code **extrallt.f** was written to extract the tally data. Separate codes (**extralle.f** and **extrallt.f**) are used to simplify **runallt.pl** execution. Perl script **runallt.pl** was designed to guide the execution of extralle.exe and extrallt.exe to form file talao for each enrichment and cooling time. File talao contains the tally bin energies and tally data for each burnup.

Analysis of the tally data in file talao was done by the new Fortran utility code **dgratio.f**. This code performs the nested-loop DG ratio calculations and identifies the bin pairs with the largest ratios. Using those bins, the DG ratios for the other burnups are calculated.

The execution of dgratio.exe for each enrichment and cooling time is guided by **runallt.pl**. The calculated data are written to files for processing by **runallt.pl** into a format suitable for plotting using gnuplot. Recall that for the $^{134}Cs/^{137}Cs$, $^{134}Cs/^{154}Eu$, and $^{154}Eu/^{137}Cs$ DG AR analyses, three files—corresponding to these three DG ratios—were created per enrichment. For the newly discovered ratio analysis, nrmax files are created per enrichment. The gnuplot data files are named mxtalo (mxtaloe3r1, mxtaloe3r2, mxtaloe3r3, …, mxtaloe3rnrmax; mxtaloe5r1, mxtaloe5r2, …, mxtaloe5rnrmax).

The gnuplot files **gnupbu3n.plt** and **gnupbu5n.plt** were created and used to plot each of the mxtaleo files for 3% and 5% enrichment, respectively. Results are presented next.

8.2. Fuel Assembly DG Ratio Analysis Results

The exploration for new DG ratios using **dgratio.f** was first done without constraints on the DG tally amplitudes and resulted in DG ratio formation using tallies with very low amplitudes; i.e., essentially noise. Such peaks likely cannot be measured by inspectors.

To ameliorate this behavior, several adjustments were attempted. First, the average tally value (for a given enrichment and cooling time) was calculated (averaged over all nonzero tally bins). Tally selection for ratio formation was limited to peaks with amplitudes that exceeded the average peak height. This approach improved results—the selected peaks were above "noise" levels, but as anticipated, the DG ARs were smaller than those for the unconstrained analysis. However, peaks with amplitudes marginally greater than the average peak height were identified. Such low-amplitude peaks could still be difficult to identify by inspectors. Some DG ratios were formed with prominent peaks, including the 0.662-MeV peak for ^{137}Cs. In addition, several of the highest DG ratios were formed using tally bins <0.2 MeV.

Second, tallies with the highest amplitudes were identified to form ratios. These large-amplitude tallies correspond to the DGs most easily measured by inspectors.

Figures 47–51 contain plots of 10 possible new DG ARs as a function of burnup for 3% enrichment at 3, 5, 10, 20, and 30 years following irradiation. The profiles exhibit monotonically increasing behavior, with appreciable slopes in most instances. Dependencies on radioactive decay are apparent, with some DG ratios showing maximum values at 3 years cooling time, others at 5 years, and others at 10 years.

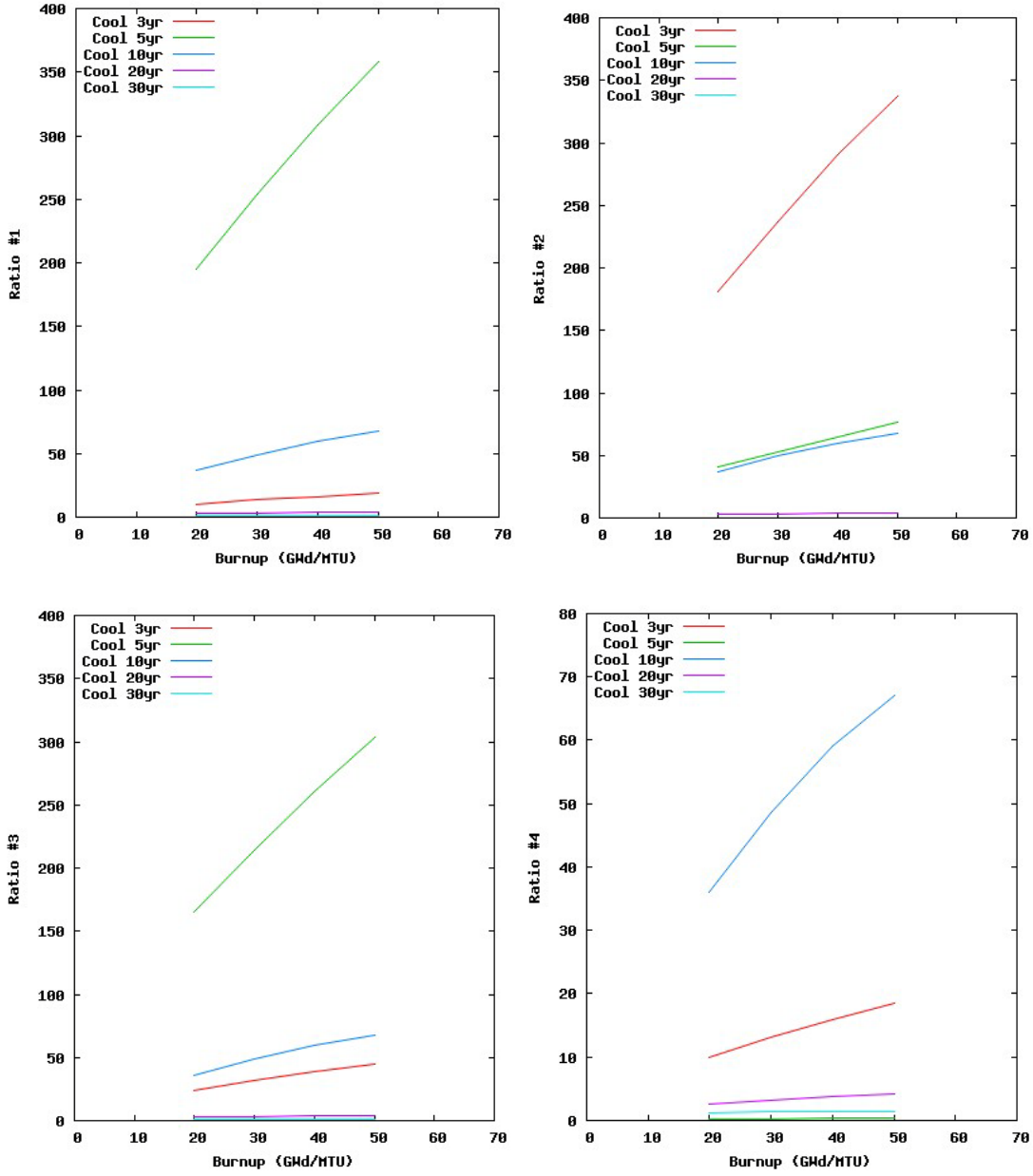

Figure 47. New DG ARs#1–4 as a function of burnup for 3% enrichment at 3, 5, 10, 20, and 30 years following irradiation.

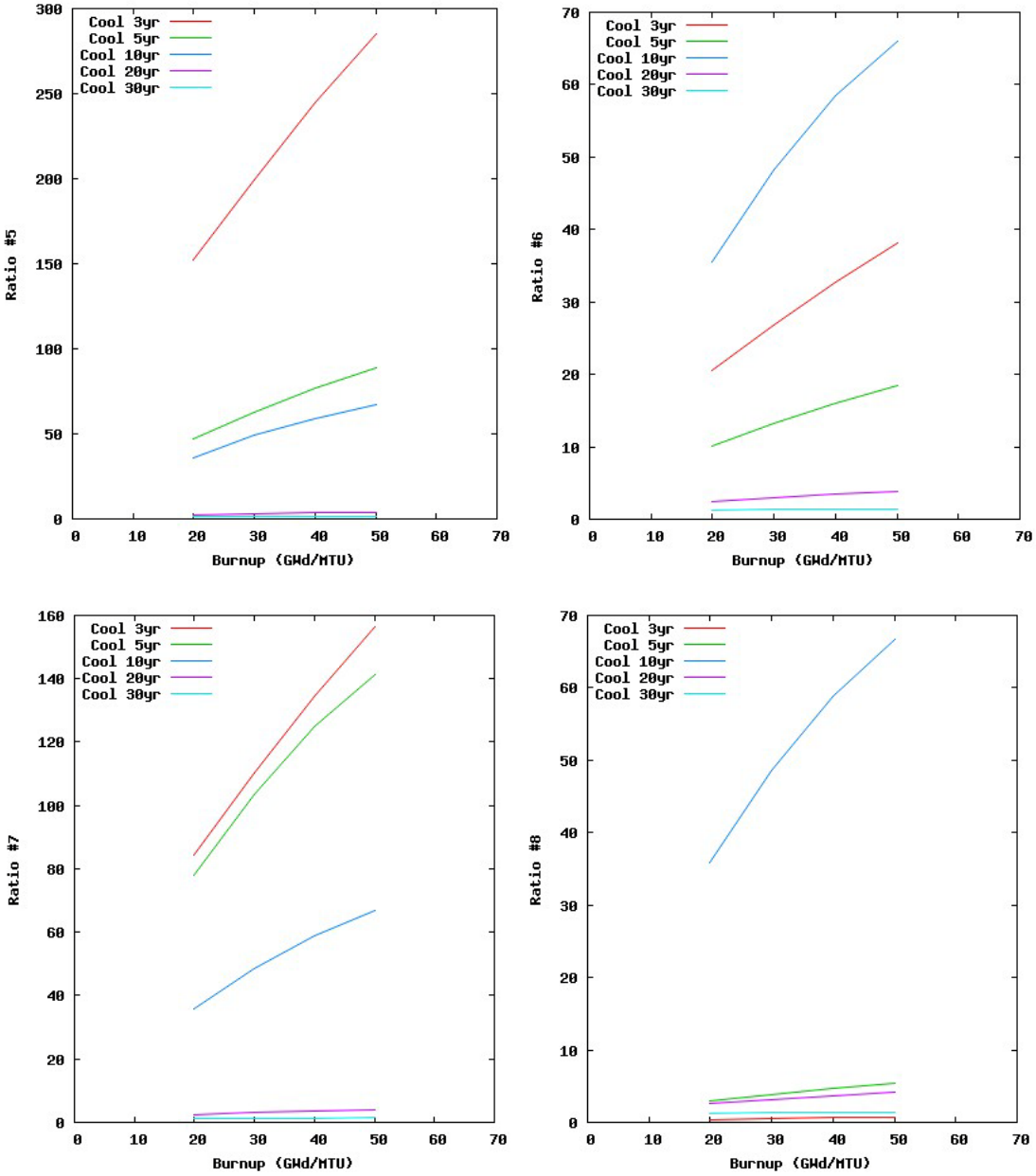

Figure 48. New DG ARs #5–8 as a function of burnup for 3% enrichment at 3, 5, 10, 20, and 30 years following irradiation.

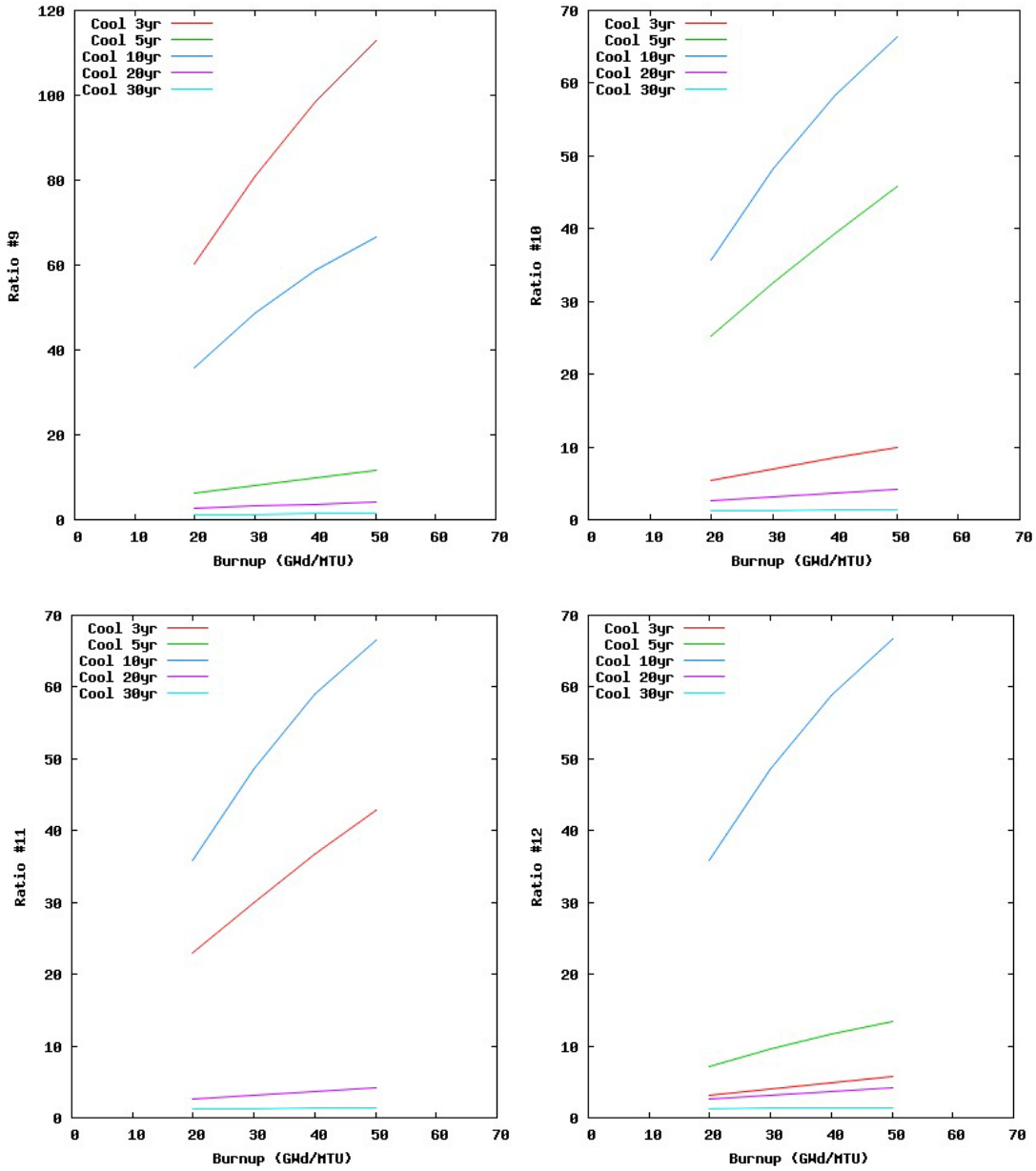

Figure 49. New DG ARs #9–12 as a function of burnup for 3% enrichment at 3, 5, 10, 20, and 30 years following irradiation.

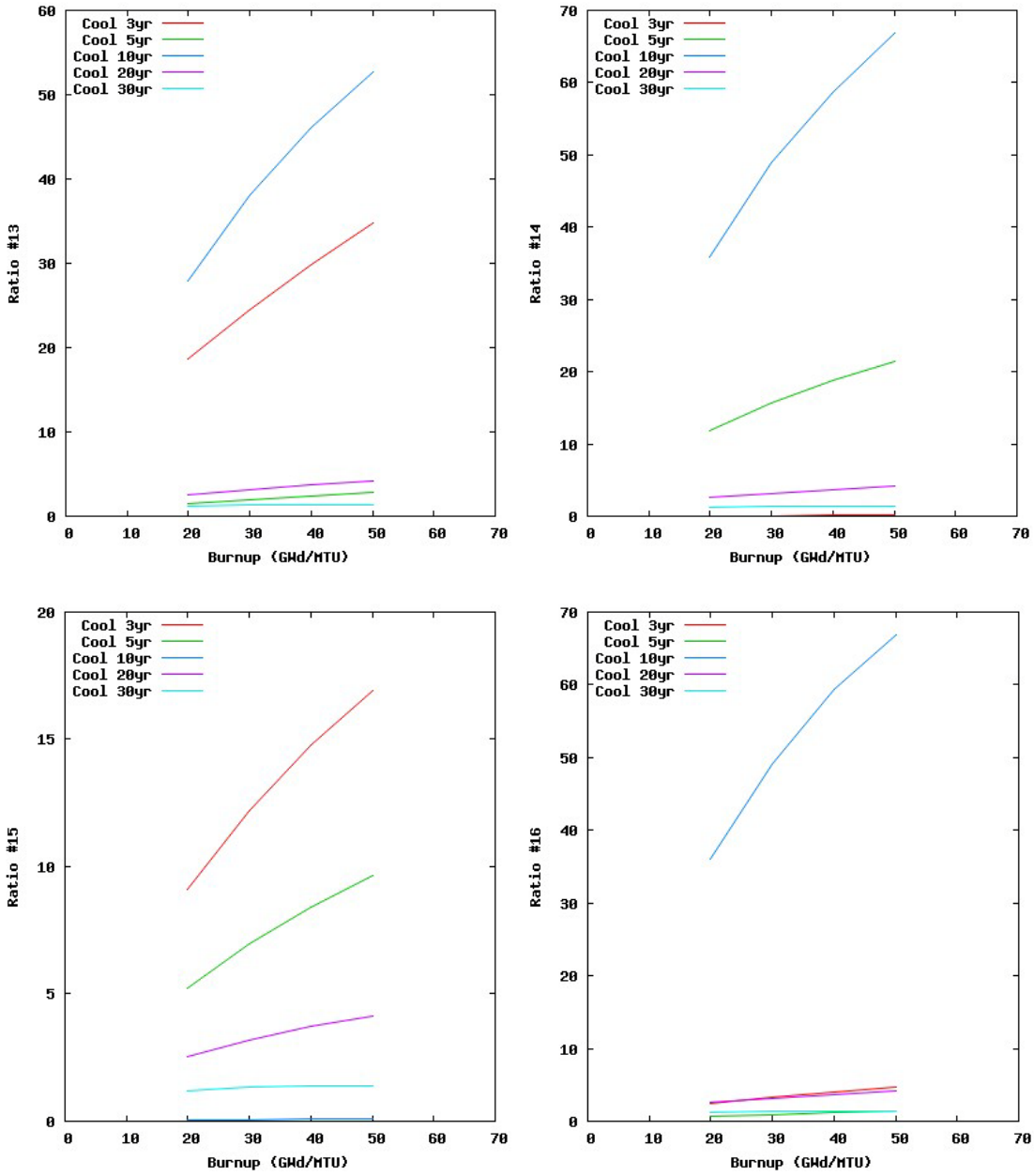

Figure 50. New DG ARs #13–16 as a function of burnup for 3% enrichment at 3, 5, 10, 20, and 30 years following irradiation.

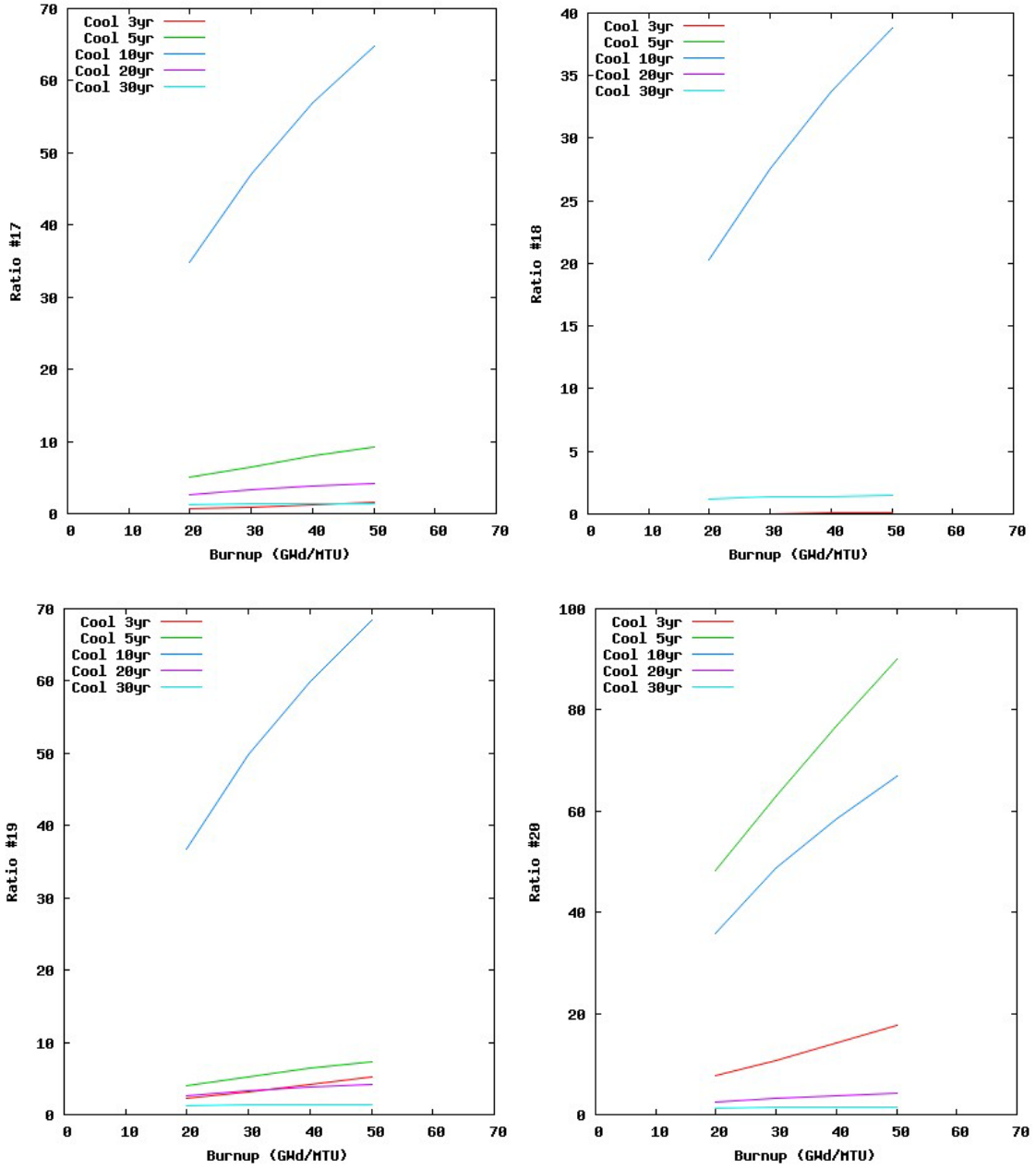

Figure 51. New DG ARs #17–20 as a function of burnup for 3% enrichment at 3, 5, 10, 20, and 30 years following irradiation.

Ratio analysis data for the 3% enrichment, 3-year cooling time dgratio.exe calculation are listed in Table 18 for fits 1–5. Listed are the fit identification number, “Fit”; the energy bin numbers for the pair of energy bins used for the fit, “EB1” and “EB2”; the upper-energy bin energies, “E1” and “E2”; the calculated DG AR, “DG AR”; and the tally data for fit bins 1 and 2 at 20 and 50 GWd/MTU, “tal eb1” and “tal eb2”.

Table 18. DG Ratio Analysis Data for 3% Enrichment, 3-Year Cooling Time

Fit	EB1	EB2	E1 (MeV)	E2 (MeV)	DG AR	Burnup 20 GWd/MTU		Burnup 50 GWd/MTU	
						tal eb1	tal eb2	tal eb1	tal eb2
1	732	807	8.02e-1	8.74e-1	1.8484	9.44e-4	9.16e-5	1.39e-3	7.28e-5
2	726	1523	7.96e-1	1.56e0	1.8623	9.16e-3	5.05e-5	1.34e-2	3.98e-5
3	726	990	7.96e-1	1.05e0	1.8560	9.16e-3	3.76e-4	1.34e-2	2.97e-4
4	1318	1523	1.36e0	1.56e0	1.8490	5.07e-4	5.05e-5	7.40e-4	3.98e-5
5	527	1523	6.05e-1	1.15e0	1.8714	7.71e-3	5.05e-5	1.13e-2	3.98e-5

Figures 52–56 contain plots of 10 possible new DG ARs as a function of burnup for 5% enrichment at 3, 5, 10, 20, and 30 years following irradiation. Behavior similar to that for 3% enrichment is evident.

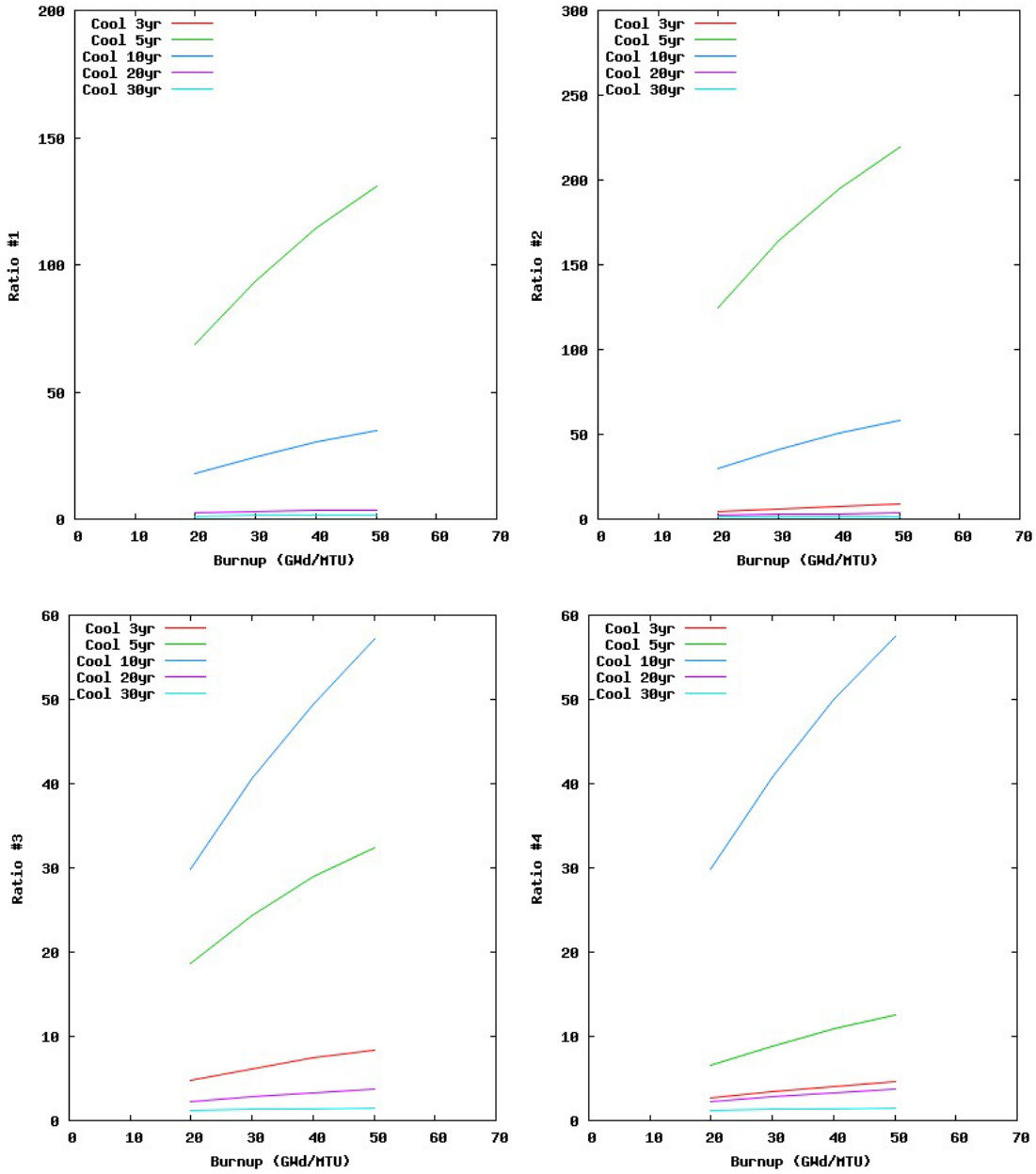

Figure 52. New DG ARs #1–4 as a function of burnup for 5% enrichment at 3, 5, 10, 20, and 30 years following irradiation.

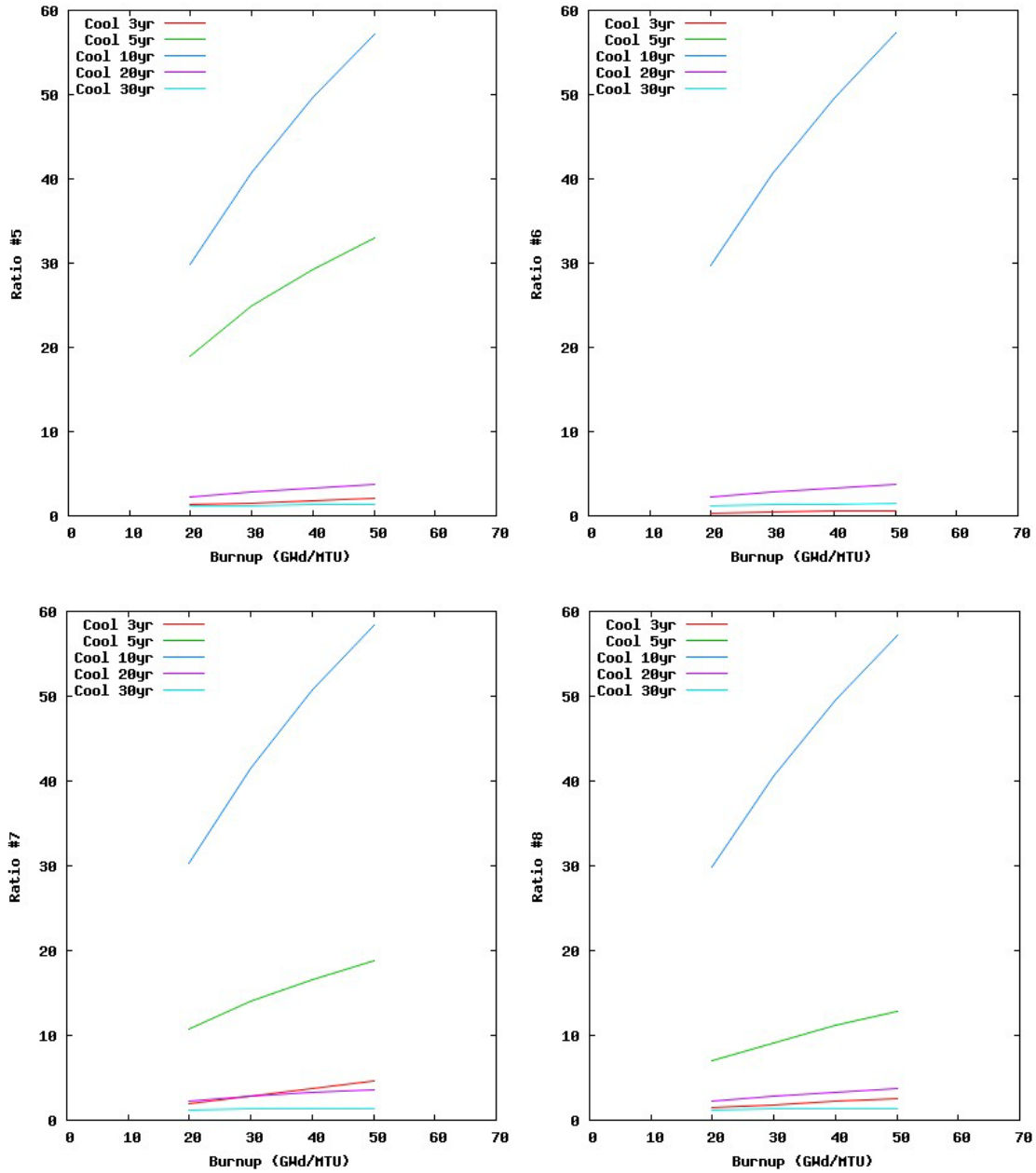

Figure 53. New DG ARs #5–8 as a function of burnup for 5% enrichment at 3, 5, 10, 20, and 30 years following irradiation.

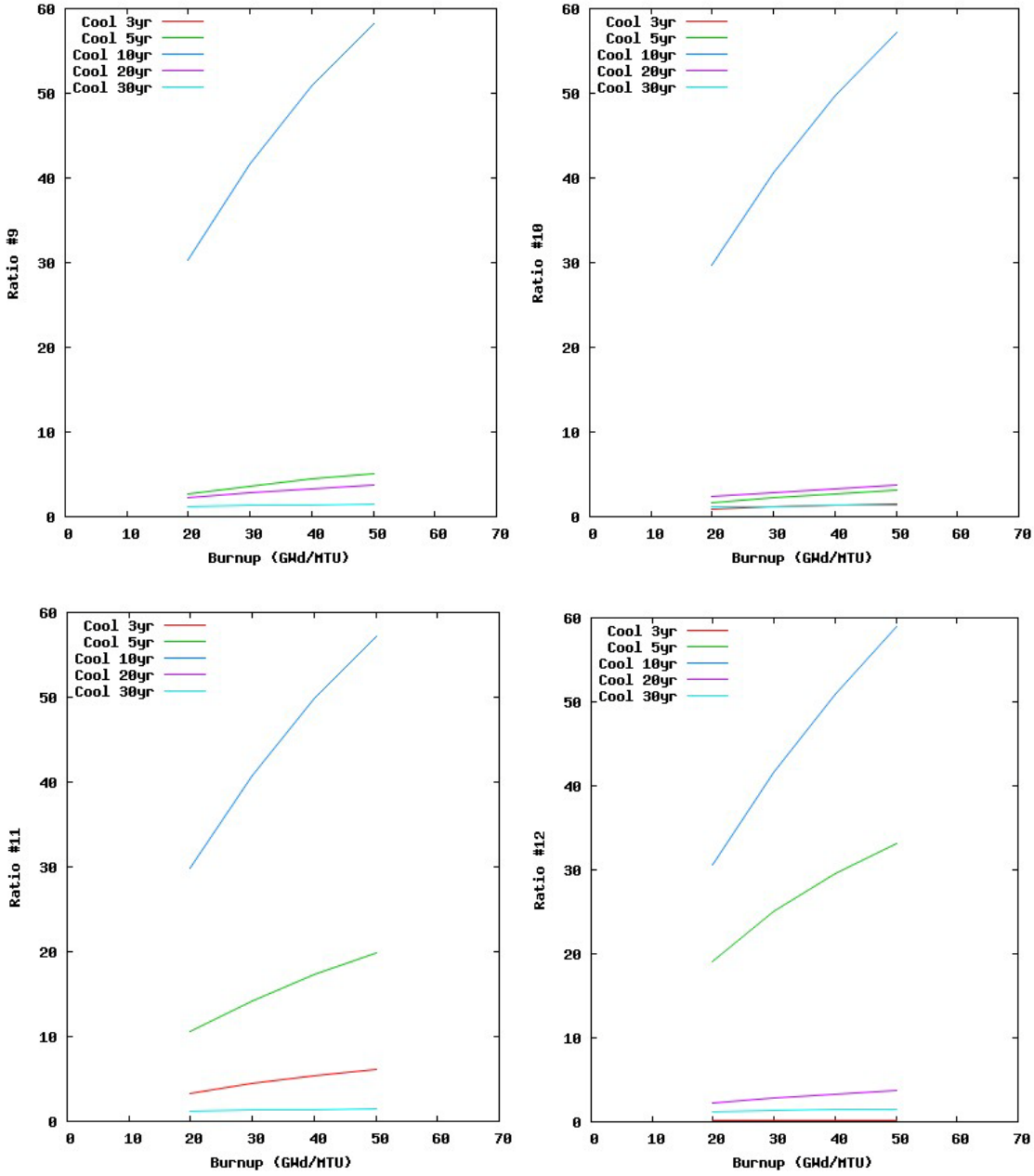

Figure 54. New DG ARs #9–12 as a function of burnup for 5% enrichment at 3, 5, 10, 20, and 30 years following irradiation.

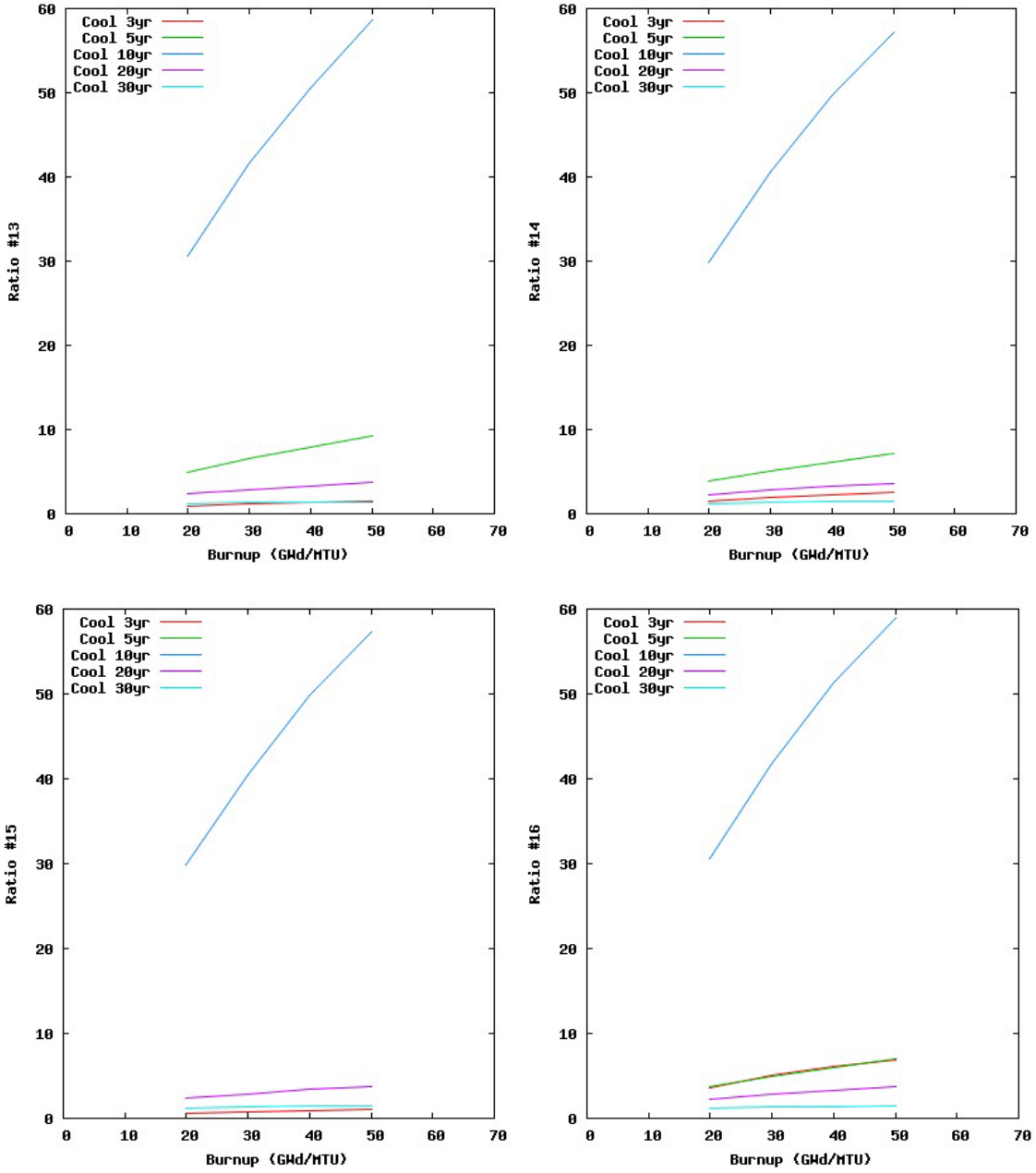

Figure 55. New DG ARs #13–16 as a function of burnup for 5% enrichment at 3, 5, 10, 20, and 30 years following irradiation.

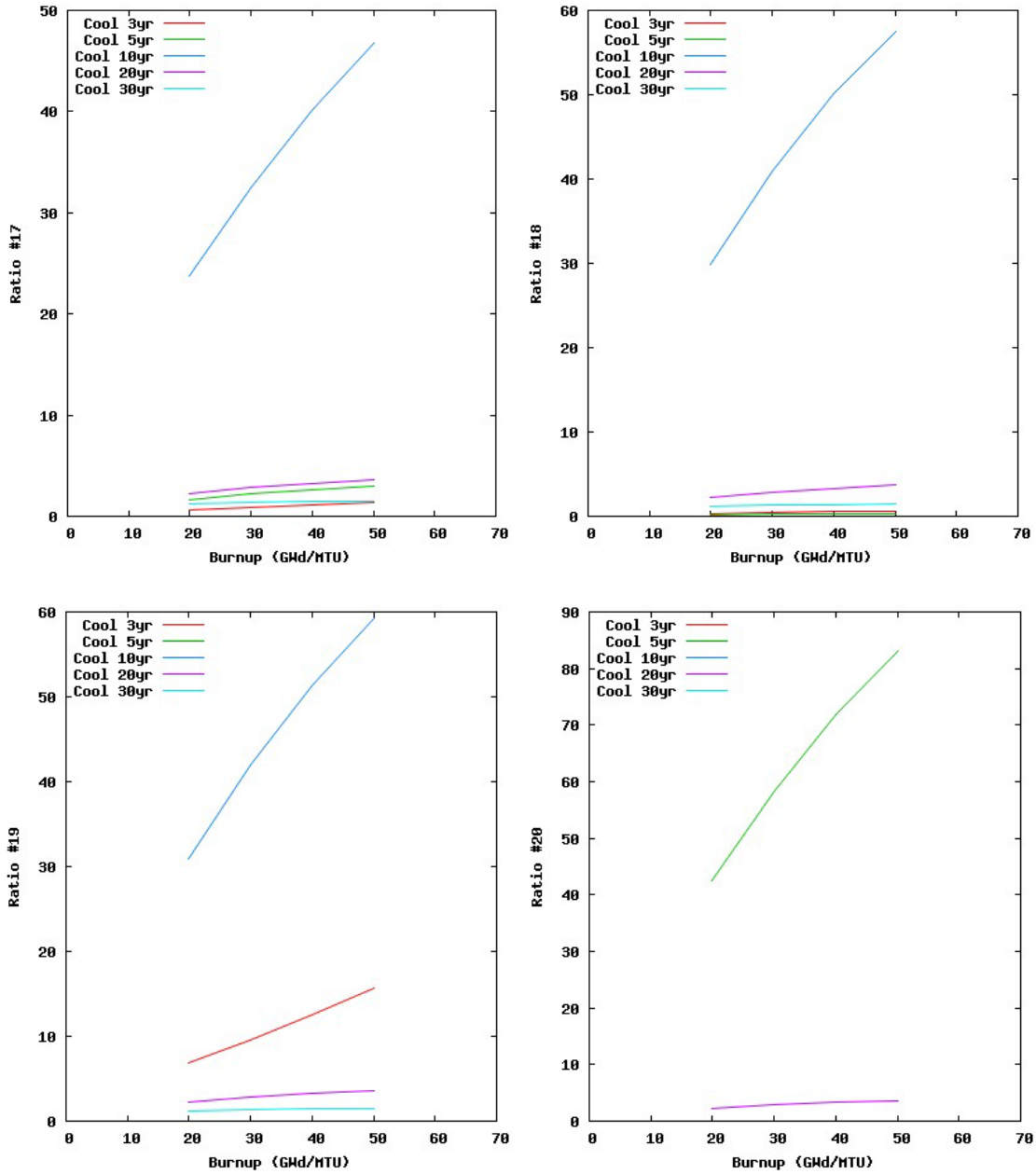

Figure 56. New DG ARs #17–20 as a function of burnup for 5% enrichment at 3, 5, 10, 20, and 30 years following irradiation.

The methodology used here to discover new DG ratios appears to function adequately. The average tally value (for a given enrichment and cooling time) is used as a tally selection baseline for peak selection (amplitudes exceeding the average peak height) for DG ratio calculations. These peaks mitigate noise in the DG AR profiles and should be identifiable by inspectors.

Execution of **runallt.pl**, inclusive of dgratio.exe execution for DG ratio discovery, for the 40 delayed-gamma models requires ~1 minute to generate 20 new DG ratios for the 3% and 5% enrichment cases.

The discovery of DG ratios using this methodology is done using only tally bin data. The methodology does not reveal the identity of the radioisotopes underlying the photon emission. Such identification will require MCNP6 upgrades (1) linking the kcode/burnup and DG emission capabilities and (2) formalizing the patch that provides a list of associated DG emission peaks and radionuclides.

Despite the identification of potential new DG ARs, there is no guarantee that they will be of use to inspectors. To reiterate, the AR technique is valid only if the measured nuclides have the same spatial distribution within the fuel pin or assembly. DG ARs are sensitive to migration effects (Hsue et al., 1978; Tsao and Pan, 1993). Migration exhibits dependence on fuel characteristics and the diffusing species (Hsue et al., 1978; Lee and Durkee, 1984). Our study examines behavior as a function of irradiation. Migration is not treated—all fuel, fission products, and actinides are *in situ*. However, this finding impacts the irradiated fuel assemblies, which is of secondary concern in this study. The central thrust of this investigation is signal analysis for electrorefining and pyroprocessing facilities.

9. FUEL ASSEMBLY DG ARs VS ACTINIDE MASS FOR NEW DG RATIOS

The preceding section presents results for potential new DG ARs as a function of burnup expressed as energy obtained from fuel irradiation (GWd/MTU). A similar process was performed to provide plots of DG emission ratios as a function of burnup characterized in terms of actinide mass.

Processing followed the recipes used in Sections 5 and 8. The same processing technique was used to obtain the mass data. The desired aggregate, or elemental, actinide mass was obtained by summing the isotopic masses using the print table 210 and 220 data. The elemental actinide mass was obtained for each cooling time for each of the eight models (two enrichments and four burnup times).

This data extraction and processing procedure was automated as follows. First, the Fortran code **extractm.f** was written to (1) parse the outp files to identify the cooldown steps in print table 210; (2) find the masses in print table 220 at the 3-, 5-, 10-, 20-, and 30-year post-irradiation cooling times; (3) sum the masses of the actinide isotopes to provide total (elemental) plutonium mass at each cooling time; and (4) write the elemental plutonium mass data to file totmo.[†] This

[†] File totmo contains the integer cooldown data (years) and elemental actinide mass data (g). This content is suitable for easy processing using the runmass.pl Perl script. For easier QA, the identical data are also written to file totmasso with ascii labeling of the quantities.

utility code dynamically determines which actinides are present and have data in the outp file at each cooldown step.

These outp files are approximately four million lines long, so these files were first zipped on Pete ("gzip") to reduce storage needs. These files were then ported to the PC. Each file was unzipped ("gunzip") for data extraction. Because of the file size, several seconds are required to unzip, parse, and extract data.

Second, the Perl script **runmassp.pl** was created to streamline the execution process for **extractm.f** for DG signal ratios as a function of elemental mass. This Perl script serves to (1) unzip/zip the outp files, (2) guide the execution of extractm.exe (Fortran executable) for each of the kcode/burnup outp files, (3) input the values in the totmo files (each contains the three ratio values), and (4) create GNUFILE plot input files containing the ratio values as a function of actinide mass for each ^{235}U enrichment and for each ratio value (for plutonium, the files dgvsmPue3r1, dgvsmPue3r2, dgvsmPue3r3, dgvsmPue5r1, dgvsmPue5r2, dgvsmPue5r3, and similar names for the other actinides).

Because the tally data from the DG sources are needed, **runmallp.pl** contains the coding contained in **runallt.pl**. The necessary tally data and DG ratios are obtained so that the GNUFILE files contain the DG emission ratios as a function of actinide mass. There are nrmax DG ratio files per enrichment for each actinide.

Execution of **runmallp.pl** for the eight kcode/burnup models and the 40 DG models requires ~20 minutes on the PC.

The following subsections contain calculated results for the four DG ARs as a function of elemental mass for 3% and 5% ^{235}U enrichment at 3, 5, 10, 20, and 30 years following irradiation. Results are given for uranium, neptunium, plutonium, americium, and curium. The abscissa values—i.e., the actinide masses—vary as a function of cooling time. These plots were created using **gndgamU.plt**, **gndgamNp.plt**, **gndgamPu.plt**, **gndgamAm.plt**, and **gndgamCm.plt** for uranium, neptunium, plutonium, americium, and curium, respectively.

9.1. DG ARs as a Function of Uranium Mass

Figures 57 and 58 contain plots of DG ARs #1–4 as a function of elemental uranium mass for 3% and 5% enrichment at 3, 5, 10, 20, and 30 years following irradiation.

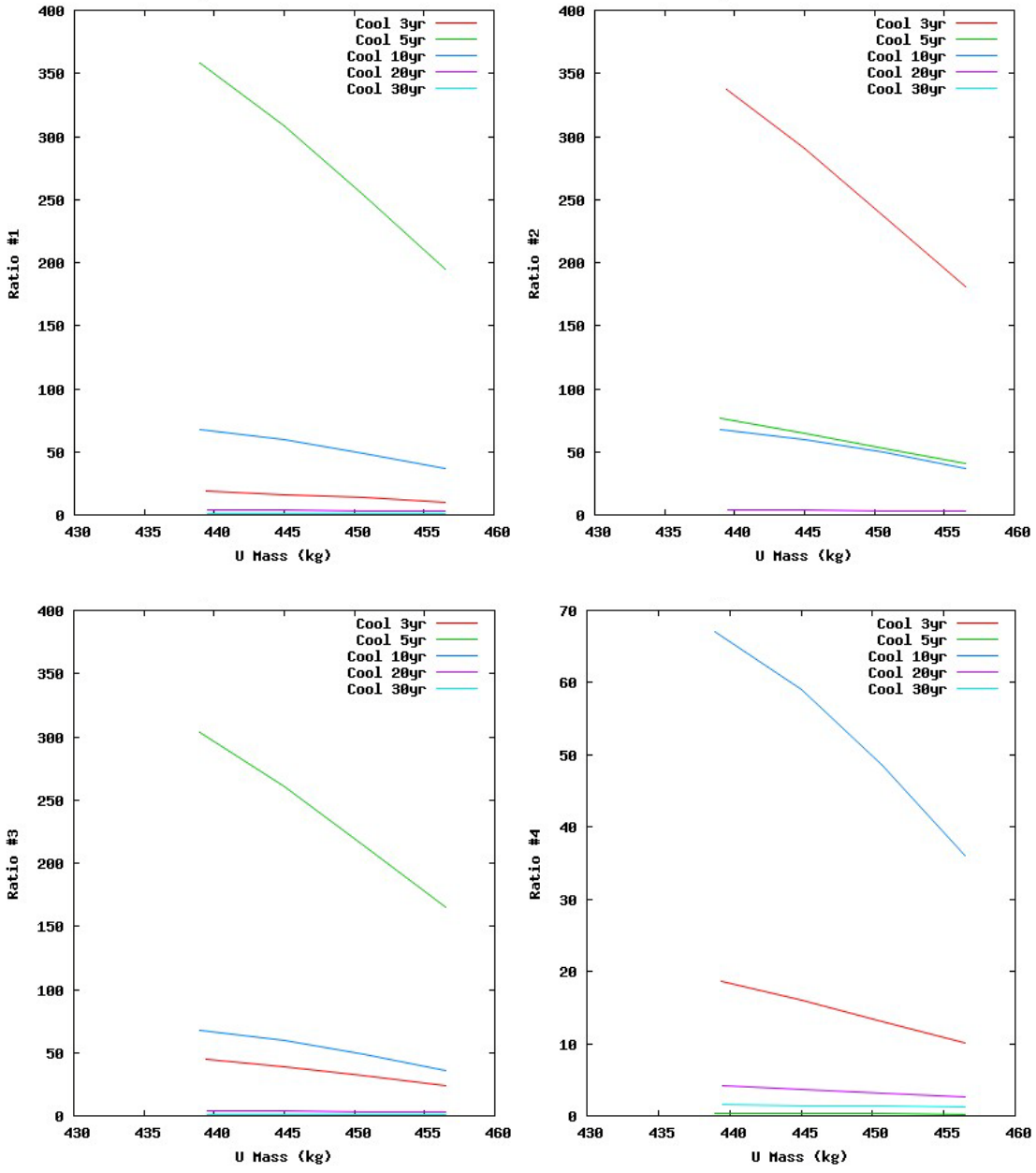

Figure 57. DG ARs 1–4 as a function of elemental uranium mass for 3% enrichment at 3, 5, 10, 20, and 30 years following irradiation.

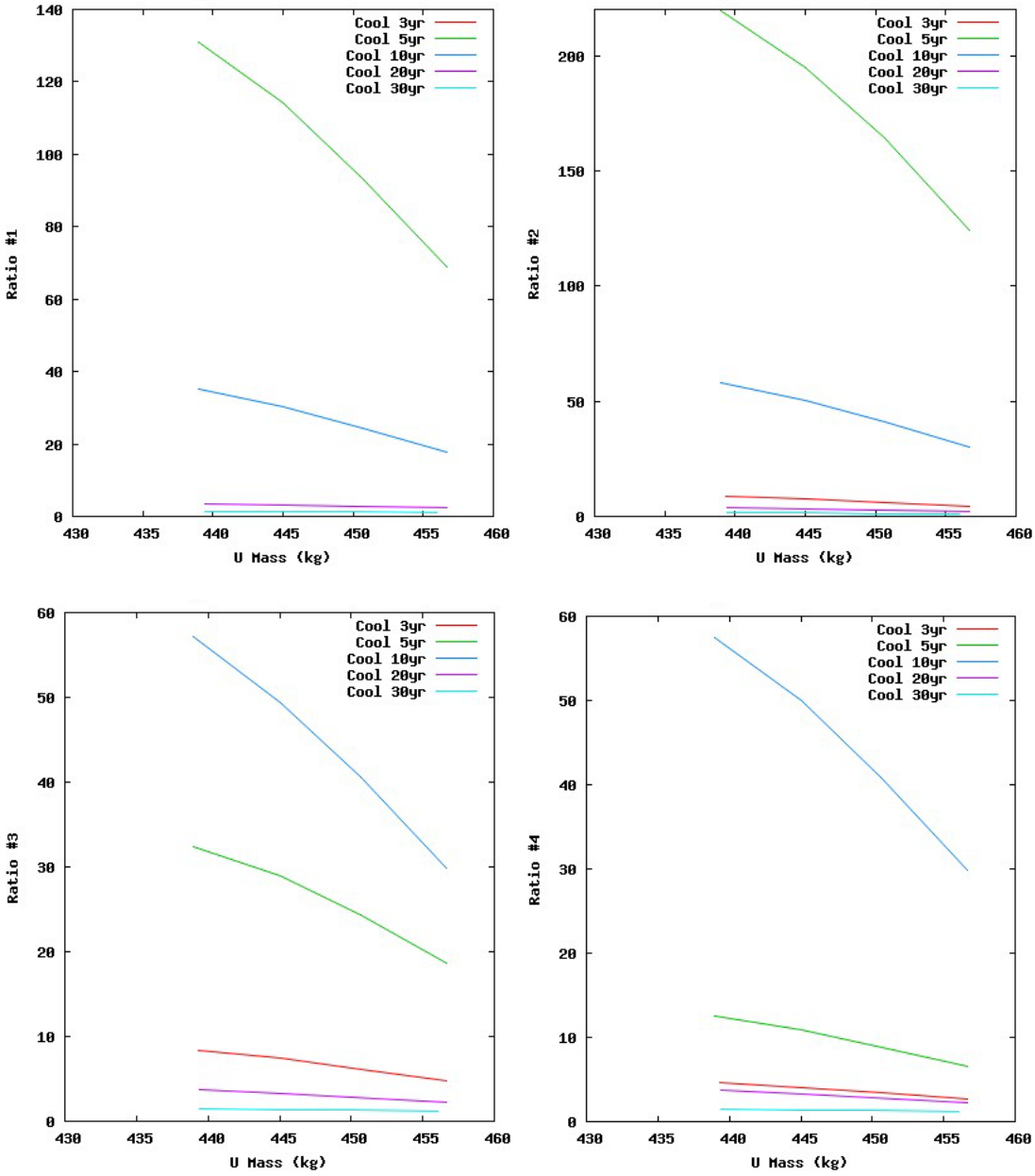

Figure 58. DG ARs 1–4 as a function of elemental uranium mass for 5% enrichment at 3, 5, 10, 20, and 30 years following irradiation.

9.2. DG ARs as a Function of Neptunium Mass

Figures 59 and 60 contain plots of DG ARs #1–4 as a function of elemental neptunium mass for 3% and 5% enrichment at 3, 5, 10, 20, and 30 years following irradiation.

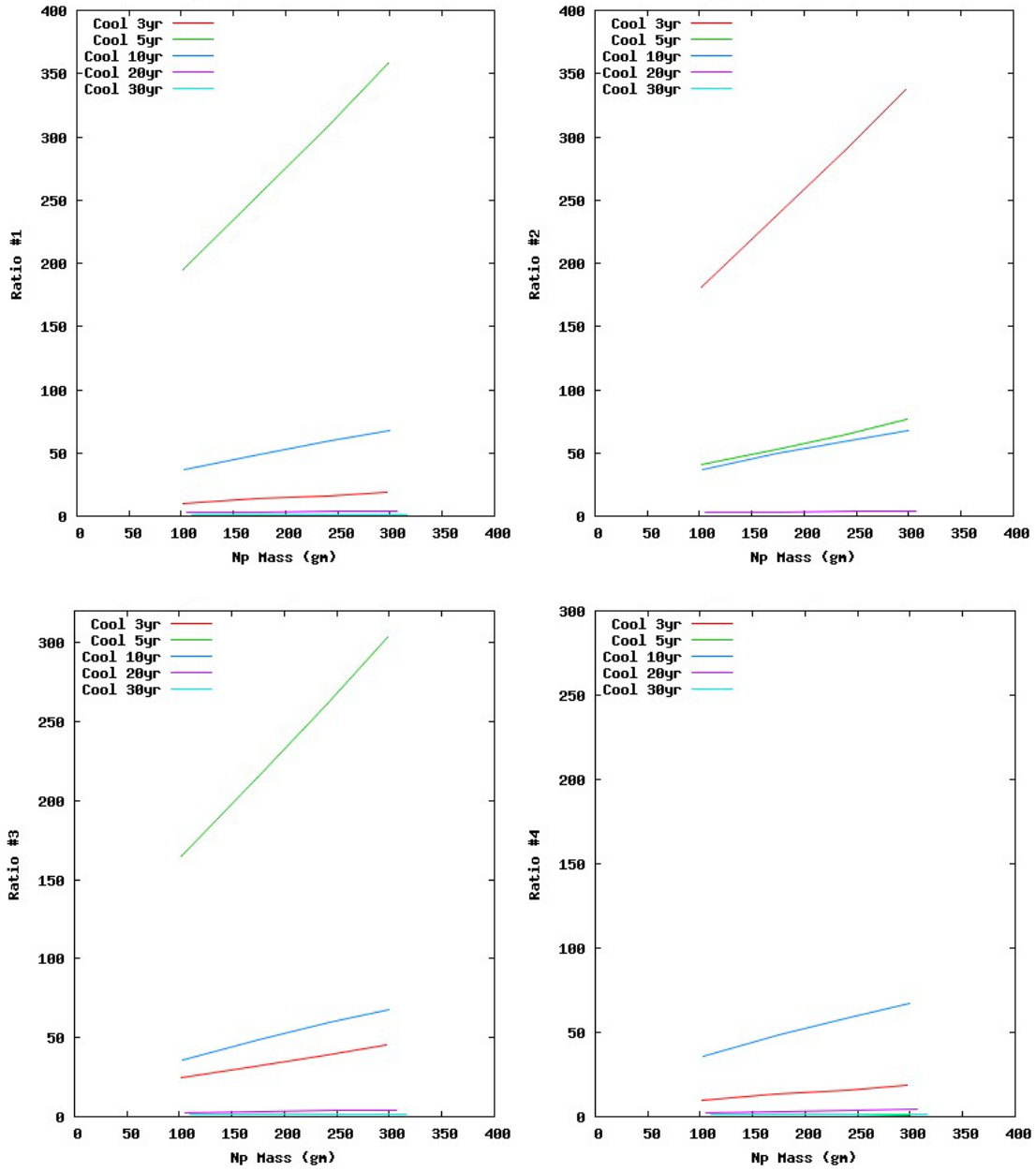

Figure 59. DG ARs 1–4 as a function of elemental neptunium mass for 3% enrichment at 3, 5, 10, 20, and 30 years following irradiation.

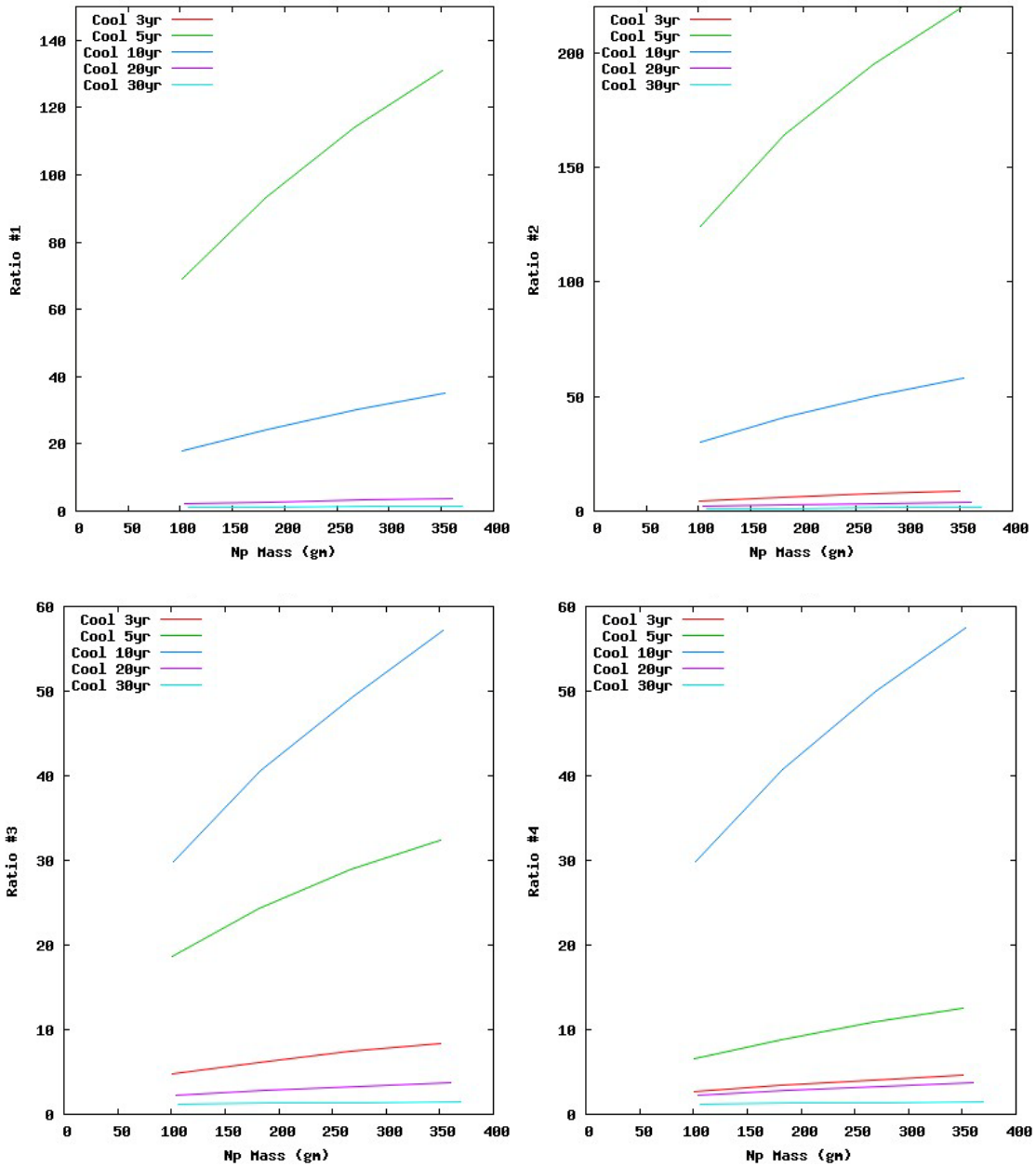

Figure 60. DG ARs 1–4 as a function of elemental neptunium mass for 5% enrichment at 3, 5, 10, 20, and 30 years following irradiation.

9.3. DG ARs as a Function of Plutonium Mass

Figures 61 and 62 contain plots of DG ARs #1–4 as a function of elemental plutonium mass for 3% and 5% enrichment at 3, 5, 10, 20, and 30 years following irradiation.

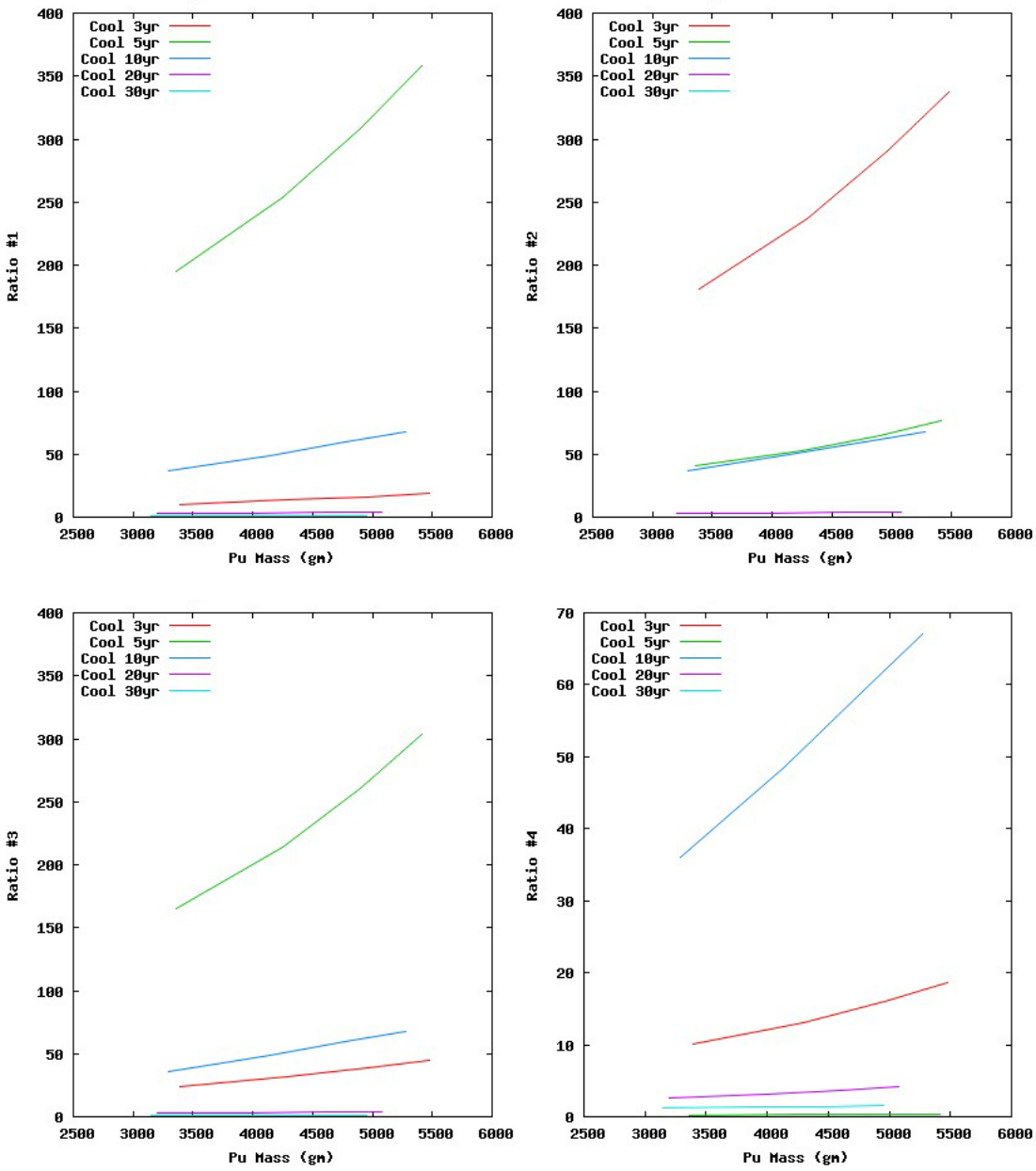

Figure 61. DG ARs 1–4 as a function of elemental plutonium mass for 3% enrichment at 3, 5, 10, 20, and 30 years following irradiation.

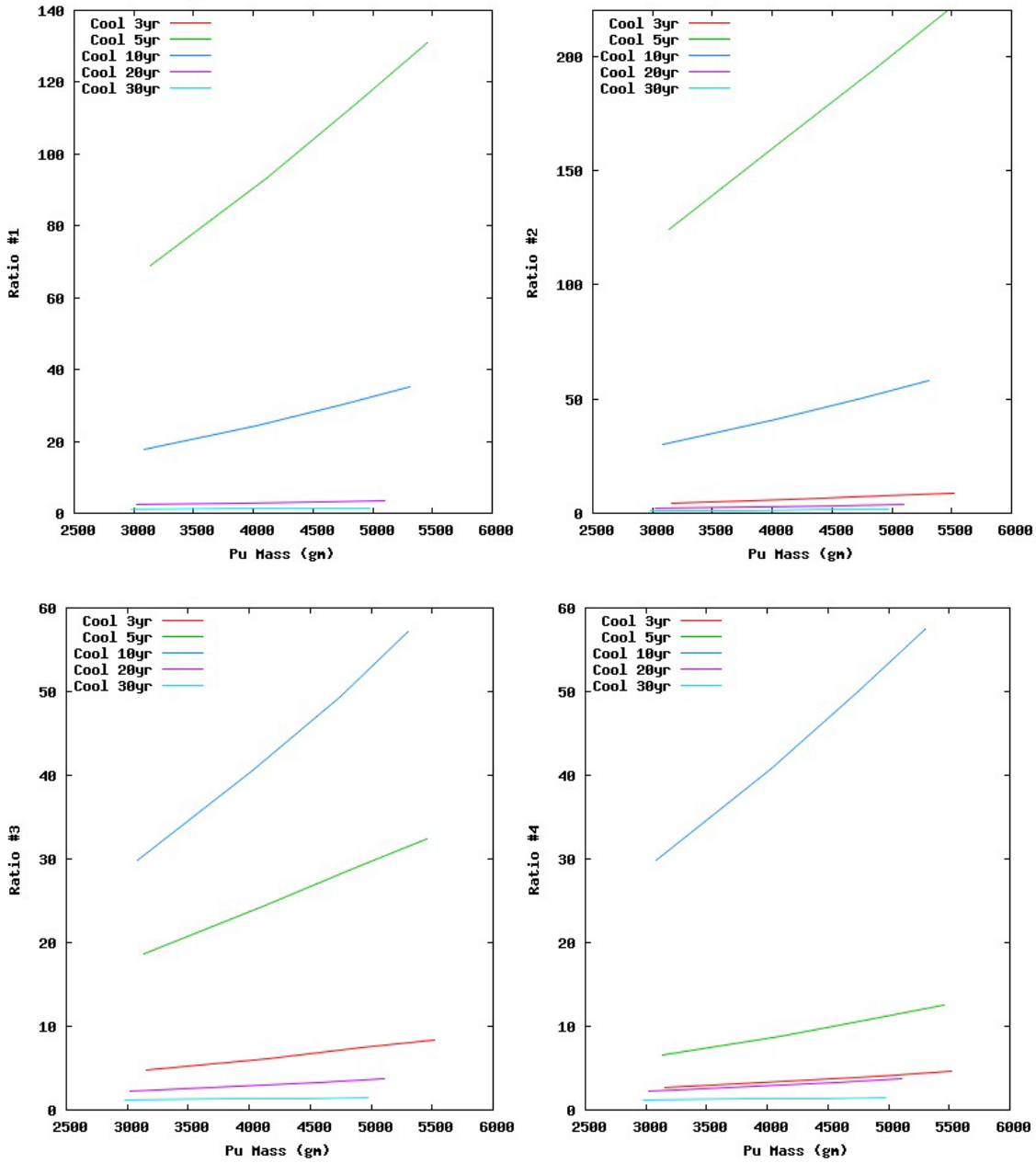

Figure 62. DG ARs 1–4 as a function of elemental plutonium mass for 5% enrichment at 3, 5, 10, 20, and 30 years following irradiation.

9.4. 9.4. DG ARs as a Function of Americium Mass

Figures 63 and 64 contain plots of DG ARs #1–4 as a function of elemental americium mass for 3% and 5% enrichment at 3, 5, 10, 20, and 30 years following irradiation.

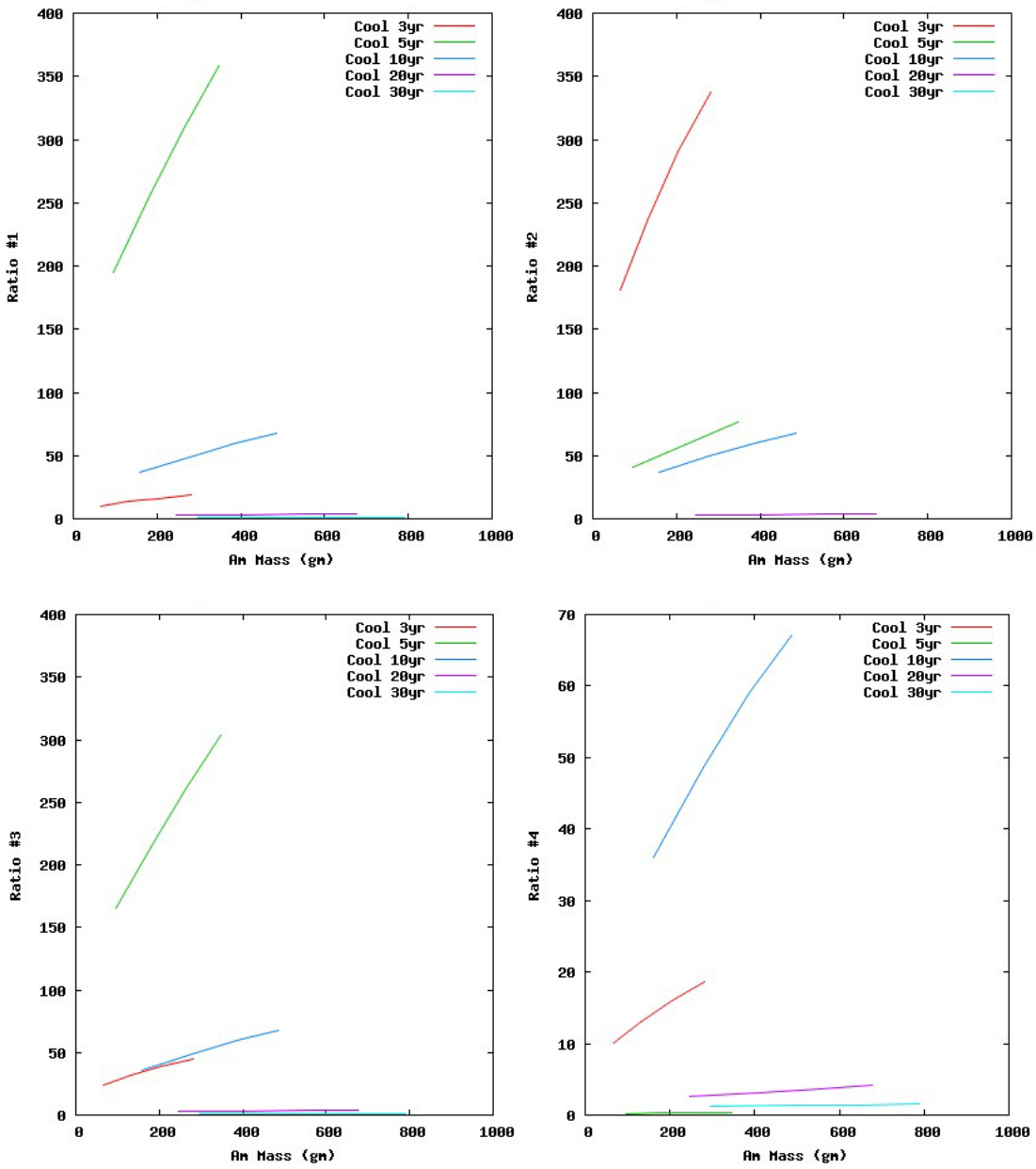

Figure 63. DG ARs 1–4 as a function of elemental americium mass for 3% enrichment at 3, 5, 10, 20, and 30 years following irradiation.

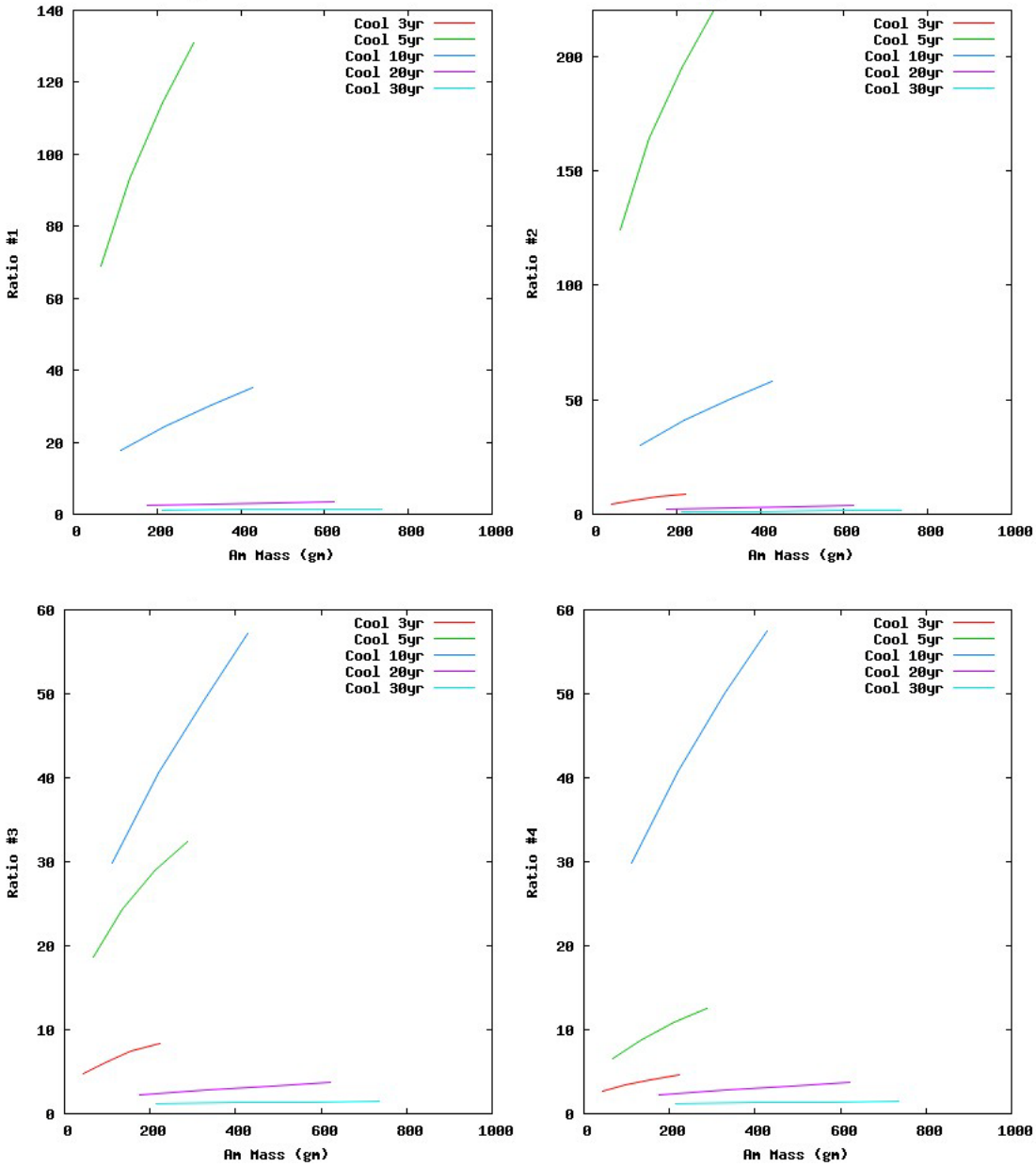

Figure 64. DG ARs 1–4 as a function of elemental americium mass for 5% enrichment at 3, 5, 10, 20, and 30 years following irradiation.

9.5. 9.5. DG ARs as a Function of Curium Mass

Figures 65 and 66 contain plots of DG ARs #1–4 as a function of elemental curium mass for 3% and 5% enrichment at 3, 5, 10, 20, and 30 years following irradiation.

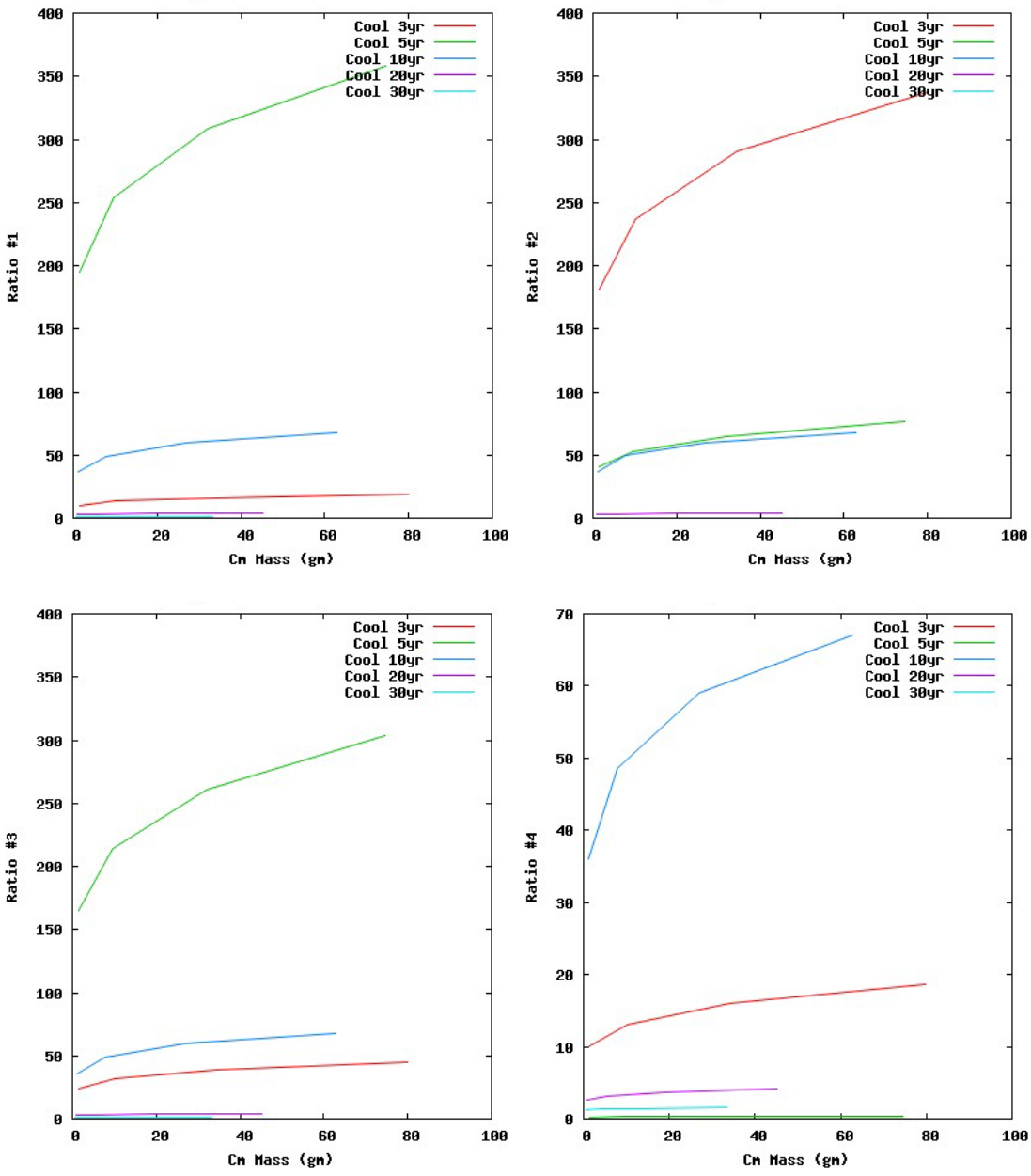

Figure 65. DG ARs 1–4 as a function of elemental curium mass for 3% enrichment at 3, 5, 10, 20, and 30 years following irradiation.

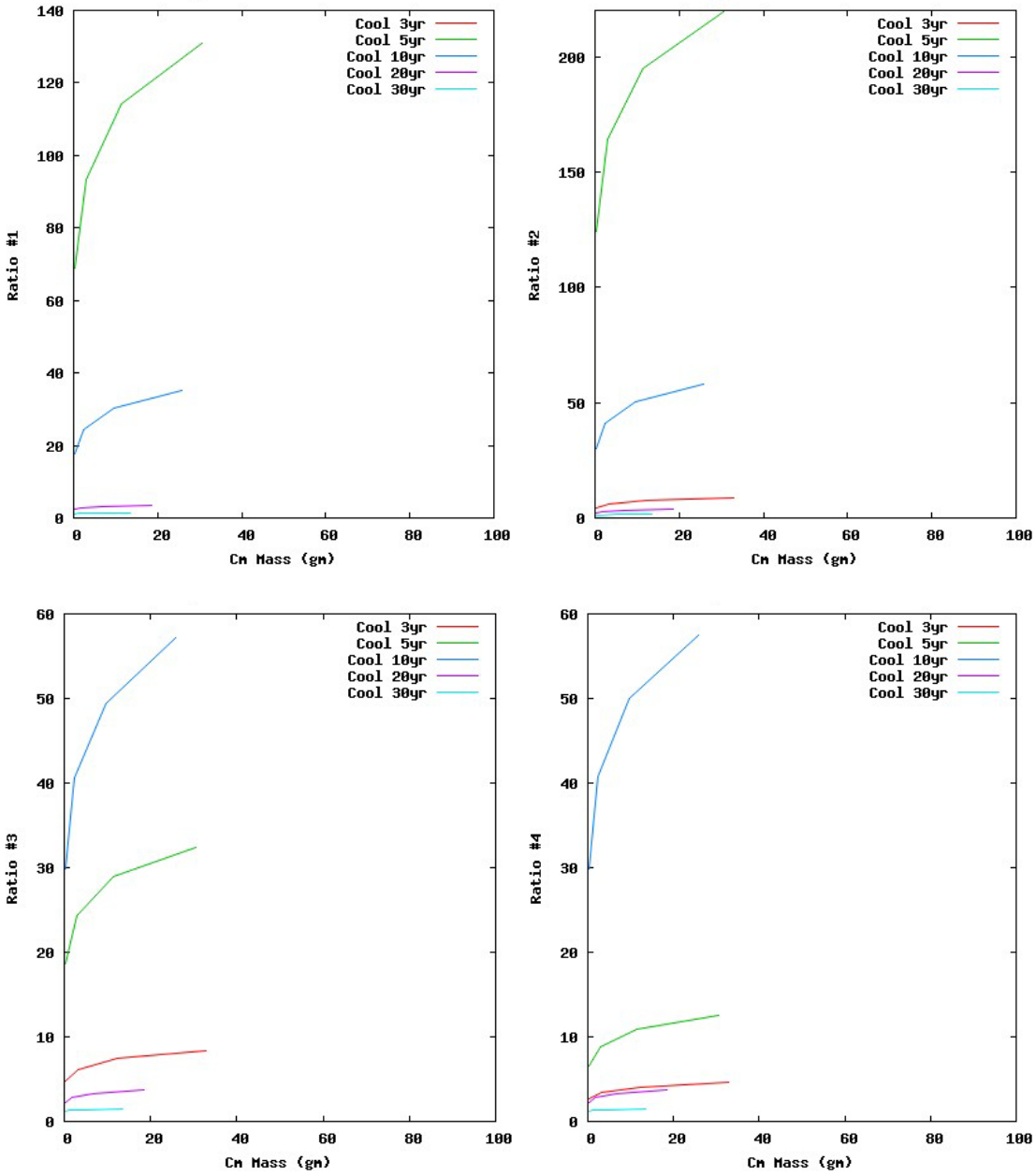

Figure 66. DG ARs 1–4 as a function of elemental curium mass for 5% enrichment at 3, 5, 10, 20, and 30 years following irradiation.

10. SUMMARY AND CONCLUSIONS

The MCNP6 Monte Carlo radiation-transport code has been used to do computer simulations of NDA analysis as a means of examining burnup and isotopic composition monitors that are suitable for pyroprocessing. The monitors examined here use DG and DN emission signatures. The entire study is broken into five parts: (1) a spent fuel assembly, (2) an electrorefiner before electrorefining, (3) an electrorefiner following electrorefining, (4) signals from other pyrochemical separations cell processing units for nominal plutonium loading, and (5) signals from other pyrochemical separations cell processing units for a 10 wt% plutonium loading reduction.

The fuel-assembly analysis was used to establish a baseline reference to which the pyroprocessing results could be compared. The assembly models were executed using the MCNP6 Tier 3 burnup inventory option to give the most comprehensive fission-product and actinide inventory available. In turn, this process provided DG and DN sources to the fullest possible extent. The analysis presented here constitutes the first reported use of the MCNP6 Tier 3 option for the signature analysis of spent fuel.

The fuel-assembly analysis used a generic Westinghouse fuel assembly model to (1) generate DG and DN sources; (2) calculate DG emission ratios for $^{134}Cs/^{137}Cs$, $^{134}Cs/^{154}Eu$, and $^{154}Eu/^{137}Cs$ as a function of burnup and actinide mass; (3) evaluate DN current as a function of burnup and actinide mass; and (4) discover potential new DG emission ratio markers.

MCNP6 was used to generate delayed neutron and delayed-gamma sources for fuel assembly models with 3% and 5% ^{235}U enrichments, 20, 30, 40, and 50 GWd/MTU; and 3-, 5- 10-, 20-, and 30-year cooling times. DG ARs were developed for conventional $^{134}Cs/^{137}Cs$, $^{134}Cs/^{154}Eu$, and $^{154}Eu/^{137}Cs$ markers as a function of burnup and of actinide mass for elemental uranium, neptunium, plutonium, americium, and curium.

DN and DG emissions were assessed using the MCNP6 surface-integrated current F1 tally. This tally calculates the number of particles crossing a surface. It is not a detector tally, so there is no detector-related uncertainty associated with the DN and DG tally data. This tally was selected to provide an initial assessment of behavior. As such, signal masking caused by detector uncertainty is excluded from the analysis. Our objective in this five-part study is to assess whether effects can be assessed and understood at this (F1) level. If desired performance can be obtained here, detector (F8 tally) studies can be undertaken later. However, if performance cannot be obtained with the F1 tally, then the additional burden (including the possible use of nonanalog variance- reduction techniques and increased execution time) associated with detector tally simulations is unwarranted.

The ratio calculation was approximated using the aggregate bin-wise photon tally data. This treatment presumed that the prominent DGs for the energy bins of interest are ^{134}Cs, ^{137}Cs, and ^{154}Eu. Currently, MCNP6 does not have the diagnostic capability required to identify the individual nuclides producing DGs that contribute to the F1 tally in each energy bin.

Our study confirms behavior reported by previous investigators for burnup-dependence of $^{134}Cs/^{137}Cs$, $^{134}Cs/^{154}Eu$, and $^{154}Eu/^{137}Cs$ markers. These ratios exhibit a quasi-linear dependence on burnup and actinide mass. Distinct profiles are apparent for different post-irradiation cooling times.

This study also sought new DG ARs. Several potential new DG markers have been found. However, the emitting nuclides cannot be identified because MCNP6 does not have the diagnostics required to identify the nuclides responsible for DGs in each F1 tally bin. Additional code development will be required to provide this diagnostic capability.

The DN currents as a function of burnup were separate and distinct for all cooling times and enrichments. The general tendencies include (1) for a given enrichment and burnup, the DN signal decreases with cooling time; (2) for a given enrichment and cooling time, the DN signal increases with burnup; (3) for a given burnup and cooling time, the DN signal decreases with increasing enrichment (constant power operation results in fewer fissions with increasing enrichment); and (4) DN signals exhibit quasi-cubic dependence on burnup for all considered enrichment and cooling times.

The analysis for DN currents as a function of element mass provided a set of observations:

- The DN currents as a function of element mass were separate and distinct for uranium, neptunium, and americium for all cooling times and ^{235}U enrichments.

- The DN current profiles as a function of plutonium and curium mass were not separate and distinct.

- The DN current decreases with increasing uranium mass. For a given uranium mass, DN current decreases with increasing cooling time. For a given uranium mass and cooling time, DN current decreases with increasing ^{235}U enrichment.

- The DN current increases with increasing neptunium mass. For a given neptunium mass, DN current decreases with increasing cooling time. For a given neptunium mass and cooling time, DN current decreases with increasing ^{235}U enrichment.

- The DN current increases with increasing plutonium mass. For a given plutonium mass, DN current is relatively insensitive to cooling time. For a given plutonium mass and cooling time, DN current decreases with increasing ^{235}U enrichment.

- The DN current increases with increasing americium mass. For a given americium mass, DN current decreases with increasing cooling time. For a given americium mass and cooling time, DN current decreases with increasing ^{235}U enrichment.

- The DN current increases virtually linearly with increasing curium mass. For a given curium mass, DN current is roughly insensitive to cooling time. For a given americium mass and cooling time, DN current is relatively insensitive to ^{235}U enrichment.

We have quantified signal versus burnup, as well as element concentration for uranium, neptunium, plutonium, americium, and curium. The IAEA is interested in total plutonium; however, several NDA techniques use the Cm/Pu ratio. In addition, criticality safety or industry-based programs may be interested in the quantification of signal vs. other elements.

Our analysis considered post-irradiation cooling times ranging between 3 and 30 years. However, MCNP6 can provide markers for cooling times immediately following irradiation.

Our study began to explore for new DG AR markers. An algorithm has been developed that provides possible new DG ARs. The identities of the nuclides used for these new DG ARs are currently unknown pending additional code development. In addition, the validity of these markers for real-world applications depends on both isotopes in a DG AR having the same spatial distributions. Our analysis has not encompassed migration effects. Consequently, the potential markers may be ineffective in actual monitoring assays. MCNP6 currently has no capability to conduct migration (diffusion) simulations.

The use of classic DG ARs is predicated on a set of five characteristics: (1) approximately equal fission yields for the major fissioning nuclides; (2) low neutron-capture cross sections (including capture by precursors); (3) long half-life relative to irradiation duration; (4) low migration (including precursors) in the fuel; and (5) readily resolvable gamma-ray spectra with high-energy gamma rays to minimize attenuation. Satisfaction of characteristics (1) – (4) leads to DG ARs that are proportional to the fluence as is seen for $^{134}Cs/^{137}Cs$ in Eq.(10). Strictly speaking, these characteristics are essentially always only approximately satisfied. As a consequence, DG ARs exhibit quasi-linear dependence on burnup at best. Nonlinear dependence increases when one or more of the characteristics is not satisfied. In Equations (1) – (14) we write the diffusion-reaction-decay equations and limiting solutions for ^{134}Cs and ^{137}Cs. In general, it is the solution to the diffusion-reaction-decay equations that is needed for the ^{134}Cs and ^{137}Cs concentrations. The concentrations in our study are provided by CINDER'90, which treats the fluence, capture, and decay but does not account for diffusion. As the results show, varying degress of nonlinearity are exhibited by the DG ARs.

The two-stage kcode/burnup and delayed-particle simulations performed for this study were executed independently. MCNP6 currently lacks the internal linkage to use inventories produced by kcode/burnup calculations in delayed-particle simulations. Our analysis thus required the use of an auxiliary VBA processing routine to create DG and DN sources using irradiated fuel inventories. We found that this VBA code was system dependent and failed to operate on different PC platforms. This study has identified the need for development of MCNP6 capability to link kcode/burnup and delayed-particle capabilities to provide user-friendly simulation capability for safeguards applications.

In Part 2 we a present a model for a pyrochemical separations cell, including an electrorefiner.

REFERENCES

Ansari S.A., Asif M., Rashid T., and Qasim K.G., 2007. "Burnup Studies of Spent Fuels of Varying Types and Enrichment," *Annals of Nuclear Energy*, **34**, 641–651.

Brown, F.B., ed., April 2003a. "MCNP–A General Monte Carlo N–Particle Transport Code, Version 5, Volume I: Overview and Theory," Los Alamos National Laboratory report LA-CP-03-0245, Ch 2 pp. 182–185.

Brown, F.B., ed., April 2003b. "MCNP–A General Monte Carlo N–Particle Transport Code, Version 5, Volume II: User's Guide," Los Alamos National Laboratory report LA-CP-03-0245, Ch. 3, pp. 31–32.

Cousin, L. and Haeck, W., 2008. "Validating the VESTA Depletion Interface Using Ariane Chemical Assay," *Transactions of the American Nuclear Society*, **101**, 694–695.

Dennis, M.L. and Usman, S., 2008. "Online Burnup Analysis of MOX Fuel Using Gamma Spectroscopy," *Transactions of the American Nuclear Society*, **99**, 181–183.

Duderstadt J.J. and Hamilton L.J. (1976), *Nuclear Reactor Analysis*, John Wiley & Sons, Inc., New York, 582.

Durkee, Joe W., Jr., James, M.R., McKinney, G.W., Trellue, H.R., Waters, L.S., and Wilson, W.B., 2009a. "Delayed-Gamma Signature Calculation for Neutron-Induced Fission and Activation Using MCNPX, Part I: Theory," *Progress in Nuclear Energy*, **51**, 813–827.

Durkee, Joe W., Jr., McKinney, Gregg W., Trellue, Holly R., Waters, Laurie S., and Wilson, W.B., 2009b. "Delayed-Gamma Simulation Using MCNPX. Part II: Simulations," *Progress in Nuclear Energy*, **51**, 828–836.

Durkee, J.W., Jr., McKinney, G.W., Trellue, H.R., Waters, L.S., and Wilson, W.B., 2009c. "Delayed-Gamma Simulation Using MCNPX," *J. Nuclear Technology*, **168**, 761–764.

Durkee, Joe W., Jr., James, Michael R., McKinney, Gregg W., and Waters, Laurie S., 2010. "MCNPX Delayed-Gamma Feature Enhancements," *Transactions of the American Nuclear Society*, **103**, 651–652.

Durkee, Joe W., Jr., James, M.R., McKinney, G.W., Waters, L.S., and Goorley, J.T., 2012. "The MCNP6 Delayed-Particle Feature," submitted to *J. of Nuclear Technology*.

Fensin, Michael L., Tobin, Stephen J., Sandoval, Nathan P., Swinhoe, Martyn T., and Thompson, Scott J., 2009. "A Monte Carlo Linked Depletion Spent Fuel Library for Assessing Varied Nondestructive Assay Techniques For Nuclear Safeguards," *American Nuclear Society Advances in Nuclear Fuel Management IV*, 1–14.

Fensin, M.L., Koehler, W.E., and Tobin, S.J., 2010. "MCNPX Simulation of a Passive Prompt Gamma System to Be Used in a Spent Fuel Plutonium Assay Strategy," *Transactions of the American Nuclear Society*, **102**, 431–433.

Fensin, M.L., Tobin, S.J., Swinhoe, M.T., Menlove, H.O., Koehler, W., Sandoval, N.P., Lee, S., Mozin, V., Richard, J., Schear, M., Hu, J., and Conlin, J., 2011. "Determining the Pu Mass in LEU Spent Fuel Assemblies – Focus on Passive Gamma Detection," Los Alamos National Laboratory report LA-UR-11-00511.

Fensin, M.L., James, M.R., Hendricks, J.S., and Goorley, J.T., 2012. "The New MCNPX Depletion Capability." Full Paper: 11-07032, International Congress on the Advancements in Nuclear Power Plants, Chicago, IL (June 24–28 2012).

Ghrayeb, S., Ivanov, K., Levine, S., and Loewen, E., 2008. "Development of Monte Carlo Models to Investigate Thorium-Based Fuel in Sodium Cooled Fast Reactors," *Transactions of the American Nuclear Society*, **99**, 203–204.

Goorley, T., James, M., Booth, T., Brown, F., Bull, J., Cox, L.J., Durkee, J., Elson, J., Fensin, M., Forster, R.A., Hendricks, J., Hughes, H.G., Johns, R., Kiedrowski, B., Martz, R., Mashnik, S., McKinney, G., Pelowitz, D., Prael, R., Sweezy, J., Waters, L., Wilcox, T., and Zukaitis, T., 2012. "Initial MCNP6 Release Overview," *J. Nuclear Technology*, to appear December 2012.

Hawari, A.I. and Chen J., 2005. "Computational Investigation of On-Line Interrogation of Pebble Bed Reactor Fuel," *IEEE Transactions on Nuclear Science*, **52**, (5) 1659–1664.

Hsue, S.T., Crane, T.W., Talbert, Jr., W.L., and Lee, J.C., 1978. "Nondestructive Assay Methods for Irradiated Nuclear Fuels," Los Alamos National Laboratory report LA-6923.

Kim, Y. and Hartanto, D., 2011. "A Physics Study on a LEU-Loaded Small Modular Fast Reactor," *Transactions of the American Nuclear Society*, **105**, 1120–1122.

Lamarsh J.R. (1972), *Introduction to Nuclear Reactor Theory*, Addision-Wesley Publishing Company, Inc., Reading, Massachusetts, 479.

Lee, C.E. and Durkee, J.W., 1984. "Multiregion Concentration Diffusion Coefficient Determination Using Davidon's Variable Metric Method," *J. Nuclear Technology*, **69**, 218–235.

McKinney, Gregg W., 2012. "MCNP6 Enhancements of Delayed-Particle Production," *PHYSOR 2012 – Advances in Reactor Physics*, Knoxville, Tennessee, USA, April 15–20, 2012, American Nuclear Society.

National Nuclear Data Center (2012), website http://www.nndc.bnl.gov/, last accessed September 19, 2012.

Organisation for Economic Co-operation and Development-Nuclear Energy Agency (2012), website http://www.oecd-nea.org/science/wpncs/buc/status.html, Benchmark Reports link

Benchmark IV-B document http://www.oecd-nea.org/science/wpncs/buc/specifications/PhaseIVB_report.pdf, last accessed September 19, 2012.

Pan, L.-K., 1989. "Destructive Gamma-Ray Analysis of Fuel Rods from the Taiwan Research Reactor," *J. Nuclear Technology*, **89**, 116–125.

Pelowitz, D.B., ed., April 2011. "MCNPX User's Manual Version 2.7.0," Los Alamos National Laboratory report LA-CP-11-00438.

Reilly, D., Ensslin, N., Smith, H., and Kreiner, S., 1991. *Passive Nondestructive Assay of Nuclear Materials*, NUREG/CR-5550, U.S. Government Printing Office, P.O. Box 37082, Washington, DC 20013-7082, p. 544.

Sandoval, N.P. and Fensin, M.L., 2008. "Burnup Automation MCNPX File Data Retrieval Tool (BAMF-DRT): Data Extraction and Input File Creation Tool Users Manual," Los Alamos National Laboratory report LA-UR-09-01259.

Sterbentz, J.W., Hawkes, G.L., Maki, J.T., and Petti, D.A., 2011. "Monte Carlo Depletion Calculation for the AGR-1 TRISO Particle Irradiation Test," *Transactions of the American Nuclear Society*, **102**, 495–496.

Trellue, H.R., McKinney, G.W., and Durkee, J., 2005. "Burnup Capability Added to MCNPX," American Nuclear Society 2005 Annual Meeting.

Tsao, C.S. and Pan, L.K., 1993. "Reevaluation of the Burnup of Spent Fuel Pins by the Activity Ratio of $^{134}Cs/^{137}Cs$," *Applied Radiation and Isotopes*, **44**, No. 7, 1041–1046.

Williams, T. and Kelley, C., gnuplot (2007), website http://www.gnuplot.info/. Last accessed on August 31, 2007

Willman, C., Hakansson, A., Osifo, O., Backlin, A., and Svard, S.J., 2006. "A Nondestructive Method for Discriminating MOX Fuel From LEU Fuel for Safeguards Purposes," *Annals of Nuclear Energy*, **33**, 766–773.

Wilson, W.B., Perry, R.T., Charlton, W.S., Arthur, E.D., Bozoian, M., Brown, T.H., England, T.R., Madland, D.G., Parish, T.A., and Stewart, J.E., 1997. "SOURCES–3A: A Code for Calculating (α, n), Spontaneous Fission, Delayed Neutron Sources and Spectra," Los Alamos National Laboratory report LA-UR-97-4365.

Wilson W.B., England T.R., George D.C., Muir D.W., and Young P.G., 1995. "Recent Development of the CINDER'90 Transmutation Code and Data Library for Actinide Transmutation Studies," Los Alamos National Laboratory report LA-UR-2181.

Wilson W.B., Cowell S.T., England T.R., Hayes A.C., and Moller P., 2007. "A Manual for CINDER'90 Version 07.4 Codes and Data," Los Alamos National Laboratory report LA-UR-07-8412. Version 07.4.1 Update: March 2008.